DOE/NASA/0156-83/1
NASA CR-167916

HIGH-TEMPERATURE MOLTEN SALT THERMAL ENERGY STORAGE SYSTEMS FOR SOLAR APPLICATIONS

Randy J. Petri
Terry D. Claar
Estela T. Ong
Institute of Gas Technology

July 1983

Prepared for
NATIONAL AERONAUTICS AND SPACE ADMINISTRATION
Lewis Research Center
Under Contract DEN 3-156

for
U.S. DEPARTMENT OF ENERGY
Office of Solar, Geothermal, Electric and Storage Systems
Division of Energy Storage Systems

DOE/NASA/0156-83/1
NASA CR-167916

HIGH-TEMPERATURE MOLTEN SALT THERMAL ENERGY STORAGE SYSTEMS FOR SOLAR APPLICATIONS

Randy J. Petri
Terry D. Claar
Estela T. Ong
Institute of Gas Technology
Chicago, Illinois 60616

July 1983

Prepared for
National Aeronautics and Space Administration
Lewis Research Center
Cleveland, Ohio 44135
Under Contract DEN 3-156

for
U.S. DEPARTMENT OF ENERGY
Office of Solar, Geothermal, Electric and Storage Systems
Division of Energy Storage Systems
Washington, D.C. 20545

ACKNOWLEDGMENT

The authors wish to thank John T. Fry for his significant contributions and efforts in the hardware assembly, experiment data collection, and post-test, metallographic analysis phases of the program.

ABSTRACT

Experimental results of compatibility screening studies of 100 salt/containment/thermal conductivity enhancement (TCE) combinations for the high-temperature solar thermal application range of 704° to 871°C (1300° to 1600°F) are presented. Nine candidate containment/HX alloy materials and two TCE materials were tested with six candidate solar thermal alkali and alkaline earth carbonate storage salts (both reagent- and technical-grade of each). Compatibility tests were conducted with salt encapsulated in ~6.0-inch x 1-inch welded containers of test material from 300 to 3000 hours. Compatibility evaluations were end-application oriented, considering the potential 30-year lifetime requirement of solar thermal power plant components. Analyses were based on depth and nature of salt-side corrosion of materials, containment alloy thermal aging effects, weld integrity in salt environment, air-side containment oxidation, and chemical and physical analyses of the salt.

A need for more reliable, and in some cases first-time-determined, thermophysical and transport property data was also identified for molten carbonates in the 704° to 871°C temperature range. In particular, accurate melting point (mp) measurements were performed for Li_2CO_3 and Na_2CO_3 while melting point, heat of fusion, and specific heat determinations were conducted on 81.3 weight percent Na_2CO_3-18.7 weight percent K_2CO_3 and 52.2 weight percent $BaCO_3$-47.8 weight percent Na_2CO_3 to support future TES system design and ultimate scale-up of solar thermal energy storage (TES) subsystems.

EXECUTIVE SUMMARY

The objectives of this thermal energy storage program were to a) select and screen the materials compatibility of reagent- and low-cost technical-grade alkali and alkaline-earth carbonate salt phase-change materials (PCM), containment materials, and thermal conductivity enhancement (TCE) materials for use in high-temperature (704° to 871°C) thermal energy storage (TES) systems utilizing advanced solar-thermal power generation concepts and b) identify carbonate salt PCM thermophysical and transport property data requirements and perform measurements accordingly to support system design and scale-up of solar thermal TES subsystems. The work performed to achieve these objectives is described in two tasks.

Task 1. Materials Compatibility Testing

This section presents the materials selection, testing matrix, procedures, and materials compatibility evaluations of 100 salt/containment/TCE materials combinations performed in ~6-inch x 1-inch test capsules at operating test temperatures of 750° to 910°/950°C (1380° to 1670°/1740°F). Nine candidate containment alloy materials and two TCE materials were tested with six candidate solar thermal carbonate storage salts (both reagent- and technical-grade).

Containment alloy testing emphasized a "core" group of materials, which included —

- AISI 304 stainless steel
- AISI 316 stainless steel
- AISI 310 stainless steel
- Incoloy 800
- Inconel 600.

Testing was also conducted on aluminum oxide-forming alloys with selected salt mixtures depending on timely availability of samples and suitable capsule fabrication. These alloys included —

- Armco 18SR/Armco 12SR
- Kanthal A-1

PAGE ____ INTENTIONALLY BLANK

- Aluminized AISI Type 304 stainless steel
- Aluminized AISI Type 316 stainless steel.

TCE materials evaluations were performed with high-conductivity copper (in both a solid and a powder metallurgy porous matrix material) and graphite (pyrolytic and ATJ grade) products in a capsule of molten carbonate with an inert gas environment (argon) maintained above the melt.

Six candidate carbonate PCM salts were investigated for high-temperature TES applications. Emphasis was given to salt compositions based on Li_2CO_3, Na_2CO_3, and K_2CO_3 from which congruent melting carbonate mixtures are available covering the temperature range of 397° to 898°C (747° to 1648°F). Reagent- and technical-grade (low-cost) versions of the candidate salts were employed for each "core" material test.

From this study, Incoloy 800 emerged as the best overall containment material during 800 to 3000 hours of testing in molten carbonates at 750° to 950°C. Effective medium-term containment may be more economically achieved with 316 SS or a modified, sigma-phase-free 310 SS.

Aluminum-oxide forming alloys [especially Kanthal A-1 (5.5 weight percent Al) and Alonized AISI 304 and 316 SS] demonstrated enhanced compatibility and are therefore attractive for containment of carbonates for high-temperature solar thermal power applications.

Copper and ATJ graphite demonstrated excellent compatibility in carbonates from 750° to 910°/950°C for up to 2700 hours. Pyrolytic graphite was found to be more chemically reactive and unstable.

The PCM salts themselves demonstrated excellent chemical and thermophysical stabilities with 1 to 5 free-cool thermal cycles for up to 3100 hours at 750° to 910°C. Technical-grade versions of the six salts generally exhibited a slightly higher, though neither prohibitive nor life-limiting, corrosive behavior with time than their reagent-grade counterparts.

Long-term containment of molten Na_2CO_3 and K_2CO_3 for storage applications above 900°C represent a considerable materials challenge requiring additional development and testing. It is recommended that further investigations focus on high-temperature materials research involving chemical alloying modifications of AISI 310 SS (decrease sigma-phase susceptibility) and aluminum-

oxide-forming materials through alloy and/or coatings development efforts to improve corrosion resistance and to define fabrication and welding requirements. Long-term (>8000-hour lab tests) corrosion compatibility and thermal cycling tests of salt/carbonate containment for TES applications in the 750° to 910°C temperature range should also be performed.

In addition, generic research into other TES media and subsystem heat exchange schemes (that is, direct-contact) should be pursued, which may potentially offer further energy, cost, and performance benefits over current, state-of-the-art molten salt TES systems for applications in the elevated temperature regime of 750° to 950°C.

TABLE OF CONTENTS

TABLE OF CONTENTS, Cont.

LIST OF FIGURES

LIST OF FIGURES, Cont.

LIST OF FIGURES, Cont.

LIST OF TABLES

LIST OF TABLES, Cont.

DETAILED DESCRIPTION OF TECHNICAL PROGRESS

Background and Introduction

Advanced concepts for the conversion of solar thermal energy to electrical power include large central receiver systems employing a closed Brayton power cycle, as well as small, dispersed power systems with Stirling, Rankine, or Brayton heat engines. To obtain high conversion efficiencies, these systems are being designed to operate in high temperature regimes of 700° to 1090°C (1300° to 2000°F).[1,2] Thermal energy storage subsystems are desirable in these applications to provide energy to the turbine or heat engine during periods of low solar insolation — early morning and late afternoon — as well as during periods of cloud cover. Latent-heat storage is particularly attractive because of its potential for attaining high energy densities (resulting in decreased system mass, volume, and cost) and absorption and release of heat over a narrow temperature range.

The Institute of Gas Technology (IGT) has been investigating the feasibility of using molten carbonates as latent-heat, phase-change materials (PCM's) for storage applications since 1976. The attractive properties and stability of alkali carbonates for use in the 450° to 540°C (850° to 1000°F) temperature range were demonstrated under ERDA Contract No. EY-76-C-02-2888, "Molten Salt Thermal Energy Storage Systems."[3] Continued work under the DOE-funded NASA Contract NAS3-20806, "High-Temperature Molten Salt Thermal Energy Storage Systems,"[4] emphasized cyclic endurance testing of an 8-kWh_{th} engineering-scale thermal energy storage (TES) module containing an alkali carbonate mixture in the 480° to 540°C (900° to 1000°F) range, screening of candidate carbonate mixtures having melting points between 660° and 890°C (1225° and 1636°F), and evaluation of thermal conductivity enhancement (TCE) materials in laboratory-scale TES modules (<1 kWh_{th} capacity). A limited amount of work was also conducted in the latter program to identify limitations of handling representative high-temperature fluoride and chloride salts.

At temperatures below approximately 650°C (1200°F), carbonates can be handled very easily and safely, and Type 316 austenitic stainless steel (SS) is compatible with molten salts for extended periods of time (5650 hours, 130 cycles between 480° and 540°C).[3] In the recently concluded work under Contract NAS3-20806,[4] Type 316 SS was generally satisfactory for containing high-temperature carbonates for short-term screening purposes (350 to 1000-

hour exposures). However, metallurgical analyses of Type 316 heat exchanger (HX) tubes exposed to Li_2CO_3 and Na_2CO_3 at 704° to 907°C (1300° to 1665°F) for several hundred hours revealed formation of an outer, porous hot-corrosion layer and subscale carburization of both the bulk grains and the grain boundaries as a result of salt interactions. Air-side oxidation of the HX was also observed. In addition, precipitated particles of brittle intermetallic sigma phase were observed throughout the bulk stainless steel matrix. Sigma-phase formation, which results from prolonged high-temperature exposure and not from salt corrosion, is deleterious to the strength and related mechanical properties of the stainless steel. Thus, selection and testing of alternate containment/HX materials was clearly required, not only on the basis of salt compatibility, but also based on the physical and microstructural stabilities of those alloys at high temperatures for extended periods (anticipated 25 to 30-year solar plant lifetime).

In light of these findings, the overall objective of the current program was to further develop latent-heat, PCM/TES technology through the selection and compatibility screening of carbonate/containment HX/TCE materials to satisfy the high-temperature [704° to 871°C (1300° to 1600°F)], TES requirements of advanced solar thermal power generation concepts. The program objectives were accomplished through the following task structure:

Task 1. Materials Compatibility Testing

The specific objectives of this task were to —

- Select six candidate latent-heat alkali/alkaline earth carbonate storage salts, five containment/HX materials, and two thermal conductivity enhancement materials having the potential of satisfying the performance, cost, and lifetime goals of advanced solar-thermal TES concepts in the 704° to 871°C (1300° to 1600°F) temperature regime.
- Perform compatibility screening tests of candidate salt/containment/TCE materials to identify the most functionally promising combinations. The screening tests were performed in two phases.
- Evaluate the effects of using low-cost technical-grade salts on corrosion and stability of containment and TCE materials.

These objectives were accomplished through the screening of nine potential containment/HX and two TCE materials with six candidate solar thermal carbonate storage salts. Compatibility evaluations were end-application oriented, with particular emphasis placed on a material's long-term (30 years)

functionality potential in light of the corrosion mechanisms observed in "welded-capsule" testing.

1.1. Materials Selection

Salt Selection

In this effort, IGT sought to explore and develop alkali/alkaline earth carbonate salts as TES phase-change materials in the 704° to 871°C (1300° to 1600°F) temperature range. These salts were selected on the basis of the desirable physical properties, thermal performance, and endurance/stability exhibited by these materials in previous programs at IGT.[3,4] Table 1 contains a listing of the carbonate mixtures originally identified and studied under Contract No. NAS3-20806 as viable candidates for Brayton or Stirling solar power system TES applications. Table 2 includes pertinent property data and experimentally determined thermal discharge characteristics.

Final candidate salts were selected for these screening tests primarily on the basis of —

- Energy density
- Cost
- Melting/solidification temperatures
- Thermal cycling performance and endurance in laboratory-scale TES modules
- Vapor pressure and high-temperature stability
- Salt impurity levels
- Toxicity, safety, hygroscopicity, and handling considerations
- Volumetric expansion on melting
- Heat capacity.

From the carbonate mixtures originally identified and studied under Contract No. NAS3-20806 as viable candidates for solar power system TES applications, the six candidate carbonate salt compositions shown in Table 3 were selected for reagent- and technical-grade salt materials compatibility testing. The solidification points of these salt mixtures span the temperature range of 686° to 891°C (1267° to 1636°F), with technical-grade salt costs

Table 1. CANDIDATE CARBONATE COMPOSITIONS TESTED UNDER CONTRACT NAS3-20806

No	Salt System	Composition wt %	Composition mol %	Melting Point °C	Melting Point °F	ΔH_f J/kg	ΔH_f Btu/lb	Heat Capacity at Melting Point c_p(s) J/kg-K	c_p(s) Btu/lb-°F	c_p(ℓ) J/kg-K	c_p(ℓ) Btu/lb-°F	Thermal Conductivity k (ℓ) W/m-K	Thermal Conductivity k (ℓ) Btu/hr-°F-ft	Density at 25°C kg/m³	Density at 25°C lb/ft³	Salt Cost $/kg	Salt Cost $/lb	Capacity Cost $/10⁶ J	Capacity Cost $/10⁶ Btu	Specific Capacity (ρ at 25°C) J/m³x10⁹	Specific Capacity (ρ at 25°C) Btu/ft³
1	Li_2CO_3-Na_2CO_3-K_2CO_3	32-33-35	43 3-31 2-25.5	397	747	276,794	119	1674.7	0.40	1632 9	0.39	2 02	1 17	2300 3	143 6	0.73	0 33	2 60	2741	6.65	17,835
2	Li_2CO_3-$CaCO_3$	55 7-44 3	63-37	662	1224	274,468	118	--	--	--	--	--	--	--	--	1.17	0.53	--	--	--	--
3	Na_2CO_3-$BaCO_3$	47 8-52.2	63-37	686	1267	172,124	74	--	--	--	--	--	--	--	--	0 18	0 08	--	--	--	--
4	Li_2CO_3-Na_2CO_3-K_2CO_3	1.21-50 0-48 8	1-55-44	706	1303	162,820	70	1674 7	0 40	1549.1	0.37	1 73	1.00	2399 6	149.8	0.24	0.11	1 49	1597	5 30	14,230
5	Na_2CO_3-K_2CO_3	50-50	56-44	710	1310	162,820	70	1674 7	0.40	1549 1	0.37	1.73	1.00	2399.6	149.8	0 24	0 11	1.49	1597	5.30	14,230
6	NaF-KF	32.5-67 5	40-60	721	1330	586,152	252	--	--	--	--	--	--	2481.3	154.9	1.23	0 56	2 11	2223	14.50	39,007
7	Li_2CO_3	100	100	723	1333	607,086	261	2637 7	0.63	2512 1	0 60	1 96	1 13	2108.0	131 6	2 05	0.93	3 38	3563	12.80	34,348
8	$CaCl_2$	100	100	772	1422	256,093	110 1	--	--	--	--	--	--	2148.0	134 1	0.09	0.04	0 34	363	5 50	14,764
9	Na_2CO_3-K_2CO_3	81 3-18 7	85-15	790-737	1454-1360	253,534	109	--	--	--	--	--	--	2513.3	156 9	0.13	0.06	0.52	551	6.37	12,090
10	Na_2CO_3	100	100	858	1576	265,164	114	1004.8	0.24	1004.8	0 24	1 83	1.06	2527.7	157 8	0 07	0.03	0.25	264	6 69	17,958
11	K_2CO_3	100	100	898	1648	200,036	86	1507.2	0.36	1507.2	0.36	1 73	1 00	2428.4	151.6	0.42	0.19	2.09	2209	4.86	13,038

D80020282

Table 2. CONTRACT NAS3-20806 LAB-SCALE TES EXPERIMENTAL RESULTS[4]

No.	Salt Code	Salt System	Composition, wt % (mol %)	Melting Point, °C (°F)	ΔH_f J/kg	ΔH_f Btu/lb	Wt. of Salt Loaded gr	Wt. of Salt Loaded lb	Discharge Solidification Range °C (°F) → °C (°F)	Time to Discharge Salt mp + 50°C → mp − 50°C, min	Heat Flux, $\bar{Q}$ mp − 50°→ mp + 50°C W/m²	Heat Flux, $\bar{Q}$ mp − 50°→ mp + 50°C Btu/hr-ft²	No. of Cycles	Hours at Operational Temperature
1	L1-1	Na_2CO_3-K_2CO_3	50-50 (56-44)	710 (1310)	162,820	70	879.8	1.94	708 (1306) → 700 (1292)	34	36,931	11,715	13	336
2	L1-2	Li_2CO_3-Na_2CO_3-K_2CO_3	1.21-49.95-48.84 (56-44)	706 (1303)	162,820	70	880	1.94	706 (1303) → 695 (1283)	46	44,422	14,091	22	528
3	L1-3	Na_2CO_3-K_2CO_3	81.3-18.7 (85-15)	790-737 (454-1360)	253,534	109	821	1.81	790 (1454) → 738 (1360)	--	48,375	15,345	38	1032
4	L2-1	Li_2CO_3	100 (100)	723 (1333)	607,086	261	720	1.58	727 (1341) → 725 (1337)	48	--	--	13	408
5	L2-2	Na_2CO_3	100 (100)	858 (1564)	265,164	113	827	1.82	868 (1594) → 862 (1584)	27	47,642	14,478	21	288
6	L2-3	K_2CO_3 (CO_2 Blanket)	100 (100)	893 (1648)	200,036	86	810	1.79	916 (1681) → 912 (1674)	21	72,513	23,002	2	96
7	L3-1	$(Li\text{-}Na\text{-}K)_2CO_3$	32-33-35 (43.3-31.2-25.5)	397 (747)	276,794	119	611.3	1.35	410 (770) → 401 (754)	86	6,954	2,206	10	504
8	L3-2	$(Li\text{-}Na\text{-}K)_2CO_3$ w/Duocel	32-33-35 (43.3-31.2-25.5)	397 (747)	276,794	119	611.3	1.35	408 (766) → 404 (759)	53	10,138	3,216	22	312
9	L3-3	$BaCO_3$-Na_2CO_3	52.2-47.8 (37-63)	686 (1267)	(172,124)	(74)	966	2.63	717 (1323) → 712 (1314)	31	41,676	13,220	36	984
10	L3-4	$CaCl_2$	100 (100)	772 (1422)	256,093	110	--	--	-- → --	--	--	--		
11	L4-1	$CaCO_3$-Li_2CO_3	44.3-55.7 (37-63)	662 (1224)	(274,468)	(118)	813.6	1.79	662 (1224) → 657 (1215)	48	40,405	12,817	25	312
12	L4-2	Li_2CO_3 (CO_2 Blanket)	100 (100)	726 (1333)	607,086	261	754	1.66	734 (1353) → 730 (1346)	54	76,583	24,293	22	672
13	L4-3	KF-NaF	67.5-32.5 (60-40)	721 (1330)	586,152	252	--	--	-- → --	--	--	--		

B80020283

Table 3. CANDIDATE ALKALI/ALKALINE EARTH CARBONATE PCM MATERIALS

	Composition, wt %	Reported Melting Point °C	(°F)	Observed Solidification Range °C	(°F)	Cost* $/kg	($/lb)
1.	$52.2BaCO_3$-$47.8Na_2CO_3$	686	(1267)	717 - 712	(1323)-(1314)	0.23	(0.10)
2.	$50.0Na_2CO_3$-$50.0K_2CO_3$	710	(1310)	708 - 700	(1306)-(1292)	0.29	(0.13)
3.	Li_2CO_3	723	(1333)	734 - 730	(1353)-(1346)	2.65	(1.20)
4.	$8.13Na_2CO_3$-$18.7K_2CO_3$	790 - 740	(1454)-(1364)	813 - 742	(1495)-(1368)	0.15	(0.07)
5.	Na_2CO_3	858	(1576)	868 - 862	(1594)-(1584)	0.06	(0.03)
6.	K_2CO_3	891	(1636)	916 - 912	(1681)-(1674)	0.51	(0.23)

* Based on technical-grade salt prices listed in Chemical Marketing Reporter, March 16, 1981.

ranging from $0.06/kg ($0.03/lb) for Na_2CO_3 to $2.65/kg ($1.20/lb) for Li_2CO_3. (See Figure 1.)

Another important aspect of salt selection took into consideration the fact that the economic feasibility of latent-heat TES concepts is contingent upon low-cost storage salt materials and cost-effective materials of construction. Therefore, one must evaluate the potential problems and limitations associated with using commercially available technical-grade carbonates. Table 4 is a listing of the pure alkali and alkaline-earth carbonates considered along with recent costs of each technical-grade salt in bulk quantities.

Since potential technical-grade salt instabilities and impurity interactions with containment and TCE materials were of immediate concern, numerous companies were identified and contacted as prospective suppliers of technical-grade carbonates. Cost information and chemical and physical property specifications on the commercially available carbonates were procurred from the chemical companies listed in Appendix A.

Regarding prospective technical-grade salt impurities, selection emphasized grades containing minimum chloride levels to reduce the risk of chloride stress corrosion cracking of containment alloys. Where possible, low sulfate levels were also sought.

In view of these considerations, the companies listed in Table 5 were selected as suppliers of the respective technical-grade carbonate salts for the salt/containment/TCE material screening tests performed in this program.

Containment Materials Selection

The selection of materials for containment and HX construction for advanced solar thermal TES applications in the elevated temperature regime of 704° to 871°C (1300° to 1600°F) was largely based on the need to improve long-term resistance to —

- Corrosion by molten salts
- Air oxidation
- Intermetallic-phase precipitation, embrittlement, or other aging effects
- Thermal cycling effects

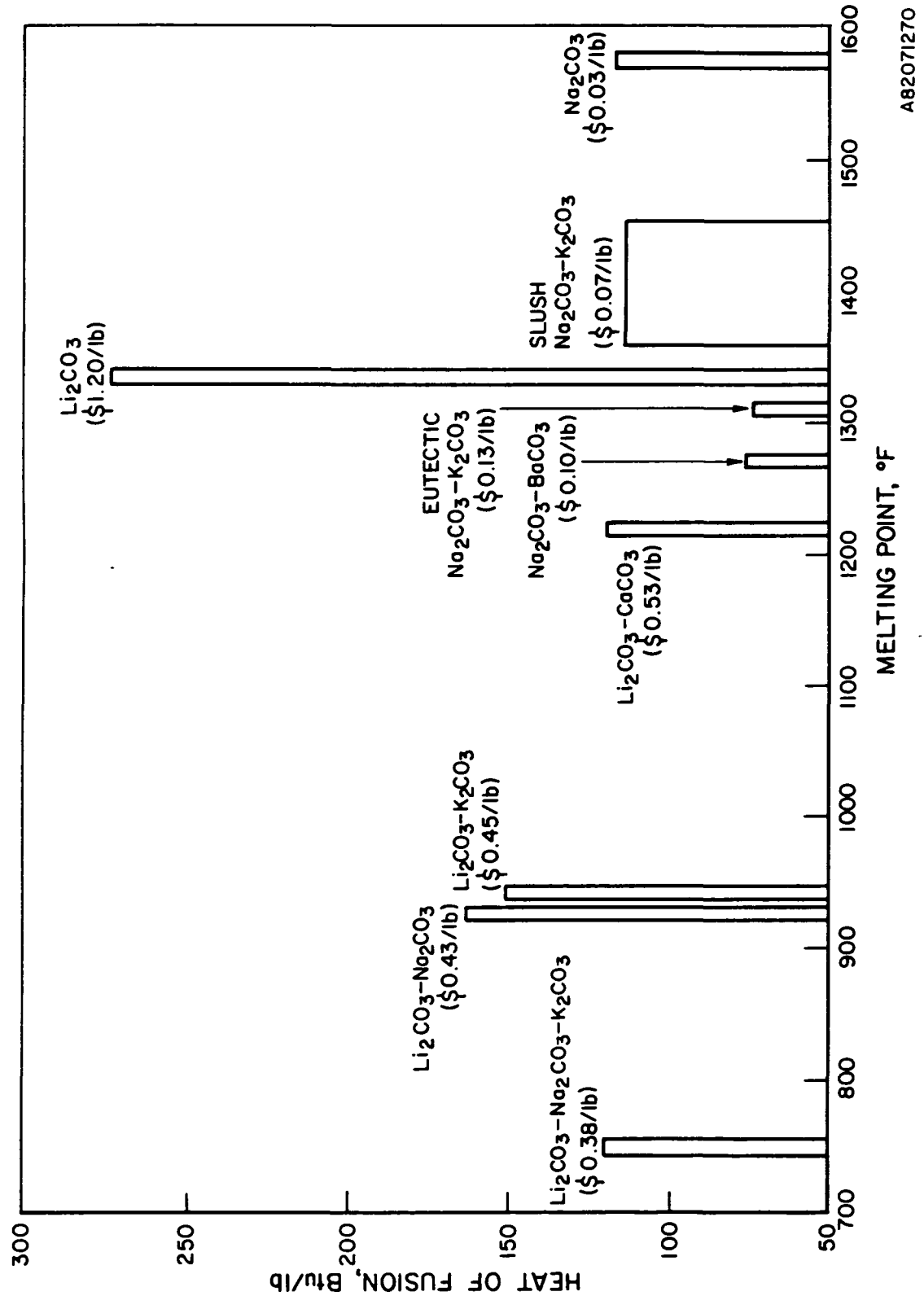

Figure 1. ALKALI/ALKALINE EARTH CARBONATES AS PHASE-CHANGE TES MATERIALS

Table 4. ESTIMATED COSTS OF TECHNICAL-GRADE ALKALI AND ALKALINE EARTH CARBONATES*

	Salt	Description	Cost,* $/kg	($/lb)
1.	Li_2CO_3	Powder, bags	2.65	(1.20)
2.	Na_2CO_3	Powder	50.06	(0.028)
3.	K_2CO_3	Granulated, purified	0.51	(0.23)
		Calcined 99% to 100% K_2CO_3	0.57	(0.26)
4.	$MgCO_3$	Powder, bags	1.17	(0.53)
5.	$CaCO_3$	Ultrafine, USP bags	0.18	(0.08)
		Natural, dry-ground, air-floated, -325 mesh, bags	0.02	(0.01)
6.	$SrCO_3$	Glass-ground, bags	0.62	(0.28)
7.	$BaCO_3$	Precipitated, bags	0.46	(0.21)
		Photo-grade, bags	0.37	(0.17)
		Electronics-grade, bags	0.37	(0.17)

* Chemical Marketing Reporter, March 16, 1981.

Table 5. CANDIDATE TECHNICAL-GRADE CARBONATE SALTS, SUPPLIERS, AND COMPOSITIONS

Supplier	Chemical Name	Grade	Typical Compositions (wt %)									Bulk Density, lb/ft^3	Melting Point, °C	Truckload Cost, $/lb
			Lithium Carbonate, Li_2CO_3											
			Li_2CO_3	Cl	H_2O	SO_4	Fe_2O_3	INS.*	CaO	Na_2CO_3				
Lithcoa	Lithium Carbonate	Fine	99.1	0.002	0.5	0.3	0.001	0.002	0.01	0.15		50	720	1.20
			Sodium Carbonate, K_2CO_3											
			Na_2CO_3	Equiv. Na_2O	Na_2SO_4	NaCl	Fe	H_2O	B	Fe_2O_3				
Stauffer	Sodium Carbonate	Regular	99.8	58.4	0.02	0.02	5 ppm						851	0.03
			Potassium Carbonate, K_2CO_3											
			K_2CO_3	Na_2CO_3	KCl	KOH	K_2SO_4	Fe	SiO_2	Pb	Hg			
Hooker Process	Potassium Carbonate	Calcined Regular	99.5	0.16	0.02	0.11	10 ppm	1 ppm	<0.1 ppm	0.5 ppm	<0.1 ppm	53	891	0.29
			Barium Carbonate, $BaCO_3$											
			$BaCO_3$	INS*	SO_3	$SrCO_3$	SiO_2	Na_2O	Fe_2O_3					
FMC	Barium Carbonate	Soft Fired	99.0	0.15	0.15	200 ppm	0.15	25 ppm				90	--	0.21

* INS. Acid Insoluble.

B83050854

- Bulk and grain boundary carburization
- Interactions with working fluids (air, helium, and sodium) or their impurities.

In addition to these chemical/thermal compatibility issues, mechanical properties of the candidate alloys were evaluated using available data to assure reliable structural compatibility for the proposed high-temperature TES applications. Properties that were evaluated in this context were —

- Stress-to-rupture at elevated temperatures
- Thermal cycling fatigue behavior
- Weldability
- Strain and thermal aging effects
- Thermal expansion coefficients between 21° and 870°C (70° and 1600°F).

Finally, factors such as materials cost, current and future availability, and ease of fabrication were also considered heavily in selecting candidate containments.

Review of the carbonate/materials corrosion literature revealed a number of papers and reports investigating alloys used in carbon-, sulfur-, and chloride-containing atmospheres in heat treatment, combustion gas scrubbing, and energy conversion applications.[7-47] Significant among the findings were —

- The establishment of the electrochemical series in molten carbonates by Ingram and Janz (Table 6).[24] It was found that only gold and platinum are sufficiently "noble" to be immune from attack, so protection of other metals [in $(Li/Na/K)_2CO_3$ ternary at 600°C] will depend on cathodic protection or on passivation.
- Potentiostatic polarization studies of Janz and Conte [in $(Li/Na/K)_2CO_3$ ternary (mp = 397°C) with CO_2 cover gas at 700°C (1292°F)][27,29] found that Types 304 and 347 SS (niobium stabilized) passivate in molten carbonates.
- Potentiostatic polarization studies of hot corrosion systems by Devereux and Owen [in molten Na_2CO_3 (mp = 858°C) with ambient air cover gas at 940°C (1724°F)][16] found that Types 304 and 316 SS and nickel exhibit abrupt reduction of current with increasing anodic potential, which also is indicative of a passivation phenomenon (potential corrosion compatibility).

Table 6. SUMMARY OF ELECTROCHEMICAL DATA IN MOLTEN CARBONATES AT 600°C (1112°F)

Metal	Electrode Potential E°, V	E(10^{-6}M), V	Oxide Pressure Log (O_2)	Oxide Precipitation pCO_2
Ba(II)	-2.90	-3.42	-56.86	+5.50
Li	-2.87	-3.91	-54.90	+6.09
Ca	-2.59	-3.11	-65.20	-2.27
K	-2.45	-3.49	-27.34	+15.0
Na	-2.43	-3.47	-35.1	+10.9
Mg	-2.41	-2.93	-60.80	-2.18
Mn	-1.38	-1.90	-38.42	-2.88
Zn	-0.89	-1.41	-31.02	-4.79
Fe(II)	-0.66	-1.18	-24.70	-4.34
Co	-0.39	-0.91	-20.88	-5.52
Ni	-0.34	-0.86	-19.16	-5.24
Pt	(+0.52)	0.00	+0.28	(-5.24)
Ag	+0.55	-0.49	+2.48	-4.50
Au	(+0.84)	+0.49	+9.4	(-4.50)

- Contrary to Grantham,[19] who suggested that up to 500°C (932°F) austenitic stainless steels are satisfactory for molten carbonate containment, but at 600°C (1120°F) nickel-based alloys are required, IGT has demonstrated the compatibility of Type 316 SS with molten carbonates (Li/K CO_3, mp = 488°C) at 650°C (1200°F) for up to 10,000 hours (in molten carbonate fuel cells) with ~32μ (~1.3 mils) corrosion in the cathodic current collector.

- Alkali aluminates, particularly the meta-aluminates, namely, $LiAlO_2$, $NaAlO_2$, and $KAlO_2$ show remarkable chemical stability in alkali carbonate systems. Because of the stability of aluminates, they have been commonly used in molten carbonate fuel cells as high surface area support materials for electrolyte matrices. The formation reaction of alkali aluminates (using α-Al_2O_3) —

$$Al_2O_3(s) + M_2CO_3(\ell) \rightleftarrows 2MAlO_2(s) + CO_2(g) \qquad (1)$$

at 727°C (1341°F) has a ΔG of -54.5 kJ/mole for $LiAlO_2$ and -14.7 kJ/mole for $NaAlO_2$ and $KAlO_2$. Because of the considerably lower free energy, the formation of $LiAlO_2$ is favored, and $LiAlO_2$ is stable over a wide range of carbonate compositions.[18,37,39-43] Thus, aluminum oxide-forming materials, with Al_2O_3 subsequently converted to alkali aluminate, should remain stable in carbonate environments.

Table 7 contains a listing of stainless steels, nickel-base alloys, superalloys, and aluminum-containing compositions, which were evaluated as candidate TES containment materials. The companies listed in Appendix B were contacted as potential suppliers of these alloys and available mechanical property, current availability, and cost data were reviewed.

From review and evaluation of the above mentioned literature data and consultations with Professor G. Janz of Rensselaer Polytechnic Institute and Professor R. A. Rapp of Ohio State University, it appeared that alloys forming Al_2O_3-rich protective films may be the preferred type of containment material for molten carbonates. The aluminum required to form these protective films can be provided either in the melted and cast alloy or by aluminized coatings. The more typical and widely available Cr_2O_3-forming alloys should be avoided if a continuous supply of oxidizing species (O_2, CO_2, H_2O, air) is maintained above the salt melt in the TES application. This is based on the fact that the protective films of $LiAlO_2$ or $NaAlO_2$ are relatively insoluble and protective when in contact with the alkali/alkaline carbonates. At 900°C, for instance, the solubility of $NaAlO_2$ was established to be only 20 molar parts per million in molten Na_2CO_3,[33] while Na_2CrO_4 is both liquid and completely soluble in Na_2CO_3 at 900°C. On the other hand, in actual TES applications as heat exchanger tubes, these alloys may face hot air or steam

7. CANDIDATE CONTAINMENT MATERIAL COMPOSITIONS

				Nb +					
58.0						0.02		7.6	W
	12.0	6.0							
	17.0	5.0			3.0	2.0			

Others

on the opposite face, and Cr_2O_3 scales are very protective against corrosion under these conditions.

Therefore, availability/cost/performance trade-offs between chromium oxide- and aluminum oxide-forming alloys need to be considered in selecting corrosion-resistant, long-term containments for specific molten carbonate TES applications. Avoidance of alloys containing significant levels of silicon, titanium, or zirconium was recommended from the standpoint of elemental solubility and acidity of those elements relative to the basicity of the carbonate melts. At the same time, alloys containing high concentrations of cobalt or chromium were avoided due to the high cost and critical nature of these elements.[48]

Contact was also made with Alon Processing Inc. (Tarentum, Pennsylvania) regarding to state-of-the-art aluminum vapor diffusion ("alonizing") techniques for providing aluminized corrosion protection layers on containment materials. In the alonizing operation, aluminum is vapor diffused into a given metal surface through a pack cementation treatment in a sealed metal retort. The depth of diffusion varies from about 3 to 15 mils, depending on the nature of the alloy and the time and temperature of the treatment. Within a given pipe length, however, the depth of diffusion is expected to be extremely uniform, and quoted to be within ± 12.7μ (0.5 mils), with a "small" pipe-to-pipe variance. The metal in the diffusion zone has an average aluminum content of about 20%, but the alloy surface layer contains about 50% aluminum. The process has found broad application for heat exchanger uses in chemical plants and petroleum refineries because of the increased resistance of aluminized steels at high temperatures to corrosion by SO_2, H_2S, and other sulfur-containing gases. Due to the nature of the process, pipe and tubing can be aluminized on the inside or the outside only or on both surfaces. In general, the process may be considered where the corrosion resistance of aluminum is desirable but its usage is restricted by its mechanical properties. Additional information and experimental literature regarding aluminum diffusion coating and cladding of metals was also reviewed and evaluated for possible application to containment and TCE materials.

Based on the evaluation of currently available corrosion literature, mechanical property data, current availability, and cost, the following "core"

group of containment materials were selected for Phase I testing with each of the reagent- and technical-grade salt mixtures listed in Table 3:

- AISI 316 SS; Fe-based (Cr_2O_3 former)
- AISI 304 SS; Fe-based (Cr_2O_3 former)
- AISI 310 SS; Fe-based (Cr_2O_3 former)
- Incoloy 800: wrought Fe-Ni-Cr-based alloy (Cr_2O_3 former)
- Inconel 600; a wrought Ni-Cr-based alloy (Cr_2O_3 former).

Figures 2 and 3 provide comparative stress-to-rupture and scaling resistance, respectively, and Figure 4 illustrates costs (relative to 304 SS) as a function of nickel plus chromium content for the five "core" alloys (from $2.36/kg for 304 SS to $26.46/kg for Inconel 600).

Aluminum oxide (Al_2O_3)-forming alloys were also investigated. Technical contacts were established at Armco Steel Corporation for obtaining samples of experimental alloys Armco 18SR and Armco 12SR. Special materials handling, preparation, and welding procedures were discussed and learned with regard to this family of alloys.

Testing of the following containment materials was performed with selected salt mixtures, depending on timely availability of samples and suitable capsule fabrication —

- Armco 18SR/Armco 12SR: Fe-Cr-Al-based sheet alloy (Al_2O_3 former)
- Kanthal A-1: Fe-Cr-Al-based cast alloy (Al_2O_3 former)
- Alonized AISI 316 or 304 SS (Al_2O_3 formers): Postponed until Phase II testing; Section 1.4 due to shut down and process scheduling delays at Alon Processing Inc.

Table 8 contains a summary of the above "core" and "supplemental" alloy compositions and costs. From the ternary phase diagram of Figure 5, it is observed that the candidate materials traverse an "approximate iso-chromium" band (12% to 25%) from 0 (for Kanthal A-1) to 75 weight percent (Inconel 600) nickel.

TCE Selection

The need for TCE materials/configurations development arises from the fact that the thermal discharge performance of a TES subsystem is controlled

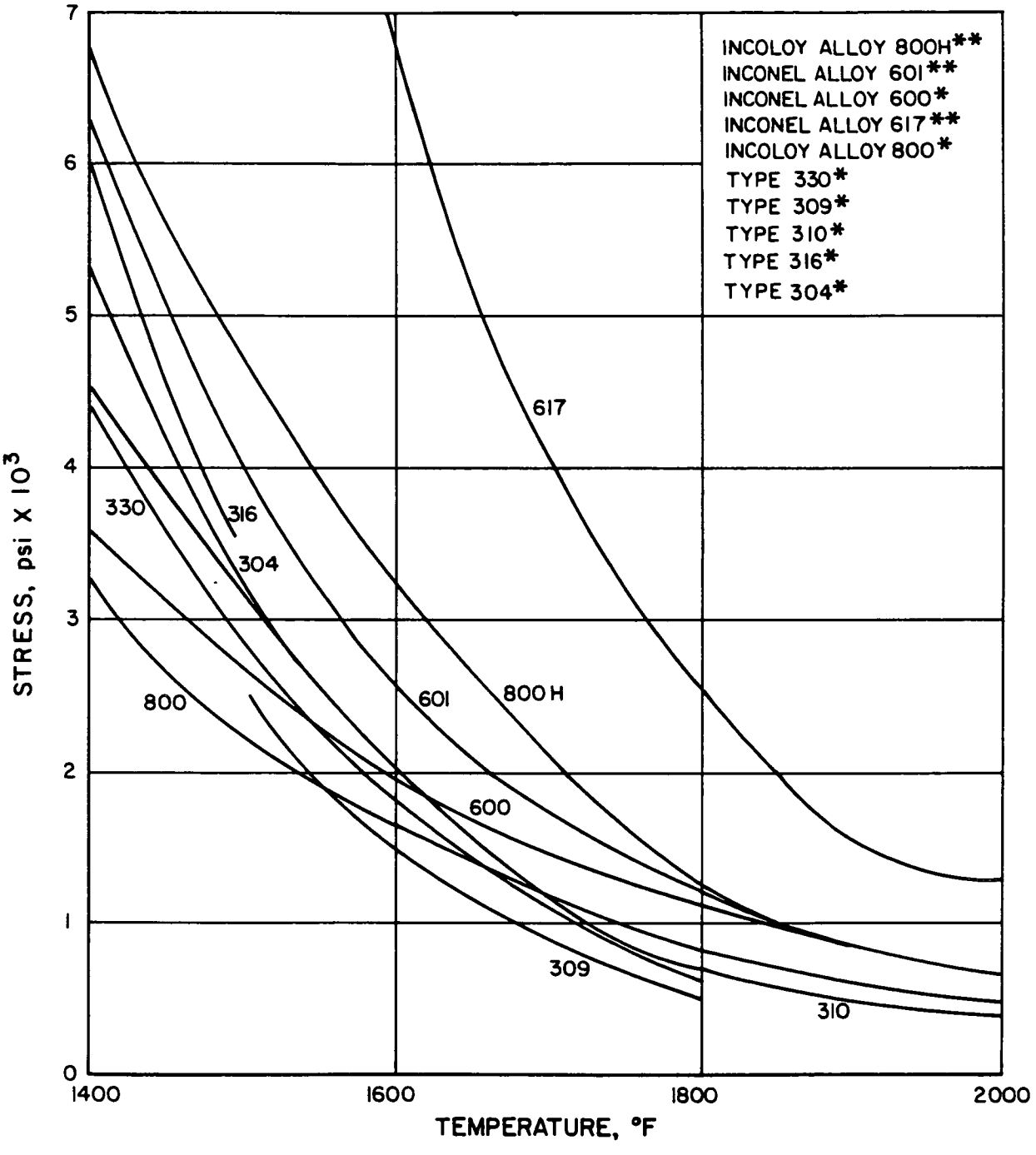

TEMPERS:

* Mill Annealed

** Solution Treated

A82071272

Figure 2. STRESS TO RUPTURE IN 10,000 HOURS

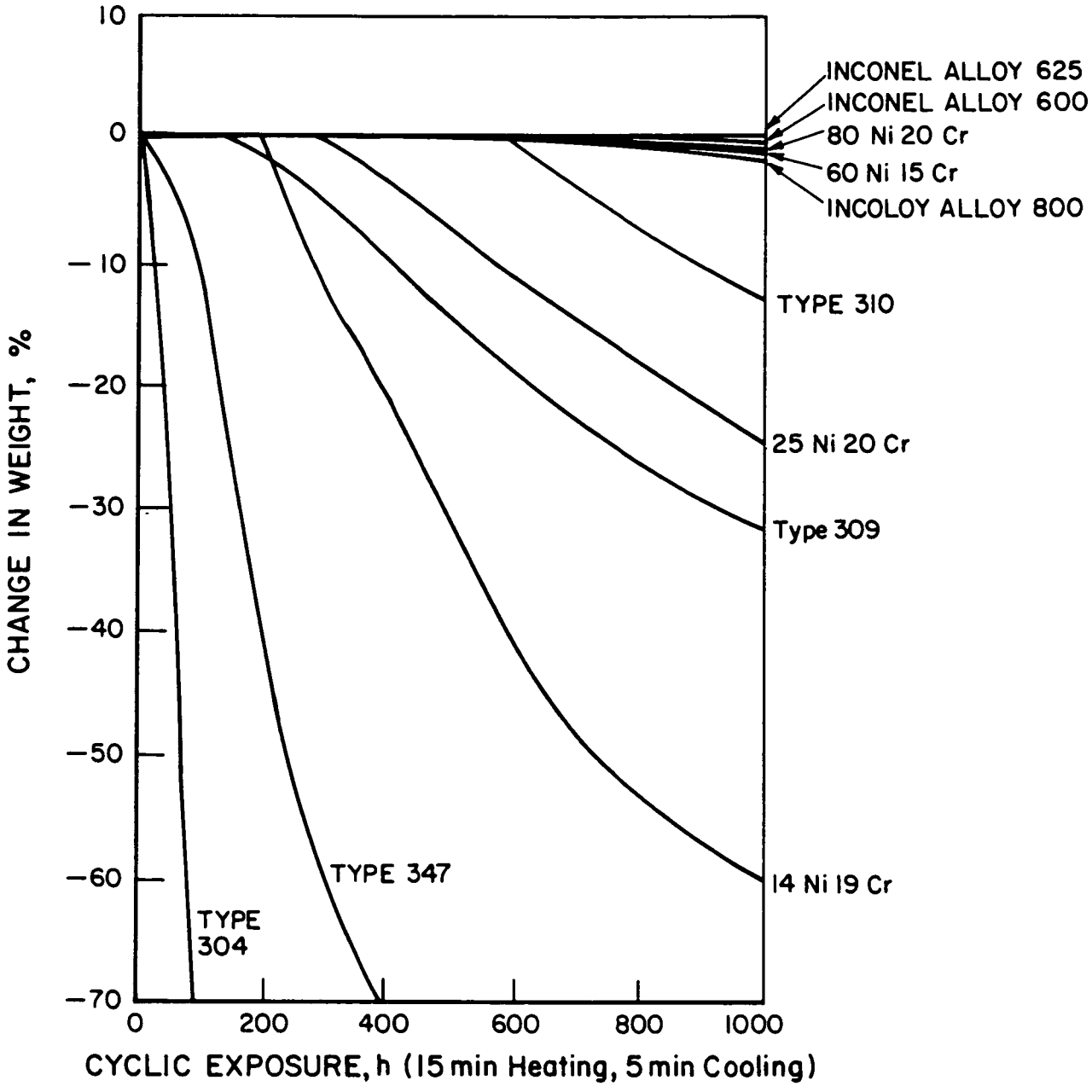

Figure 3. SCALING RESISTANCE OF CANDIDATE TES CONTAINMENT ALLOYS AT 980°C (1800°F)[24]

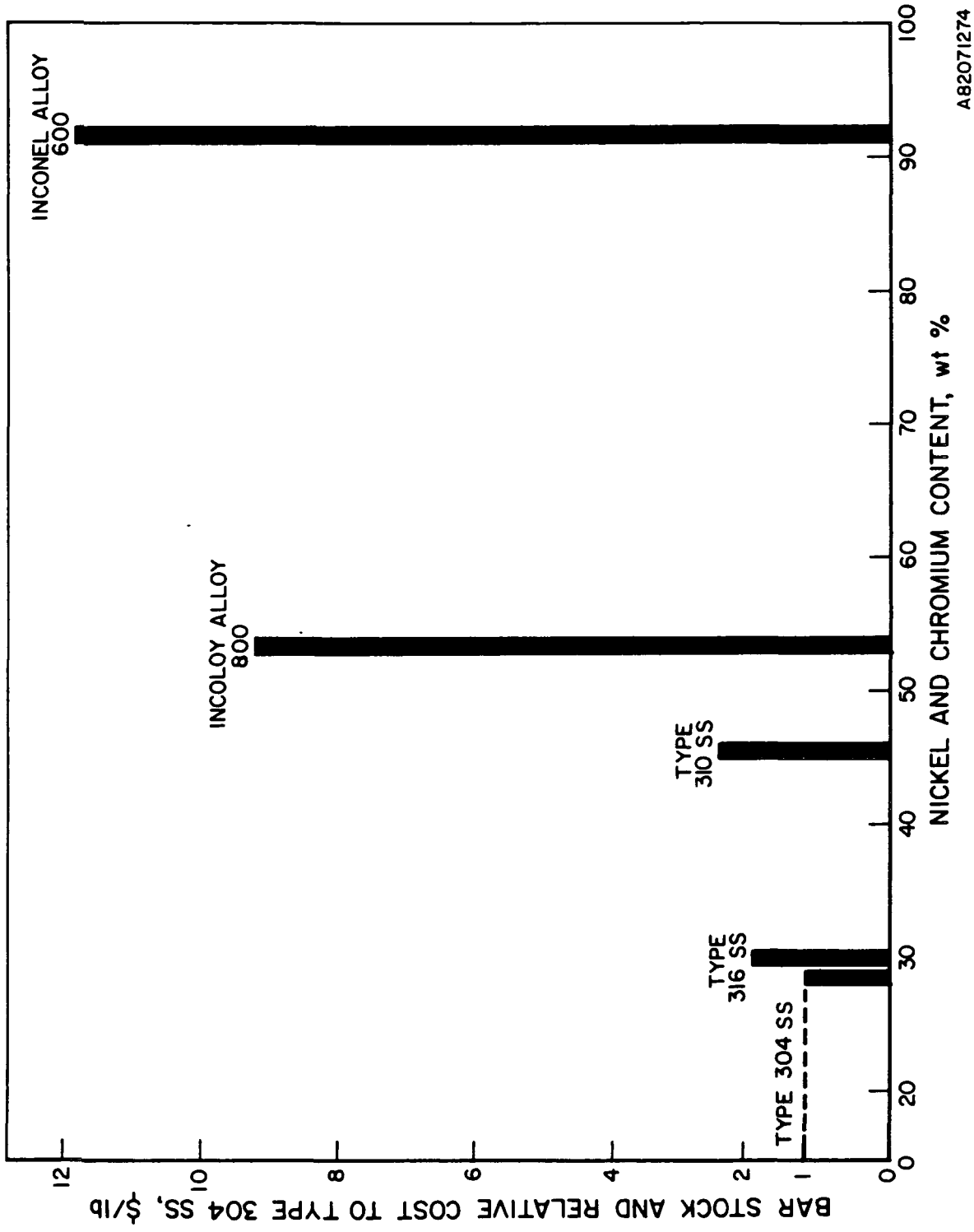

Figure 4. COST OF CANDIDATE TES CONTAINMENT ALLOYS

Table 8. CANDIDATE CONTAINMENT MATERIALS

"Core" Tests	Composition, wt %							Cost Bar,	
	Mn	Cr	Ni	Mo	Fe	Al	Cu	$/kg	($/lb)
AISI 304 SS	2.0	19.0	9.5	--	69.0	--	--	2.36	(1.07)
AISI 316 SS	2.0	17.0	12.0	2.50	60.0	--	--	4.10	(1.86)
AISI 310 SS	2.0	25.0	20.5	--	51.0	--	--	5.25	(2.38)
Incoloy 800	1.5	21.0	32.5	--	46.0	0.40	0.75	20.50	(9.30)
Inconel 600	0.5	15.5	76.0	--	8.0	--	0.20	26.46	(12.00)
Supplemental Tests									
Armco 18SR/12SR	0.15/0.20	17.5/12.0	0.3/0.2	--	79.0/85.1	1.8/1.25	--	2.27	(1.03)
Kanthal A-1	--	22.0	--	--	70.0	5.50	--	11.90	(5.40)
Alonized AISI 316 and 304 SS									

B83050855

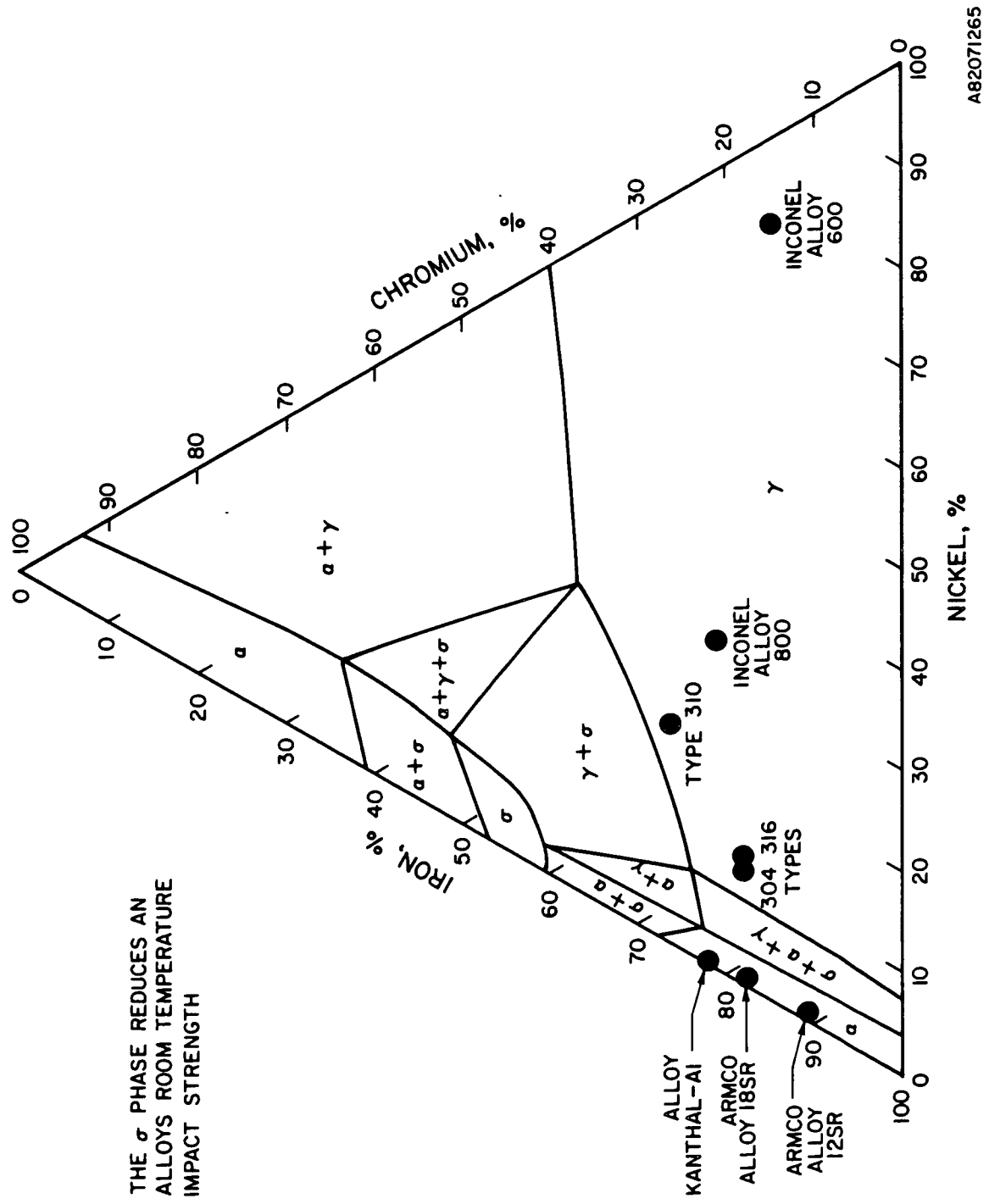

Figure 5. CANDIDATE TES HX MATERIALS REPRESENTED ON Fe-Ni-Cr TERNARY PHASE DIAGRAM [649°C (1200°F)]

by the rate at which the latent heat-of-fusion released at the solid/liquid interface is transported to the heat exchanger surface (typically a tube) through the growing layer of solid salt. Thus, TCE materials selection criteria include thermal conductivity, expected chemical compatibility with the carbonate environment, cost, availability, and ease of fabrication into a desirable TCE configuration.

A listing of potential TCE materials is provided in Table 9. Although aluminum is very attractive as a TCE material because of its high thermal conductivity of 220 W/m-K (127 Btu/h-ft-°F) (approximately 100 times that of solid carbonates and 10 times that of austenitic stainless steels), it cannot be used for the 704° to 871°C (1300° to 1600°F) solar thermal TES applications because of its 660°C (1220°F) melting point. Copper also has a very high thermal conductivity of 178 Btu/h-ft-°F and a reasonable melting point (1083°C; 1981°F) but is expected to oxidize in the carbonate TES environments with air cover gases. Although iron- and nickel-based materials are compatible at these temperatures, they are more costly and have much lower thermal conductivities than aluminum and copper, greatly reducing their attractiveness as TCE materials. Pyrolytic graphite is also reported to have a high thermal conductivity [208 W/m-K (120 Btu/h-ft-°F)], but again oxidation is expected in a high-temperature carbonate environment. Additionally, TCE concepts in the form of specially configured metal alloys or thin corrosion-resistant coatings applied to high thermal conductivity substrate materials were considered for possible carbonate TES applications.

The testing of a 95 volume percent porous, open-celled structure of continuous aluminum TCE (brand named Duocel, Energy Research and Generation, Inc.) was performed in a $(Li\text{-}Na\text{-}K)_2CO_3$ ternary eutectic (mp = 397°C) for over 4000 hours at 450°C (840°F) under Contract No. NAS3-20806. Use of this TCE configuration resulted in a 45% increase in heat conduction through the solid salt to the air working fluid in lab-scale testing.[4]

Metal foam products of the type above are generally available in open- and closed-cell configurations. Because closed-cell foams lack the permeability required for PCM heat transfer applications, only open-cell structures were considered here. In general, open-cell foams may be prepared by electroplating, powder metallurgy, or casting.

Table 9. POTENTIAL TCE MATERIALS

Material	Melting Point °C	Melting Point (°F)	Thermal Conductivity at 500°C (932°F) W/m-K	Thermal Conductivity at 500°C (932°F) Btu/hr-ft-°F	Heat Capacity Room Temp J/kg-K	Heat Capacity Room Temp Btu/lb-°F	Materials Cost* $/kg	Materials Cost* $/lb	Materials Cost* $/m³	Materials Cost* $/ft³
Aluminum	660	(1220)	220	127	921	0.22	1.74	0.79	4,732	134
Copper	1083	(1981)	308	178	385	0.09	1.65	0.75	14,726	417
Iron	1536	(2797)	38	22	461	0.11	3.02	1.37	23,766	673
Molybdenum	2610	(4730)	116	67	255	0.06	9.70	4.40	99,128	2807
Nickel	1453	(2647)	57	33	502	0.12	4.76	2.16	42,448	1202
316 Stainless Steel	1370	(2478)	21	12	502	0.12	2.80	1.27	22,531	638
ATJ Graphite	sublimes		78	45	837	0.20	9.85	4.47	22,107	626
Pyrolytic Graphite	sublimes		208**	120**	837	0.20	--	--	--	--
Silicon Carbide	2700	(4892)	87	50	836	0.20	--	--	--	--
CS Graphite	sublimes		76	44	837	0.20	1.10	0.50	2,401	68

* Costs based on 100% of theoretical density.

** a-b Plane.

B80020284

The first method is limited to relatively large pore sizes and metals that can be electroplated; such as copper, nickel, cobalt, or chromium. The powder metallurgical technique is limited in dimensions by the size of the high-temperature vacuum furnace used in the sintering process. Powder metallurgy is, however, able to prepare foams from a wide variety of metals, including copper, nickel, tungsten, molybdenum, tantalum, and superalloys. Also, foam samples with very small pore sizes down to 250μm (10 mil) can be prepared by this method.

Both the electroplating and powder metallurgy methods start out with a matrix of organic foam, which is burned out during the process leaving hollow ligaments of triangular shape as connecting members. Depending on the porosity of the ligament walls, the interior volume of the ligaments may also be filled with PCM material. The casting process results in slightly more expensive solid ligament foam and is currently limited to metals with low melting points, such as aluminum or magnesium.

A number of companies were contacted as suppliers of high-conductivity porous graphite (pyrolytic and Grade ATJ), pyrolytic boron nitride, copper, and nickel foam and reticulated mesh products. Their product line specifications were reviewed and samples received. These companies appear in Appendix C.

Consultations with Professor Rapp further confirmed the narrowed solar thermal (700° to 900°C) TCE selection to the testing of high-conductivity copper and graphite products in a capsule of molten carbonate with an inert gas environment maintained above the melt.

A high-porosity [96% porosity, 25.4 pores per cm (10 pores per inch)], thick ligament [508μ (~20 mils)] powder metallurgy copper matrix from Rocket Research Inc. was chosen as the preferred test sample due to the superior strength of its thick ligaments. Thick wall [760μ (~30 mils)] copper tubing [0.31 cm (0.125 in.) OD] was also obtained to evaluate both solid and reticulated versions of copper as a TCE material.

Pyrolytic (PG) and ATJ graphite samples from Union Carbide were also selected for simultaneous (PG and ATJ) carbonate compatibility testing.

1.2. Test Matrix

The matrix of test variables for the materials compatibility screening was developed on the basis of the general matrix pattern shown in Table 10. The overall matrix was to include six salt compositions, both reagent- and technical-grade salt components, at least five containment materials, two TCE materials, and a variable related to containment fabrication processing effects.

The synthesis of this salt, containment/HX, and TCE materials selection subtasks resulted in the test matrix of Table 10. The 70 materials combinations represented by an "X" indicate the "core" matrix of capsules that were tested. The five main containment materials were tested with each salt mixture and grade, while copper and graphite were screened only with the technical grade of each of the salt mixtures. Supplemental testing was also conducted on Armco 18SR/12SR capsules with Kanthal A-1 specimens inside.

1.3. Compatibility Screening Tests

Introduction

After identification and procurement of candidate salt, containment/HX, and TCE materials, the materials combinations were subjected to the initial phase of compatibility screening tests. These tests were performed in closed, heli-arc welded capsules of the candidate containment materials containing the reagent- or technical-grade salts plus, in some cases, other candidate containment materials or TCE materials coupons.

We conducted as many compatibility screening tests as materials availability deemed possible in sealed containment metal capsules, based on the observations made during high-temperature salt testing under NAS3-20806.[4] Above 650°C (1200°F), it is advantageous to test salts in closed containers rather than open aluminum oxide crucibles in order to —

- Prevent salt creepage and resultant cross-contamination between salts at the high test temperatures being investigated
- Eliminate a continuous supply of oxidizing species or provide an inert (non-oxidizing) environment to minimize resultant containment/TCE corrosion
- Eliminate the experimental difficulties associated with possible cracking failure of alumina materials during thermal cycling from high temperature.

Table 10. SALT/CONTAINMENT AND HX/TCE MATERIALS CORE SCREENING TEST MATRIX

			Containment Materials					Supplemental	TCE Materials	
			1	2	3	4	5	6	1	2
No.	Salt System Composition, wt %	Grade	304 SS	316 SS	310 SS	Inconel 600	Incoloy 800	Armco 18SR/12SR (Kanthal A-1 inside)	Graphite	Copper
1	52.2 $BaCO_3$-41.8 Na_2CO_3	Reagent	X	X	X	X	X			
2	52.2 $BaCO_3$-41.8 Na_2CO_3	Technical	X	X	X	X	X	X	X*	X*
3	50.0 Na_2CO_3-50.0 K_2CO_3	Reagent	X	X	X	X	X			
4	50.0 Na_2CO_3-50.0 K_2CO_3	Technical	X	X	X	X	X	X	X*	X*
5	Li_2CO_3	Reagent	X	X	X	X	X			
6	Li_2CO_3	Technical	X	X	X	X	X	X	X*	X*
7	81.3 Na_2CO_3-18.7 K_2CO_3	Reagent	X	X	X	X	X			
8	81.3 N_2CO_3-18.7 K_2CO_3	Technical	X	X	X	X	X	X		
9	Na_2CO_3	Reagent	X	X	X	X	X			
10	Na_2CO_3	Technical	X	X	X	X	X	X	X**	X**
11	K_2CO_3	Reagent	X	X	X	X	X			
12	K_2CO_3	Technical	X	X	X	X	X		X**	X**

* In 304 SS capsule.

** In Inconel 600 capsule.

B83050856

Figure 6 schematically summarizes the general design and fabrication of the test capsules. Depending on availability of candidate material tubing, the capsules were nominally 2.54 cm (1 in.) in outer diameter (OD) x 12.7 cm (5 in.) long.

Experimental Test Components: Salt/Containment/TCE Materials Preparation, Testing Procedures, and Data Collection

Salt Preparation

All reagent- and technical-grade carbonate salt mixtures underwent similar pretest preparation processes and preliminary evaluations as follows:

- Weighing, mixing in a Norton Ball Mixer and final milling in a Sweco vibratory mill to -50 mesh particle size [<300μ (11.8 mils)]
- Mechanical cold-pressing of the salt mixtures into cylindrical pellets with the following nominal characteristics —
  - Height: 1.8 to 2.4 cm (0.7 to 0.93 in.)
  - Diameter: 2.1 cm (0.8125 in.)
  - Mass: 8 to 15 g (0.02 to 0.03 lb)
  - Density: 65% to 75% of theoretical
- Individual volume change-on-fusion experiments and calculations to establish salt filling level in capsules and capsule surface/salt volume ratios (to result in a final welded capsule ~50% to 70% filled with molten salt).

Cognizance of the total water content of these cold-pressed pellets is important from two operational standpoints:

- Molten carbonate physical chemistry; possible hydroxide formation in the presence of $H_2O(g)$ —

$$M_2CO_3(\ell) + H_2O(g) \rightleftarrows 2MOH(\ell) + CO_2(g) \quad (2)$$

with the hydrolysis constant, $K_h = \dfrac{X^2_{MOH} P_{CO_2}}{X_{M_2CO_3} P_{H_2O}}$ (3)

- Gas-phase (water vapor) pressure buildup in the gas phase of the welded test capsules.

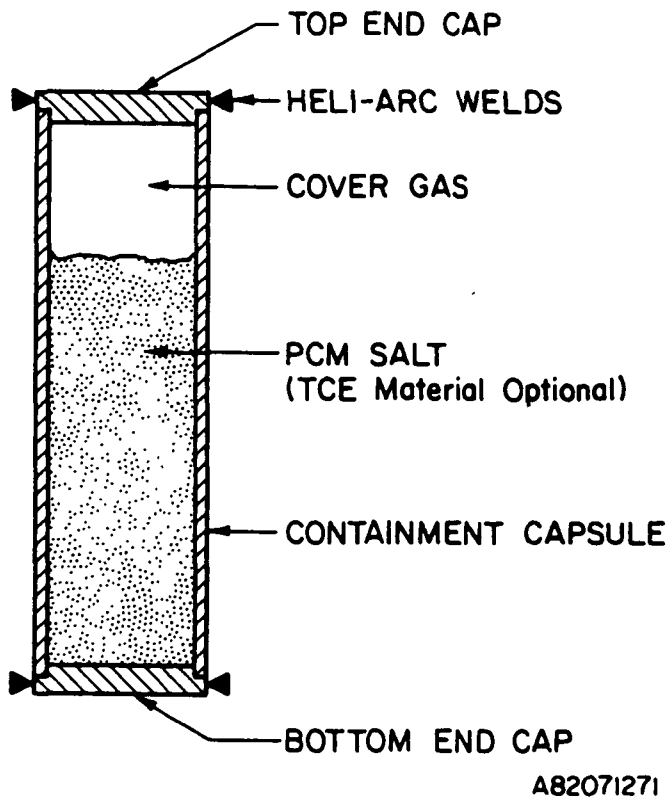

Figure 6. SCHEMATIC DIAGRAM OF SALT/CONTAINMENT/TCE MATERIAL COMPATIBILITY CAPSULE

In view of these considerations, further safeguards were taken to yield reliable compatibility data —

- Immediately after pressing, all pellets were separated and stored in "Whirl-Pak" pre-sealed, surgical-type plastic specimen bags with one "Mini-Pak" indicating a silica-gel desiccant package inside a 14% relative humidity dry-room.

- Gravimetric water content analyses of the "as-pressed" dry-room stored pellets appear in Table 11. The test was conducted by weight loss after 4 hours at 150°C (at this temperature, all unbound water and hydrates will evolve).

  — As one can observe, pure K_2CO_3 and K_2CO_3-containing compositions appear to be the most hygroscopic.

- Of these salts, any one that possessed 0.4 weight percent H_2O or more was dehydrated for 4 hours at 150°C within 24 hours of actual capsule loading, cooled in a desiccator, and again placed in "Whirl-Pak" specimen bag with a desiccant package.

Containment/HX Materials Preparation

Consultations with numerous materials fabricators and distributors revealed availability and delivery constraints that eventually necessitated the use of three general capsule designs.

Testing of AISI Type 304 and 316 SS was performed in capsules of the following specifications (Figure 7):

- Standard 1.9 cm (0.75 in.), Schedule 40 welded threaded-pipe nipples and end caps

  — Nipple ID = 2.12 cm (0.834 in.)

  — Nipple OD = 2.67 cm (1.05 in.)

  — Nominal wall thickness = 0.287 cm (0.113 in.)

  — Nipple height = 11.43 cm (4.5 in.)

  — End-cap wall thickness (excluding thread) ≈ 0.254 cm (0.10 in.)

  — Standpipe threads = 6.3 per centimeter (16 per in.)

  — Final capsule height ≈ 13.7 cm (5.4 in.).

Testing of AISI Type 310 SS, Incoloy 800, and Inconel 600 was conducted in machined capsule bodies and end caps as follows (Figure 8):

Table 11. MEASURED WATER CONTENT (Bound and Unbound) OF "AS-PRESSED" CARBONATE PELLETS

No.	Salt System Composition, wt %	Grade	H_2O, %*	Dehydrate for 4 h at 150°C**
1	52.2 $BaCO_3$-41.8 Na_2CO_3	Reagent	0.19	
2	52.2 $BaCO_3$-41.8 Na_2CO_3	Technical	0.25	
3	50.0 Na_2CO_3-50.0 K_2CO_3	Reagent	1.66	X
4	50.0 Na_2CO_3-50.0 K_2CO_3	Technical	4.39	X
5	Li_2CO_3	Reagent	0.04	
6	Li_2CO_3	Technical	0.05	
7	81.3 Na_2CO_3-18.7 K_2CO_3	Reagent	0.44	X
8	81.3 Na_2CO_3-18.7 K_2CO_3	Technical	1.48	X
9	Na_2CO_3	Reagent	0.05	
10	Na_2CO_3	Technical	0.05	
11	K_2CO_3	Reagent	2.44	X
12	K_2CO_3	Technical	2.95	X

* H_2O % = % weight loss after 4 h at 150°C.

** Dehydrate 4 h at 150°C within 24 h of capsule loading.

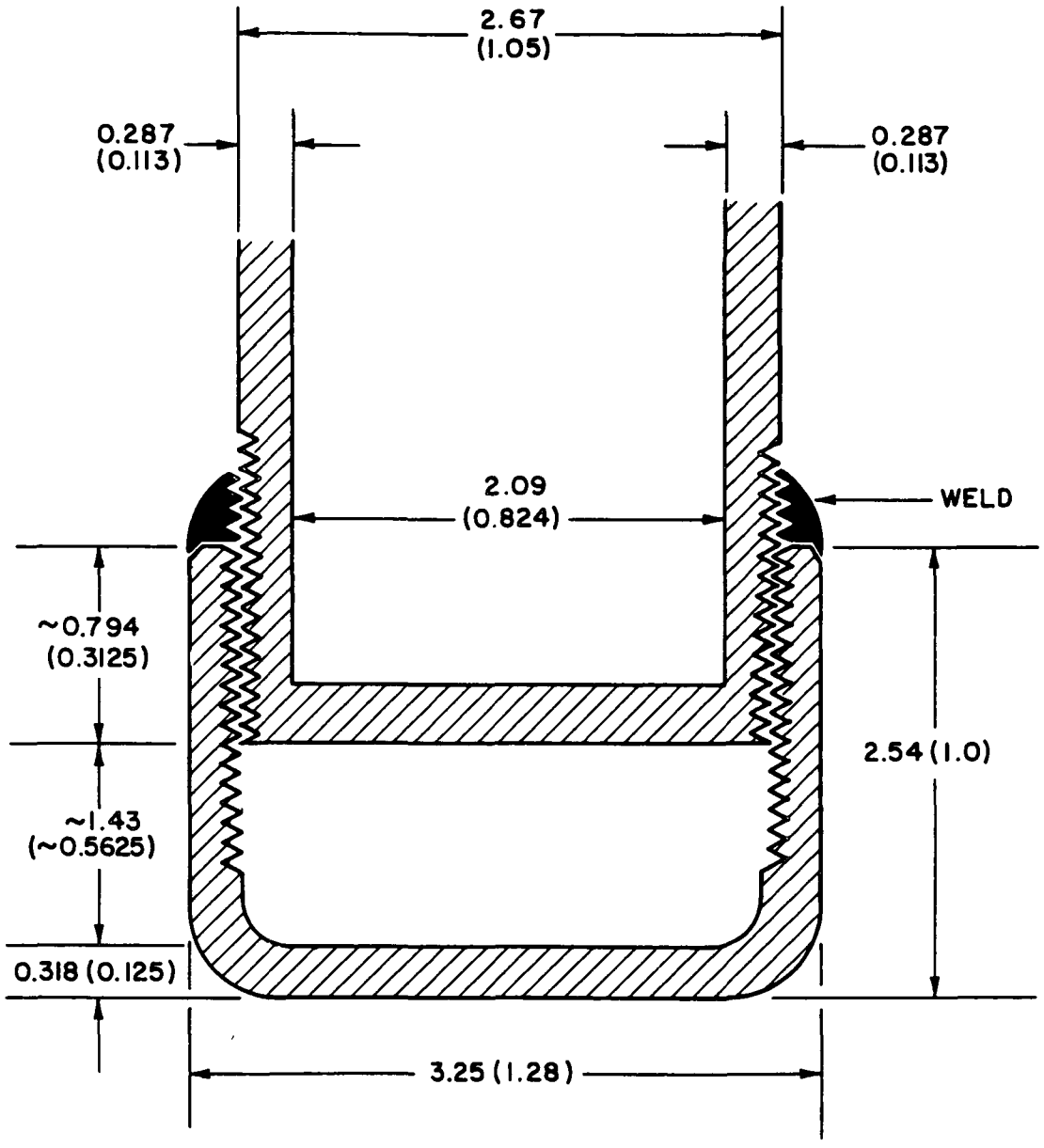

Figure 7. THREADED STANDARD NIPPLE AND END-CAP CAPSULE DESIGN WELD AREA CROSS SECTION (Used with 304 SS and 316 SS)

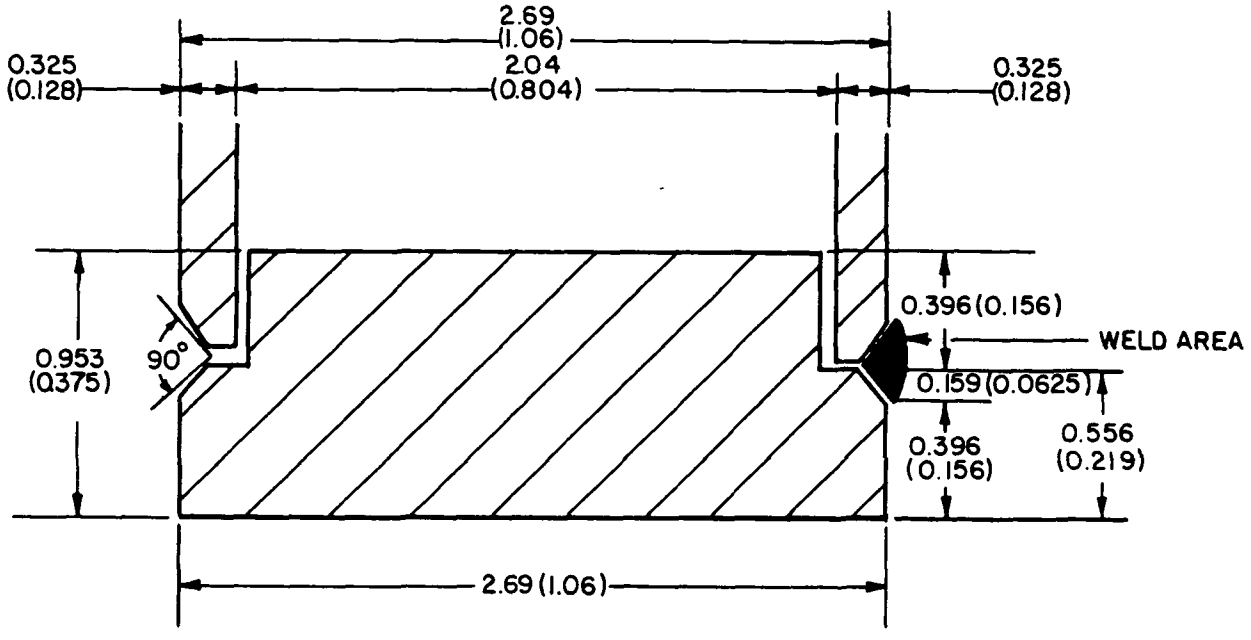

NOTE: ALL DIMENSIONS IN CENTIMETERS (Inches).

A82071287

Figure 8. MACHINED CAPSULE AND END-CAP DESIGN WELD AREA CROSS SECTION (Used With 310 SS, Incoloy 800, and Inconel 600)

- Standard 1.9 cm (0.75 in.), Schedule 40 seamless pipe (for machining capsule body) and bar stock (for machining end caps, as shown in Figure 8)
  - Pipe ID = 2.09 cm (0.824 in.)
  - Pipe OD = 2.67 cm (1.05 in.)
  - Nominal wall thickness = 0.287 cm (0.113 in.)
  - Bar stock diameter = 2.86 cm (1.125 in.)
  - Final capsule height = 11.43 cm (4.5 in.).

In addition, Armco 18SR/12SR samples were machined into test capsules according to the following specifications (Figure 9):

- Capsule body: Armco 12SR, 3.81 cm (1.5 in.) T.I.G. welded tubing
  - Tube ID = 3.48 cm (1.37 in.)
  - Tube OD = 3.81 cm (1.5 in.)
  - Nominal wall thickness = 0.165 cm (0.065 in.)
- Capsule end cap: Armco 18SR, machined from 0.10 cm (0.040 in.)-thick plate then fusion welded to Armco 12SR capsule body (Figure 9).

Prior to batch fabrication/loading/welding of the containment capsules, a preliminary pretest analysis was conducted to evaluate and confirm unaffected capsule design and weld characteristics.

A 304 SS capsule (representative of the nipple/end cap design) and Inconel 600 (representative of the machined capsule/end cap design) were heli-arc welded (308L SS and I-82 filler metal, respectively) and sectioned in the weld area for both capsule types. (Figures 7 and 8, respectively, illustrate the basic cross-sectional shape, dimensions, and weld areas of these designs.) Figures 10 and 11, respectively, show these weld areas after sectioning and metallographic examination. The 304 SS design weld was found to (advantageously) completely penetrate the base metal along ~80 mils of the capsule ID. The Inconel 600 capsule's weld penetrated through ~50% of the capsule wall thickness of 0.287 cm (0.113 in.). The higher magnification photograph of the sample (Figure 12) shows the three-part interface between the relatively columnar weld metal (left), the Inconel 600 end cap (machined from solid bar stock — bottom), and capsule wall (top right). The weld appears to be sound, with no carbide precipitation in the joining metals. It

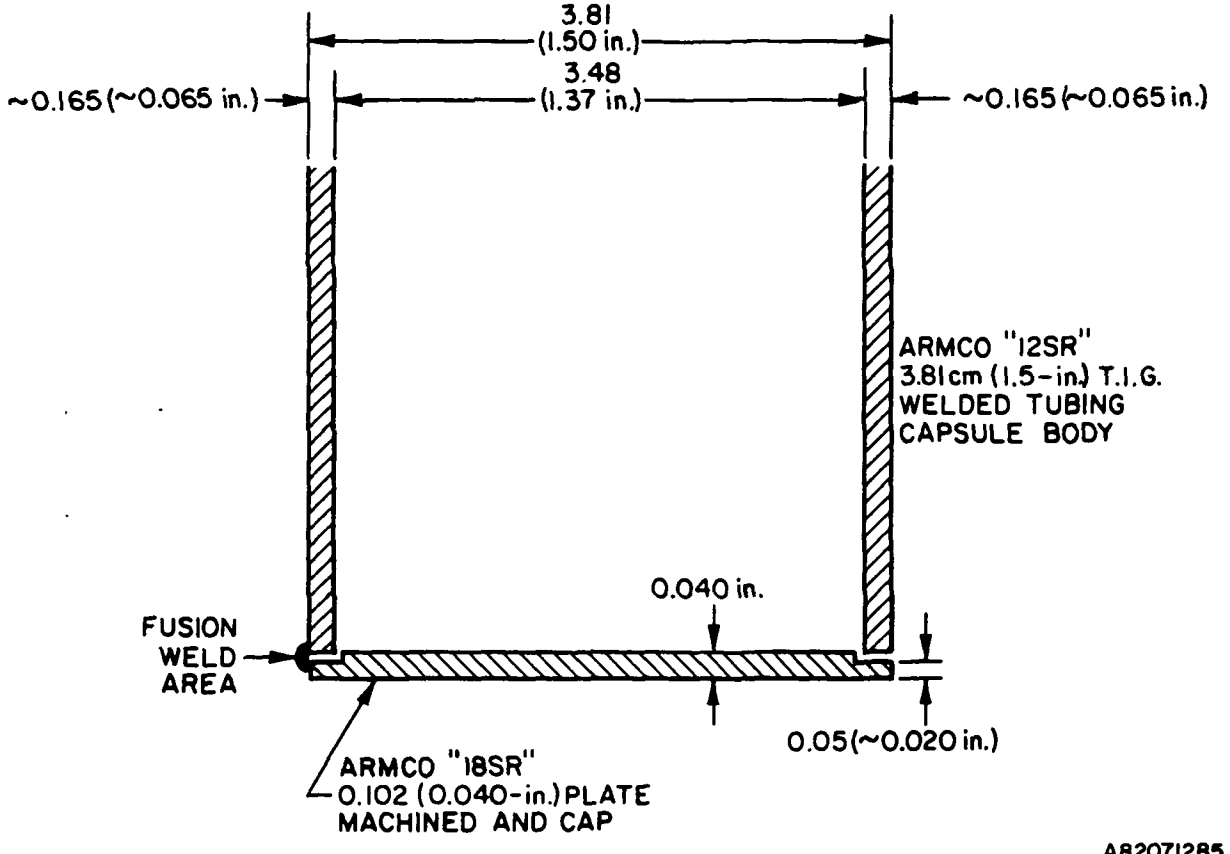

Figure 9. MACHINED ARMCO 12SR CAPSULE BODY/ARMCO 18SR END-CAP DESIGN WELD AREA CROSS SECTION (TIG Fusion Weld)

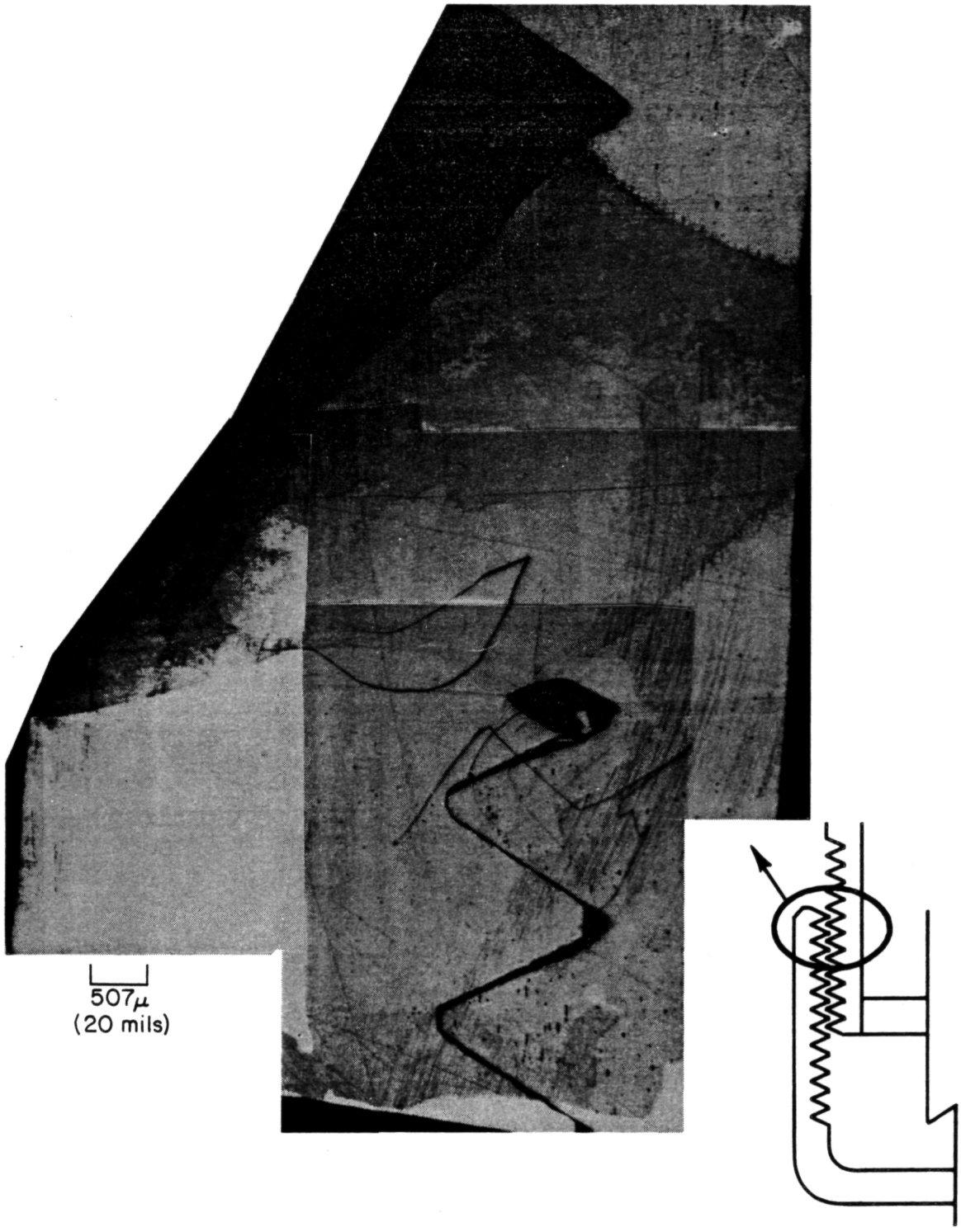

Figure 10. PRETEST SECTION OF THREADED NIPPLE AND END-CAP CAPSULE WELD AREA (25X, Etchant: Electrolytic, 10% Oxalic Acid)

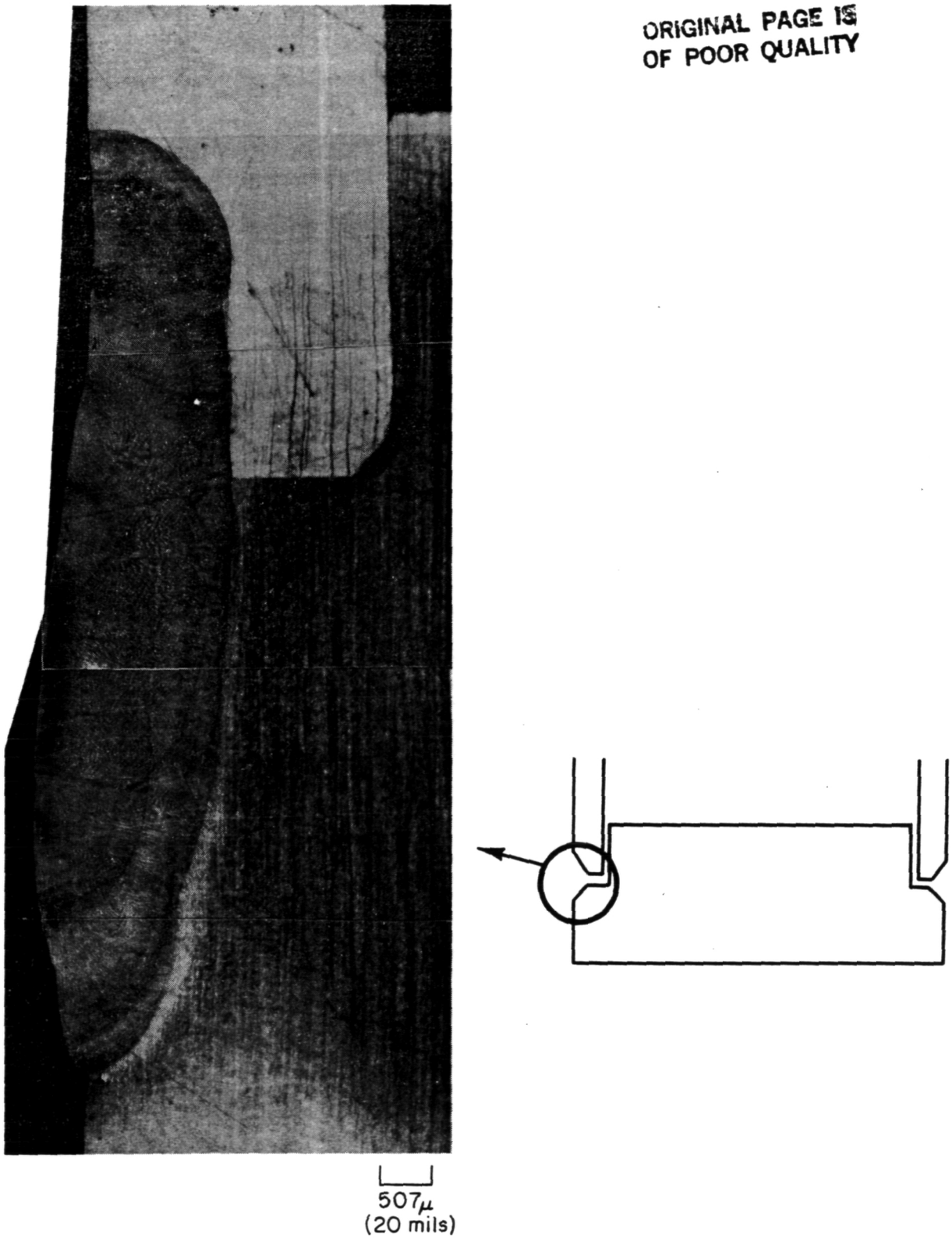

Figure 11. PRETEST SECTION OF MACHINED CAPSULE AND END-CAP DESIGN WELD AREA (Inconel 600) (25X, Etchant: Electrolytic, 10% Oxalic Acid)

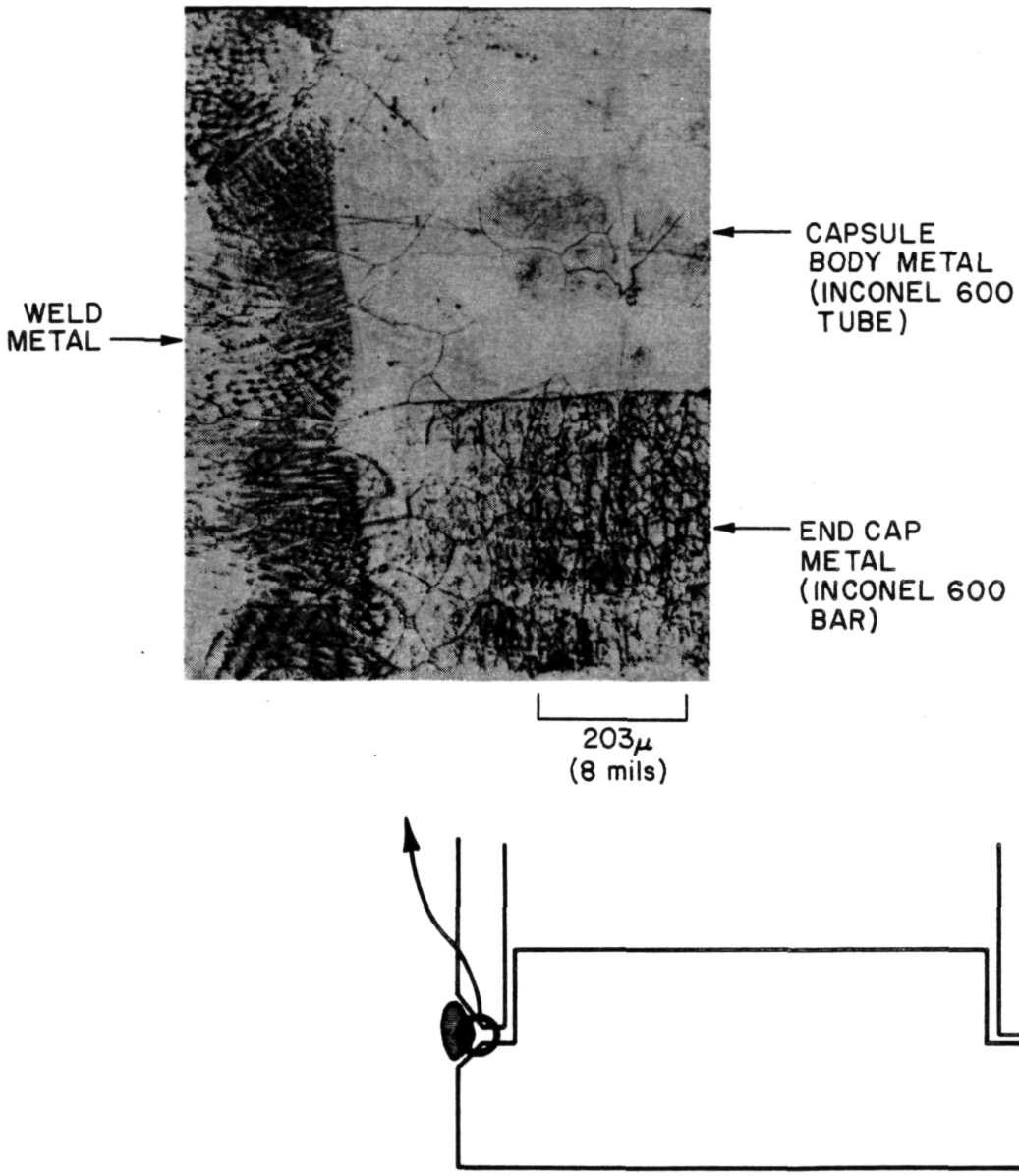

Figure 12. HIGHER MAGNIFICATION MICROGRAPH OF THE WELD/END-CAP/ CAPSULE INTERFACE OF FIGURE 11 (125X, Etchant: Electrolytic, Oxalic Acid)

was decided to maintain longer metal melting times when welding this design capsule, so as to result in a 70% weld penetration.

Prior to salt loading or initial welding, all TES test capsule components were cleaned and ultrasonically degreased in a 50% toluene/50% methanol solution and handled with white-gloves during loading and welding.

Typical final test capsule preparation/fabrication procedures entailed the following steps:

- Salt preparation
- Capsule machining (one end cap drilled for final weld pressure relief)
- Cleaning
- Degreasing (ultrasonically in a 50% toluene/50% methanol solution)
- Initial capsule welding (leaving one end open)
- Salt pellet dehydration
- Salt pellet loading (and other containment/TCE sample loading)
- Final capsule welding, cooling, then pressure relief hole weld-filling (in air or 100% argon in glove box)
- X-ray inspection at 0° and 90°C
  - Weld inspection criterion; Section VIII of the ASME Boiler and Pressure Vessel Code[50]
- Installation into compatibility test furnace.

The photographs of Figures 13 and 14 illustrate the final fabricated form of the nipple-and-end-cap and machined capsule body designs, respectively.

TCE Preparation

As noted above, copper (both as a reticulated matrix and a solid form) and high-conductivity graphite (pyrolytic and ATJ) were selected for compatibility testing in the 704° to 871°C (1300° to 1600°F) solar thermal temperature range.

Prior to capsule loading, each sample was stored in a clean environment dry room with 14% relative humidity. For the low and medium range temperature tests (750° and 850°C, respectively) samples of copper (solid and reticulated)

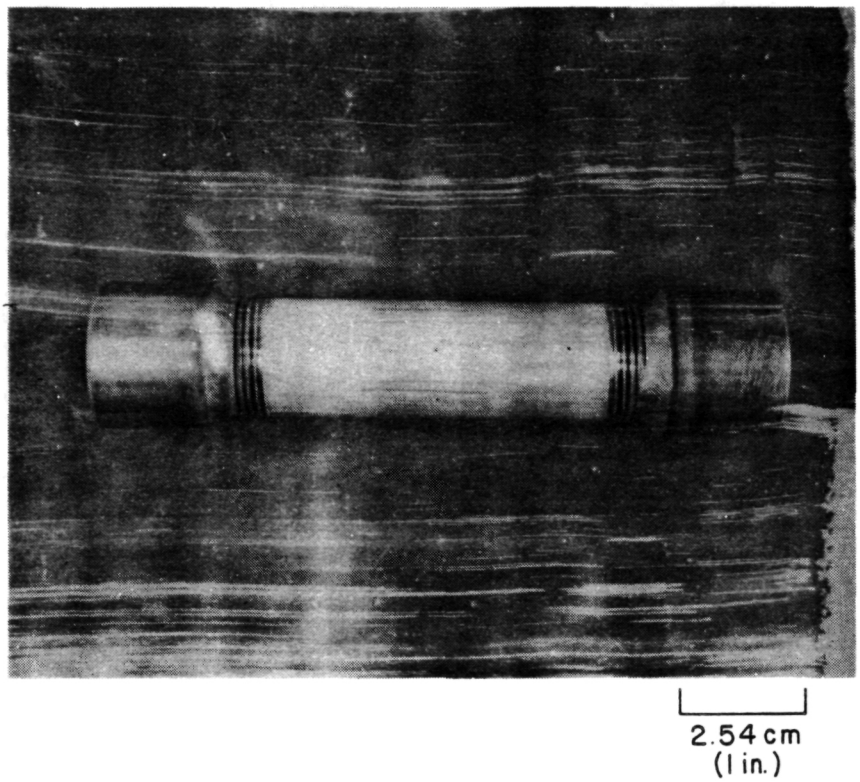

Figure 13. TYPICAL FINAL-WELDED DESIGN FOR 304 SS AND 316 SS

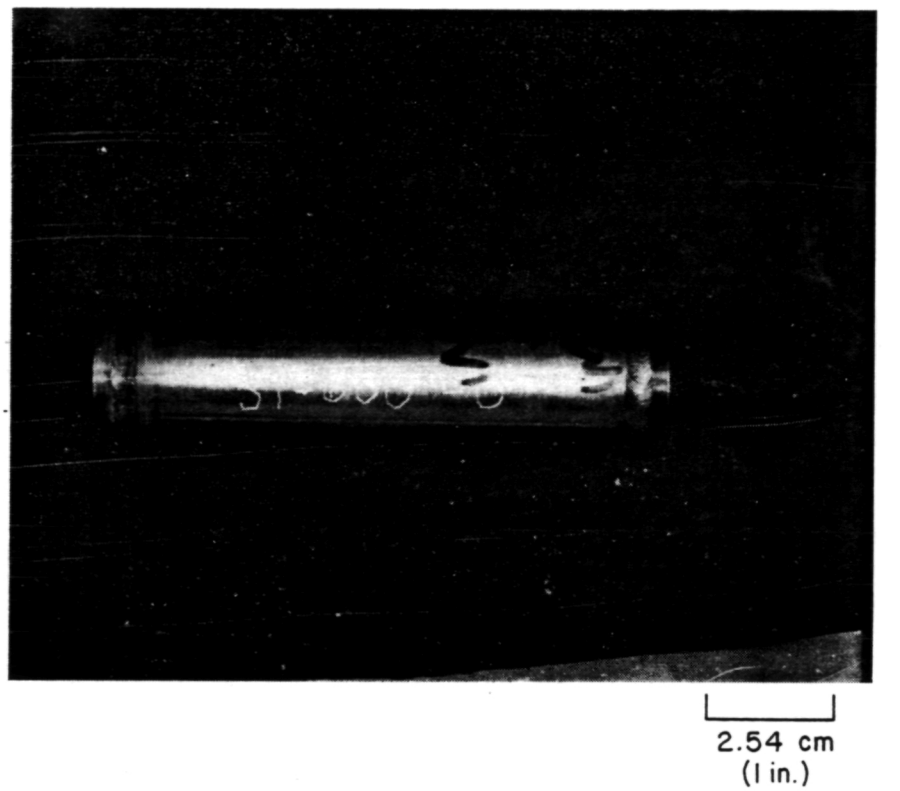

Figure 14. TYPICAL FINAL-WELDED TEST CAPSULE DESIGN FOR 310 SS, INCOLOY 800, AND INCONEL 600

and graphite (P.G. and ATJ) were loaded into individual type 304 SS capsules containing technical grades of —

- 52.2 wt % $BaCO_3$-44.8 wt % Na_2CO_3 (tested at 750°C)
- 50.0 wt % Na_2CO_3-50.0 wt % K_2CO_3 (tested at 750°C)
- Li_2CO_3 (tested at 850°C).

For the highest test temperature (~920°C), samples of copper and graphite were loaded into individual Inconel 600 capsules containing technical grades of Na_2CO_3 and K_2CO_3.

All of these TCE-oriented test capsules were then final welded in a glove box, evacuated of air then back-filled with 100% argon and welded. The welded capsules were then positioned in their respective furnaces for the compatibility screening tests.

Testing Procedures and Data Collection

To facilitate the materials compatibility testing, three high-temperature, box-type furnaces (Blue-M, Stabil-Glow) were employed to bracket the solar thermal application range of 704° to 870°C (1300° to 1600°F). The furnaces possessed a continuous service operating range to 1093°C (2000°F) and an intermittent regime to 1204°C (2200°F) (with Modella Heating Elements, 1316°C). Temperature was regulated through solid-state Honeywell Dialatrol controllers with adjustable full-time proportioning, yielding a calibrated temperature accuracy of approximately ±2%.

Actual testing during Phase I was conducted at three temperature levels — 750°C (1382°F), 850°C (1562°F), and 950°C (1742°F) — thereby dividing the salt matrix into three parts. Each salt was thus maintained at 50° to 130°C (90° to 234°F) above its reported melting point during the corrosion tests (Table 12).

The compatibility capsules were positioned in the furnaces as illustrated in Figure 15. Each capsule was placed vertically into individually drilled 3.81 cm (1.5 in.) deep holes in a bed of 7.62 cm (3 in.) thick firebrick. This was to provide vertical support and a porous firebrick capsule-to-capsule barrier to prevent creepage of salt into neighboring test containments (and heating elements) in the event of a leak. Initial capsule furnace position installations were also referenced with the 0° X-ray angle to facilitate post-

Table 12. FURNACE TESTING TEMPERATURE LEVELS

No.	Salt System Composition, wt %	Grade	Melting Point °C	Melting Point °F
	Furnace I 750°C (1382°F)			
1	52.2 $BaCO_3$-41.8 Na_2CO_3	Reagent	686	1267
2	52.2 $BaCO_3$-41.8 Na_2CO_3	Technical	686	1267
3	50.0 Na_2CO_3-50.0 K_2CO_3	Reagent	710	1310
4	50.0 Na_2CO-50.0 K_2CO_3	Technical	710	1310
	Furnace II 850°C (1562°F)			
5	Li_2CO_3	Reagent	723	1333
6	Li_2CO_3	Technical	723	1333
7	81.3 Na_2CO_3-18.7 K_2CO_3	Reagent	737-790	1360-1454
8	81.3 Na_2CO_3-18.7 K_2CO_3	Technical	737-790	1360-1454
	Furnace III 950°C in Phase I, 910°C in Phase II			
9	Na_2CO_3	Reagent	858	1576
10	Na_2CO_3	Technical	858	1576
11	K_2CO_3	Reagent	898	1648
12	K_2CO_3	Technical	898	1648

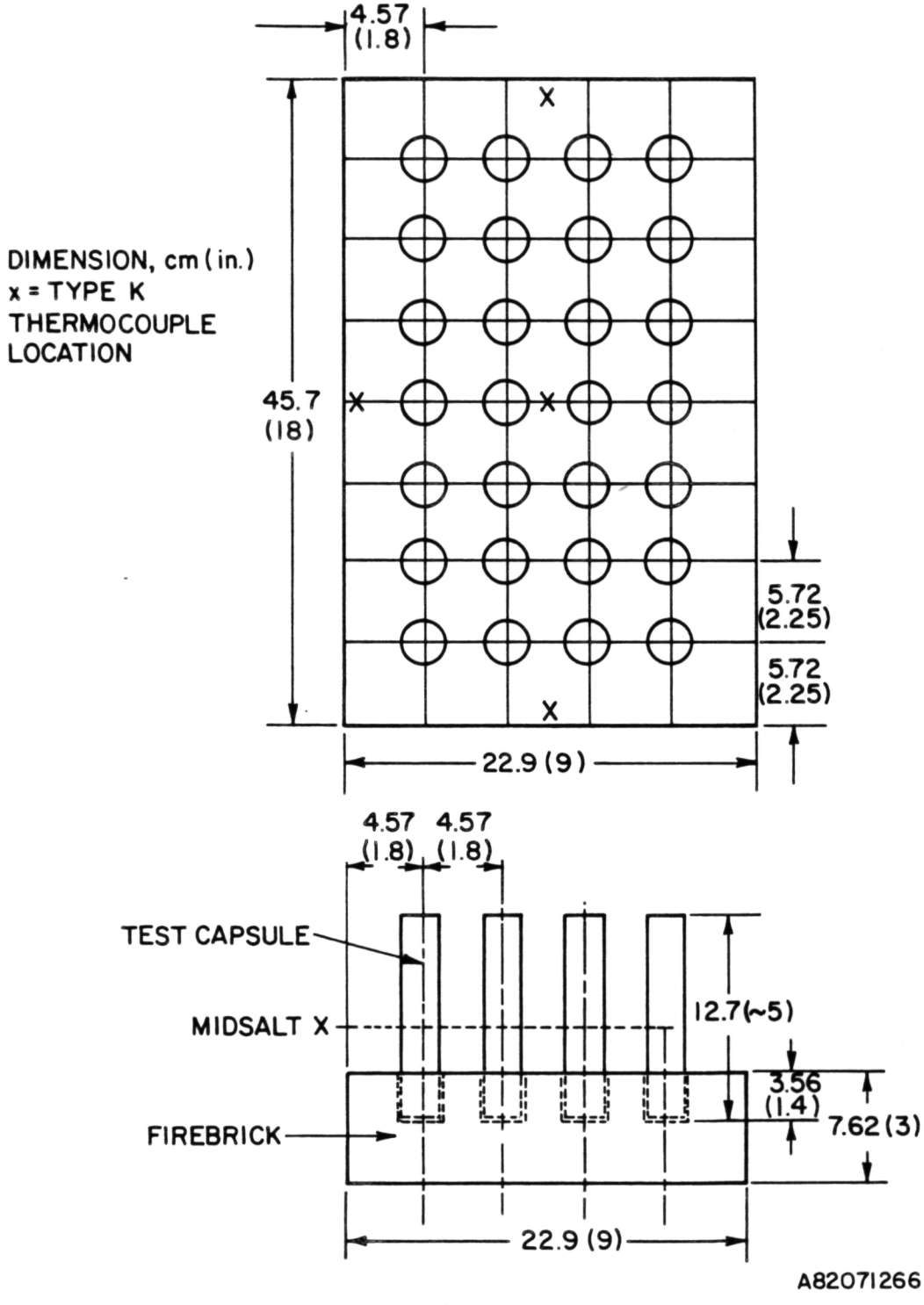

Figure 15. COMPATIBILITY TEST FURNACE LAYOUT

test cross-comparison with pretest X-rays for breach location correlation, where possible. In-furnace temperatures were monitored (4 times per 24 hours) longitudinally in four locations (as in Figure 15) —

1. Front (along width median)
2. Mid-length (along width median)
3. Back (along width median)
4. Mid-length (nearest side heater coil panel).

In addition to X-ray pretest capsule evaluation, temperature, and visual capsule integrity monitoring, complete individual test histories were maintained (as in the format of Figure 16) in order to facilitate correlation of pre- and post-test observations and results.

Although the furnaces were operated at varying heat-up (to temperature) and down (cooldown to room temperature or 300°C for failed capsule removal) times, total capsule test time was recorded to reflect solely hours spent at the operational test temperatures indicated in Table 12.

After the end of each test, the containment/TCE and salt materials were examined to evaluate their stabilities. The salt compositions were chemically analyzed and verified both before installation and after shutdown for CO_2 content, cation composition (Li, K, Na, Ba, etc.), and relative levels of iron, nickel, and chromium (elements indicative of corrosive chemical reaction between salt and containment materials). Finally, each unit was sectioned at mid-salt and top-salt (meniscus) level, visually examined to note overall compatibility, and then metallographic cross sections were conventionally mounted, ground, and polished for light microscopy to determine the nature and extent of corrosion.

Materials Compatibility Evaluations

Screening Evaluation Criteria

A number of factors must be considered in any evaluation of TES system component compatibility. In addition to possessing the desirable individual properties and characteristics necessary for testing selection, salt, containment/HX, and TCE materials compatibility, evaluations were based on —

CAPSULE CODE: _ S _ _ - _ _ _ _ - _ _

START-UP DATE: _ _ / _ _ / 80 TIME: _ _ : _ _ _ M

SHUT-DOWN DATE: _ _ / _ _ / 80 TIME: _ _ : _ _ _ M

HOURS OPERATED: _____ Hours

OVEN No.: _____

COMMENTS: _____

- SALT - Date Loaded _ _ / _ _ / 80

Composition		Melting Point	Mass Salt Loaded	Height per Pellet	No. of Pellets	Volume Salt Loaded	% of Capsule vol = Salt
Salt	Wt. %						
		_____°C	_____ gr	_____cm	_____	_____cm^3	_____
		_____°F	_____lbs	_____in		_____in^3	

- CONTAINMENT MATERIAL

Capsule Body	End Caps	Mass of Capsule After Loading Salt and Welding
		_____gr _____lbs

- TCE MATERIAL - Yes ☐ No ☐

Material	Mass	Form	Dimensions	Volume	Density	Picture?
	_____gm _____lbs		____ x ____ x ____cm ____ x ____ x ____in	_____cm^3 _____in^3	_____gr/cm^3 _____lbs/in^3	

- CAPSULE WELDING

Welded by	Weld Rod	Date Welded	Atmoshpheres Above Salt	Who did Atmospheres	Date of Atmospheres	Welds X-rayed?	Welds Accepted?
		_ _ / _ _ / 80			_ _ / _ _ / 80		

Comments: _____

- TEST CAPSULE

Design Type	Inside Dimensions	Volume Inside	Date Fabrication Complete	Date Cleaned	Comments
	_ _ H x _ _ D cm _ _ H x _ _ D in	_____cm^3 _____in^3	_ _ /_ _ / 80	_ _ / _ _ / 80	

- OPERATION

Oven Temp. Setting	Thermal Cycled	Temp. Cycle	Time at Lowest Temp.	Total Cycle Time	Capsule Leaks?	Pictorial History?
	Yes ☐ No ☐					

B82071281

Figure 16. TES CORROSION TEST CAPSULE HISTORY FORM

- Depth and nature of salt-side corrosion of containment/HX and TCE materials
- Containment alloy thermal aging effects
- Weld integrity in salt environment
- Air-side containment oxidation
- Chemical and physical analyses of the salt.

Evaluation of Salt/Materials Compatibility

The salts/materials investigated in this subtask for their compatibility for latent heat storage were in the high design (high thermal conversion efficiency) solar thermal temperature regime 538° to 871°C (1000° to 1600°F).

As mentioned earlier, prior to batch fabrication/loading/welding of the containment capsules, a preliminary pretest analysis was conducted to assess unaffected capsule and weld integrity characteristics. Additionally, two 304 SS test capsules were prepared and loaded with technical-grade Na_2CO_3 for the beginning-of-life quality and test procedures appraisal —

- One welded in air
- One welded in a glove box, evacuated of air, then back filled with 100% argon and welded
- Both short-term furnace tested at 910°C (1670°F) for 72 hours.

From the pretest weld evaluation and testing of these 304 SS nipple and end cap capsules, it was found that care must be taken in "washing" the filler metal into the weld area gaps (Figure 7) on capsules of this design.

Seventy-seven compatibility test capsules of 304 SS, 316 SS, 310 SS, Inconel 600, Incoloy 800, and Armco 18SR/12SR, containing the test matrix salts and selected samples of Kanthal A-1, copper, and graphite, were then prepared and installed into the three Blue-M furnaces for the Phase I screening tests (Table 10). In addition to some prolonged exposure tests, an additional 24 compatibility capsules were tested during Phase II.

The following discussion details the operational/post-test history of the Phase I and II testing matrix. It was during the initial phase of testing that some of the significant problems associated with molten salt/welded containment systems in this high-temperature regime were encountered.

Identification and resolution of these problems and results from the Phase I screening tests were used as the basis for identifying the most promising salt, containment/HX, and TCE materials combinations for further Phase II screening tests.

Beginning of Life

Capsules of Inconel 600 and Incoloy 800 with technical-grade 50 wt % Na_2CO_3-50 wt % K_2CO_3 developed beginning-of-life leaks in their weld areas after 72 hours of operation. Sectioning and metallographic examination of the capsules containing leaks revealed incomplete weld penetration, crevice corrosion, and intergranular microcracking (Figure 17) due to partial separation of the end cap from the capsule body wall (5 to 12 mils). Replacement capsules were subsequently prepared (using longer metal melting times to yield more complete weld penetration) and then installed. Such capsules subsequently attained 763 hours of leak-free operation.

An overview summary of the Phase I testing appears in Tables 13 and 14. In addition to the early-in-life capsule failures noted above, 10 test capsules developed significant salt leakage within the first 600 hours of continuous operation; 9 of these failed capsules were from the highest temperature (950°C) furnace.

Post-test examinations of these capsules indicated that the leaks were associated with —

- Inadequate weld penetration
- Observed capsule wall/end cap interface separation
- Evidence of crevice corrosion (a design/fabrication problem not necessarily indicative of salt/material long-term corrosion compatibility, but nonetheless causing a capsule test to terminate).

Additionally, calculations indicated that the evolution of adsorbed H_2O from the carbonate pellets during heat-up (at the highest furnace temperature when in these totally closed capsules) caused pressure buildup in the gas phase over the melt, which in turn created capsule hoop (tensile) stresses possibly exceeding the yield (resulting in bulging), or rupture strength (resulting in cracks and failures) of the containment materials at the testing temperatures.

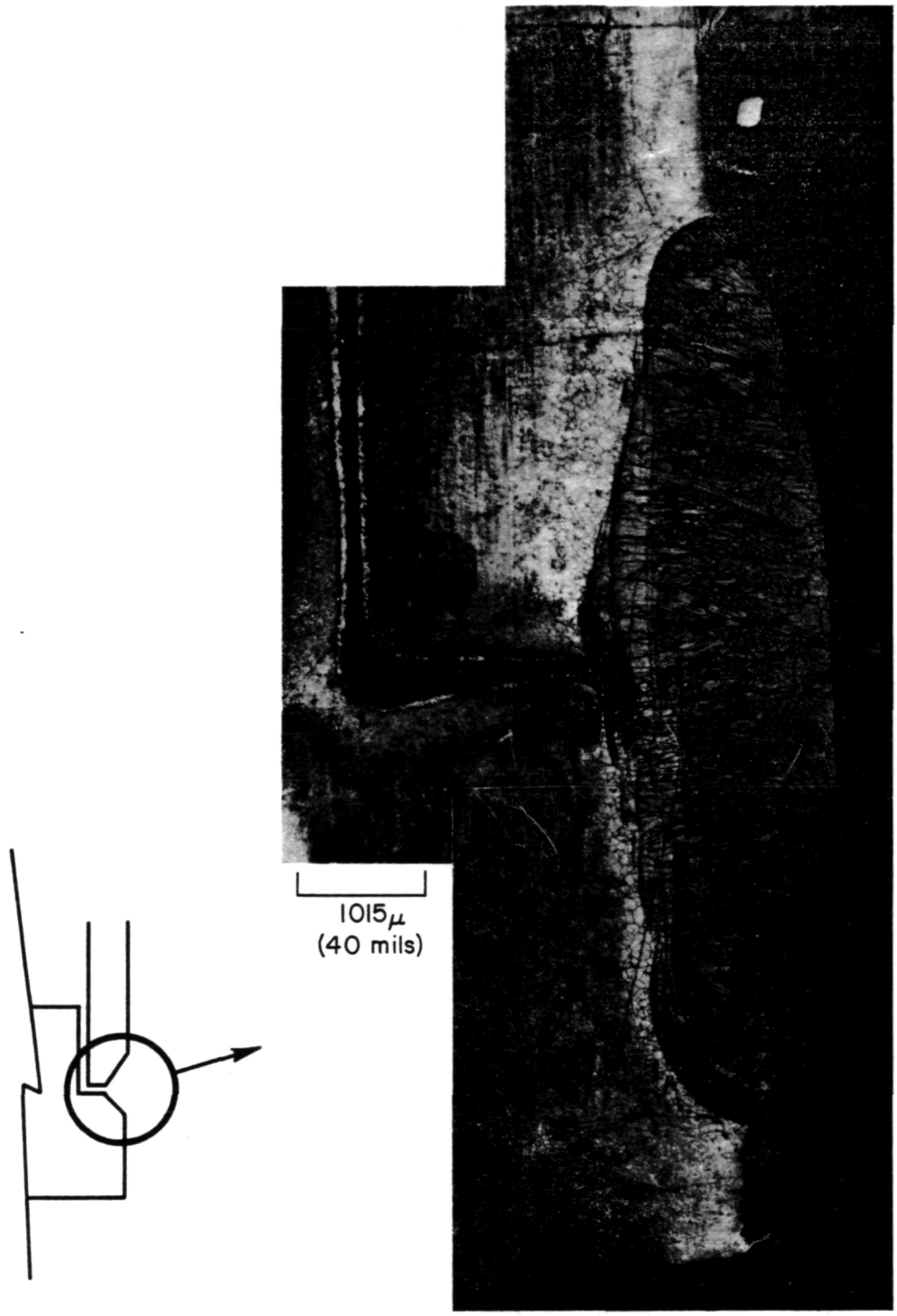

Figure 17. POST-TEST WELD CROSS SECTION MICROGRAPH OF SALT SIDE INCONEL 600 CAPSULE WITH TECHNICAL-GRADE Na_2CO_3 FOR 72 HOURS AT 910°C (25X, Etchant: Electrolytic, 10% Oxalic Acid)

Table 13. PHASE I COMPATIBILITY TEST SCHEDULE SUMMARY

Containment Material	Inside Sample (TCE, etc.)	Capsule Design	Weld Type	Weld Filler Metal	Capsule Environment	No. Installed	No. Failed	No. Sectioned
304 SS	--	N/E-C*	Tig Fillet	SS 308L	Air	12	4	8
316 SS	--	N/E-C	Tig Fillet	SS 316L	Air	12	4	5
310 SS	--	MC/E-C	Tig Fillet	SS 310L	Air	12	2	7
Inconel 600	--	MC/E-C**	Tig Fillet	I-82	Air	12	4 (1 redone)	8
Incoloy 800	--	MC/E-C	Tig Fillet	I-82	Air	12	1 (1 redone)	8
304 SS	P.G. and ATJ	N/E-C	Tig Fillet	SS 308L	Argon 100%	3	0	0
304 SS	Copper: Solid and reticulated	N/E-C	Tig Fillet	SS 308L	Argon 100%	3	0	0
Inconel 600	P.G. and ATJ	MC/E-C	Tig Fillet	I-82	Argon 100%	2	0	0
Inconel 600	Copper: Solid and reticulated	MC/E-C	Tig Fillet	I-82	Argon 100%	2	0	0
310 SS	HK-40	MC-E-C	Tig Fillet	SS 310L	Air	2	0	0
Armco 12SR capsule body with Armco 18 SR end caps	Kanthal A-1	MC/E-C	Tig Fusion	--	Air	5/77 (2 redone)	1/16 (2 redone)	0/36

* Nipple and end cap.

** Machined capsule body and end cap.

B83050857

Table 14. PHASE I POST-TEST COMPATIBILITY EVALUATION PLAN

			Containment Materials (Hours of Operation)						TCE Materials (Hours of Operation)	
No.	Salt System Composition, wt %	Grade	1 304 SS	2 316 SS	3 310 SS	4 Inconel 600	5 Incoloy 800	6 Armco 18SR/12SR (Kanthal A-1 inside)	1 Graphite P.G. and ATJ	2 Copper Solid Tube and Reticulated Matrix
	OVEN I 750°C									
1	52.2 $BaCO_3$-41.8 Na_2CO_3	Reagent	[1882]	[1882]	[1603]	[1882]	[1882]			
2	52.2 $BaCO_3$-41.8 Na_2CO_3	Technical	[1882]	1882	1603	1882	1882	1056	1243	1243
3	50.0 Na_2CO_3-50.0 K_2CO_3	Reagent	[1882]	[1882]	[1603]	[1882]	[1882]			
4	50.0 Na_2CO_3-50.0 K_2CO_3	Technical	[1882]	[1882]	1603	[1603]	1603	[1056]	1243	1243
	OVEN II 840°C									
5	Li_2CO_3	Reagent	[1931]	(672)	[1603]	(288)	[1931]			
6	Li_2CO_3	Technical	[1931]	1931	[1603]	1931	1931	1056	1243	1243
7	81.3 Na_2CO_3-18.7 K_2CO_3	Reagent	[1931]	[1931]	[1603]	[1931]	[1931]			
8	81.3 Na_2CO_3-18.7 K_2CO_3	Technical	[1931]	1931	1603	[1931]	1931	1056		
	OVEN III 950°C									
9	Na_2CO_3	Reagent	(288)	(288)	(763)	(288)	[816]			
10	Na_2CO_3	Technical	[(552)]	(288)	(763)	(288)	[816]	[1034]	1154	1154
11	K_2CO_3	Reagent	(288)	[(288)]	[1490]	[1803]	[816]			
12	K_2CO_3	Technical	[(552)]	816	[1490]	[816]	[816]		1154	1154

KEY

(○) = Failed Capsule.

[□] = Capsule to be sectioned and metallographically examined.

B83050858

Because of these experimental difficulties, the following modifications were planned and implemented for Phase II salt preparations —

- After initial mixing, milling, and cold-pressing, all salts were dehydrated in a vacuum oven for 4 hours at 150°C.
- After this dehydration step, test capsules were immediately loaded with salt and finally heli-arc welded.

Containment/Salt Compatibility Tests at 750°C

A summary of post-test metallographic examination results from containment/salt compatibility tests conducted at 750°C is given in Table 15 for the candidate alloys of AISI 304, 316, and 310 austenitic stainless steels; Inconel 600; and Incoloy 800. The carbonate salts tested at this 750°C temperature were both reagent and technical grades of 52 wt % $BaCO_3$-48 wt % Na_2CO_3 (686°C mp) and of 50 wt % Na_2CO_3-50 wt % K_2CO_3 (710°C mp). Some additional results on AISI 304 compatibility with these salts at 750°C are presented in Table 16. The AISI 304 capsules in these tests contained specimens of copper or graphite TCE materials and had an argon cover gas, rather than air.

The AISI 304 and 316 SS materials showed generally comparable corrosion characteristics in these 750°C tests, although 304 SS generally had slightly thicker oxide scale on the inner capsule surfaces than 316 SS. The oxide scale thicknesses increased with time of exposure. For 304 SS in technical-grade 52 $BaCO_3$-48 Na_2CO_3, scale thicknesses ranged from 2 to 3 mils after 984 hours, 3 to 4 mils after 1882 hours, and 4 to 5 mils after 2635 hours. (See Figure 18.) Post-test analysis of the technical-grade salt revealed its constitutent's general chemical stability, although indicating an increase in iron content from <0.01% to 0.36% (Table 17) after 1882 hours at 750°C in 304 SS. Figure 19 is an optical micrograph of the corrosion scale and underlying metal from the 304 SS capsule tested for 2635 hours in this salt.

The 50 Na_2CO_3-50 K_2CO_3 salt composition appeared to be more agressive toward both 304 SS and 316 SS than 52 $BaCO_3$-48 Na_2CO_3, and in turn, technical-grade 50 Na_2CO_3-50 K_2CO_3 was more corrosive than the reagent-grade salt. The effect of salt grade and the somewhat better corrosion resistance of 316 SS over 304 SS after 1882 hours of testing are shown in the micrographs of Figures 20 and 21, and chemical analysis results in Table 18. Comparison of the scale microstructures in these figures reveals that the scales formed on

Table 15. RESULTS OF CONTAINMENT/SALT COMPATIBILITY TESTS AT 750°C

	Alloy	1	2	3	4	5
No.	Salt, wt %	AISI 304 SS	AISI 316 SS	AISI 310 SS	Inconel 600	Incoloy 800
1	$52BaCO_3$-$48Na_2CO_3$ Reagent	1882 h 5-6 mil scale	1882 h 4-5 mil scale Minor carburization	1603 h 1-2 mil scale Sigma phase	1882 h 1-2 mil scale Extensive carburization	1882 h <1 mil scale Moderate carburization
2	$52BaCO_3$-$48Na_2CO_3$ Technical	984 h 2-3 mil scale 1882 h 3-4 mil scale	3106 h Capsule failure	2947 h 1-2 mil scale Sigma phase	3106 h 1.3 mil scale Extensive carburization	3106 h 1 mil scale Moderate carburization
3	$50Na_2CO_3$-$50K_2CO_3$ Reagent	1882 h 4-5 mil scale	1882 h 3-4 mil scale	1603 h 1-2 mil scale Sigma phase	1882 h 2-3 mil scale Extensive carburization	1882 h 1-2 mil scale
4	$50Na_2CO_3$-$50K_2CO_3$ Technical	984 h 6 mil scale Minor carburization 1882 h 8-10 mil scale Minor carburization	984 h 4 mil scale 1882 h 5-6 mil scale	2947 h 12-14 mil reaction layer Sigma phase	1603 h 2-3 mil scale Extensive carburization	3106 h 2-3 mil scale 3106 h 4-5 mil scale

B83050859

Table 16. AISI 304 SS/SALT COMPATIBILITY TESTS CONDUCTED WITH TCE MATERIALS (Argon Cover Gas)

Containment Material	Salt*	TCE Materials**	Exposure	Results
304 SS	$52BaCO_3$-$48Na_2CO_3$	PG, ATJ	1320 hr at 750°C	7-9 mils oxidation + carburization
304 SS	$52BaCO_3$-$48Na_2CO_3$	Cu	2635 hr at 750°C	4-5 mil oxide scale
304 SS	$50Na_2CO_3$-$50K_2CO_3$	PG, ATJ	2539 hr at 750°C	16-18 mil oxide scale Subscale carburization
304 SS	$50Na_2CO_3$-$50K_2CO_3$	Cu	2635 hr at 750°C	12-14 mil oxidation + carburization
304 SS	Li_2CO_3	PG, ATJ	2635 hr at 850°C	7-8 mil oxide scale
304 SS	Li_2CO_3	Cu	2635 hr at 850°C	7-8 mil oxide scale

* Technical-grade salts, wt % composition.

** PG: Pyrolytic graphite
ATJ: Union Carbide ATJ graphite
Cu: Porous reticulated and tubular copper.

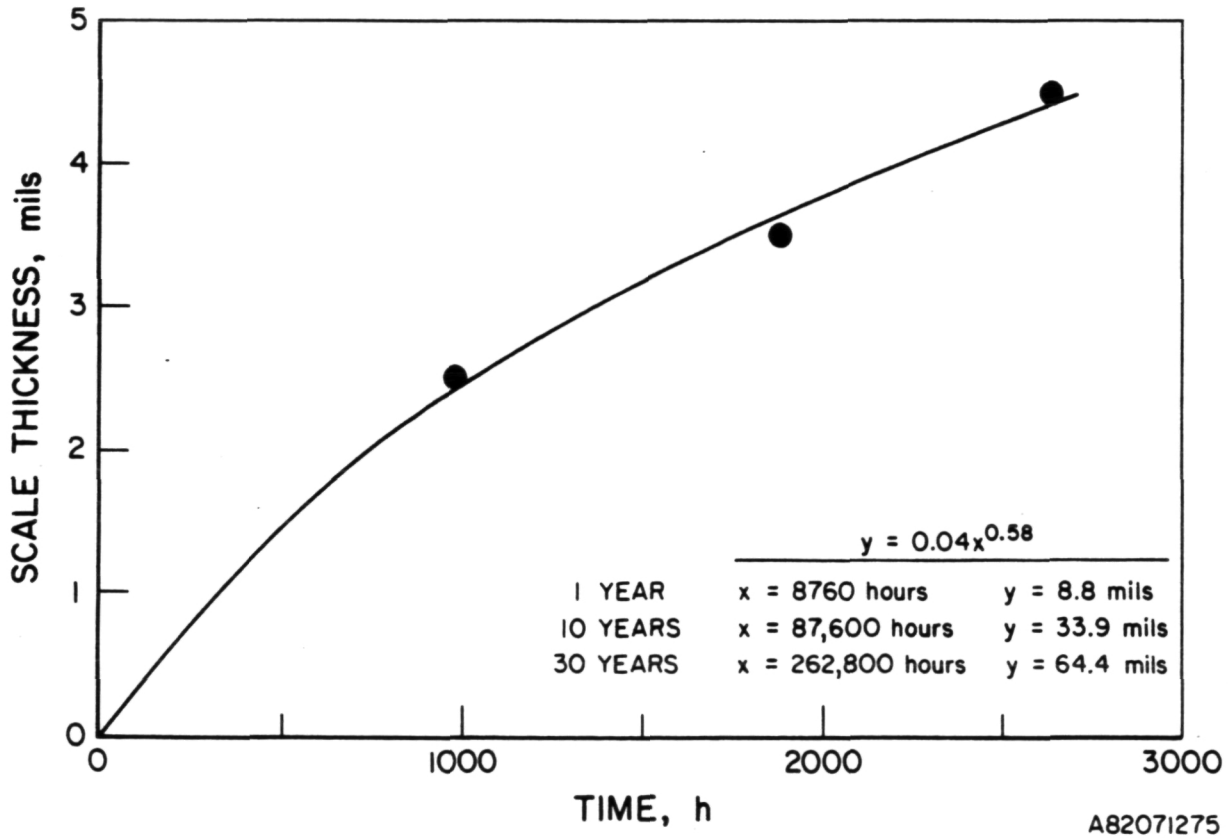

Figure 18. GROWTH OF OXIDE SCALE ON AISI 304 IN TECHNICAL-GRADE 52 wt % $BaCO_3$-48 wt % Na_2CO_3 AT 750°C

Table 17. PRE- AND POST-TEST CHEMICAL ANALYSIS OF $52BaCO_3$-$48Na_2CO_3$ AT 750°C

Salt	Grade	In Containment	Chemical Analysis, wt %						Hours
			$CO_3^=$	Na	Ba	Fe	Cr	Ni	
Pre-Test									
$52Ba_2CO_3$-$48Na_2CO_3$	Technical	--	43.6	18.7	36.1	<0.01	<0.02	<0.01	--
Post-Test									
$52Ba_2CO_3$-$48Na_2CO_3$	Technical	304 SS	42.5	20.3	32.8	0.34	0.08	0.05	1882
$52Ba_2CO_3$-$48Na_2CO_3$	Technical	Inconel 600	42.8	18.9	34.9	0.02	0.02	0.15	3106
$52Ba_2CO_3$-$48Na_2CO_3$	Technical	Incoloy 800	43.1	19.0	33.9	0.04	<0.01	0.01	3106

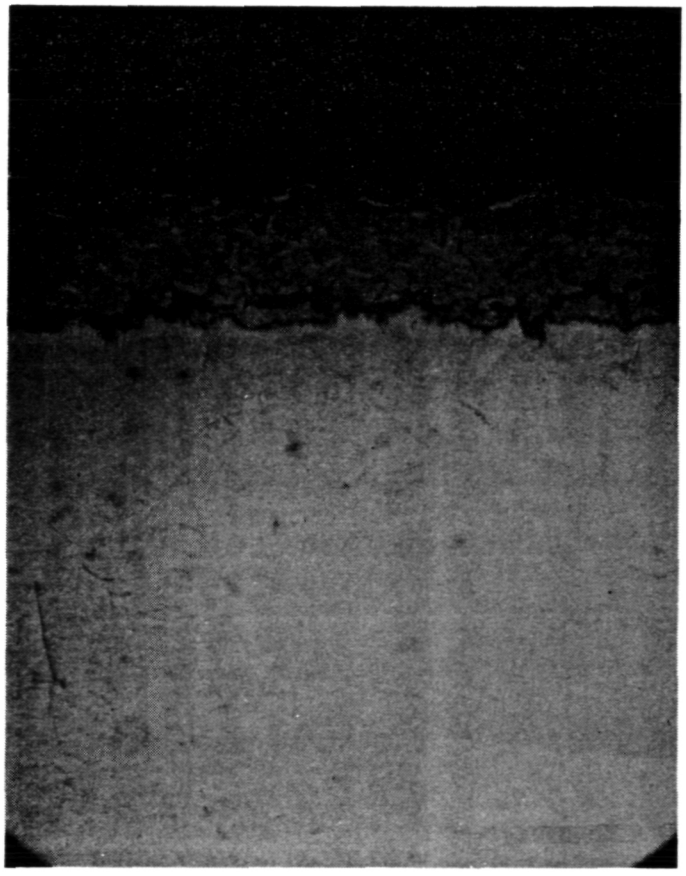

Figure 19. OPTICAL MICROGRAPH OF 304 SS TESTED IN TECHNICAL-GRADE $52BaCO_3$-$48Na_2CO_3$ FOR 2635 HOURS AT 750°C (Ar Cover Gas/Cu TCE) (160X, Etchant: Electrolytic, 10% Oxalic Acid)

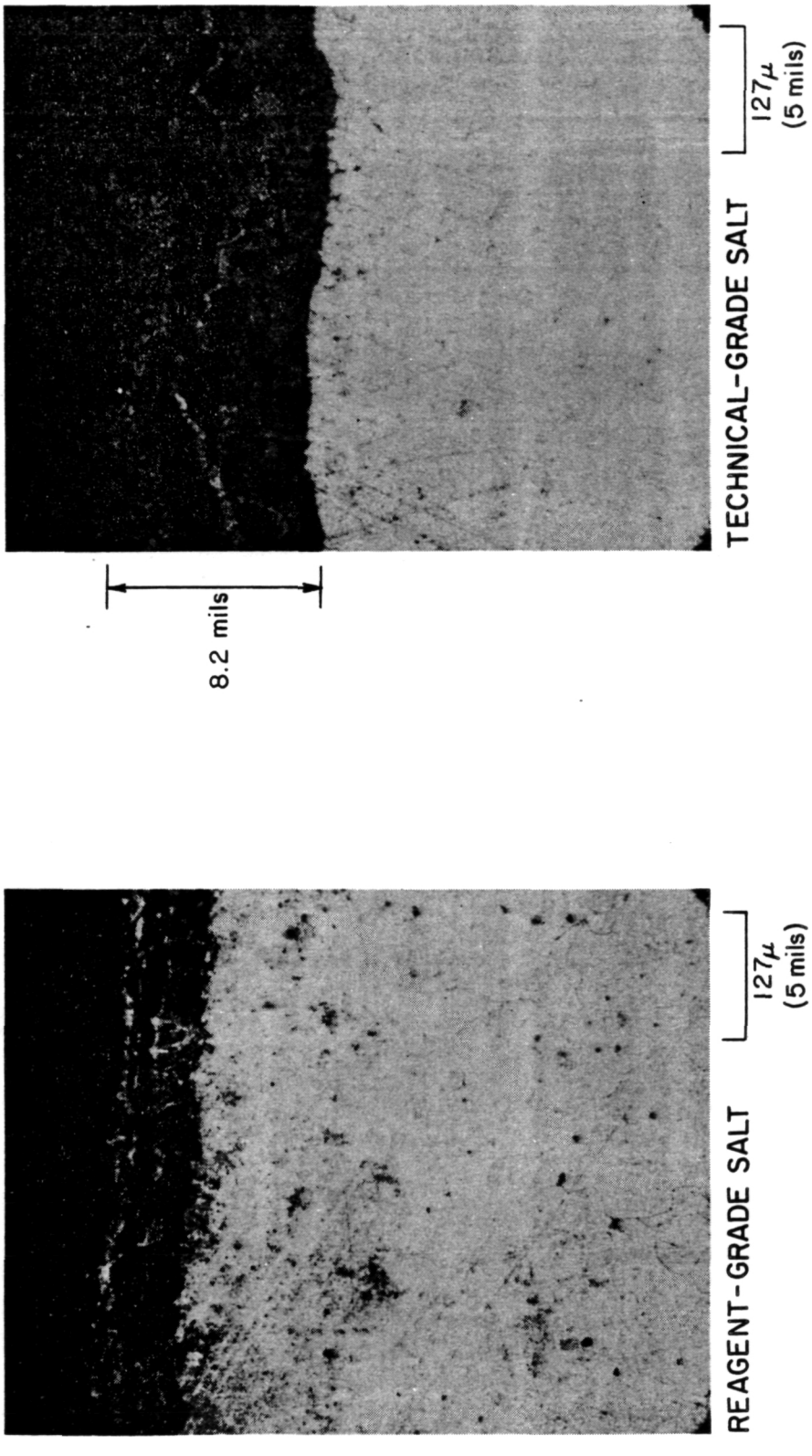

Figure 20. CORROSION LAYERS ON AISI 304 SS AFTER 1882 HOURS OF TESTING AT 750°C IN 50 wt % Na_2CO_3-50 wt % K_2CO_3 SALT (160X)

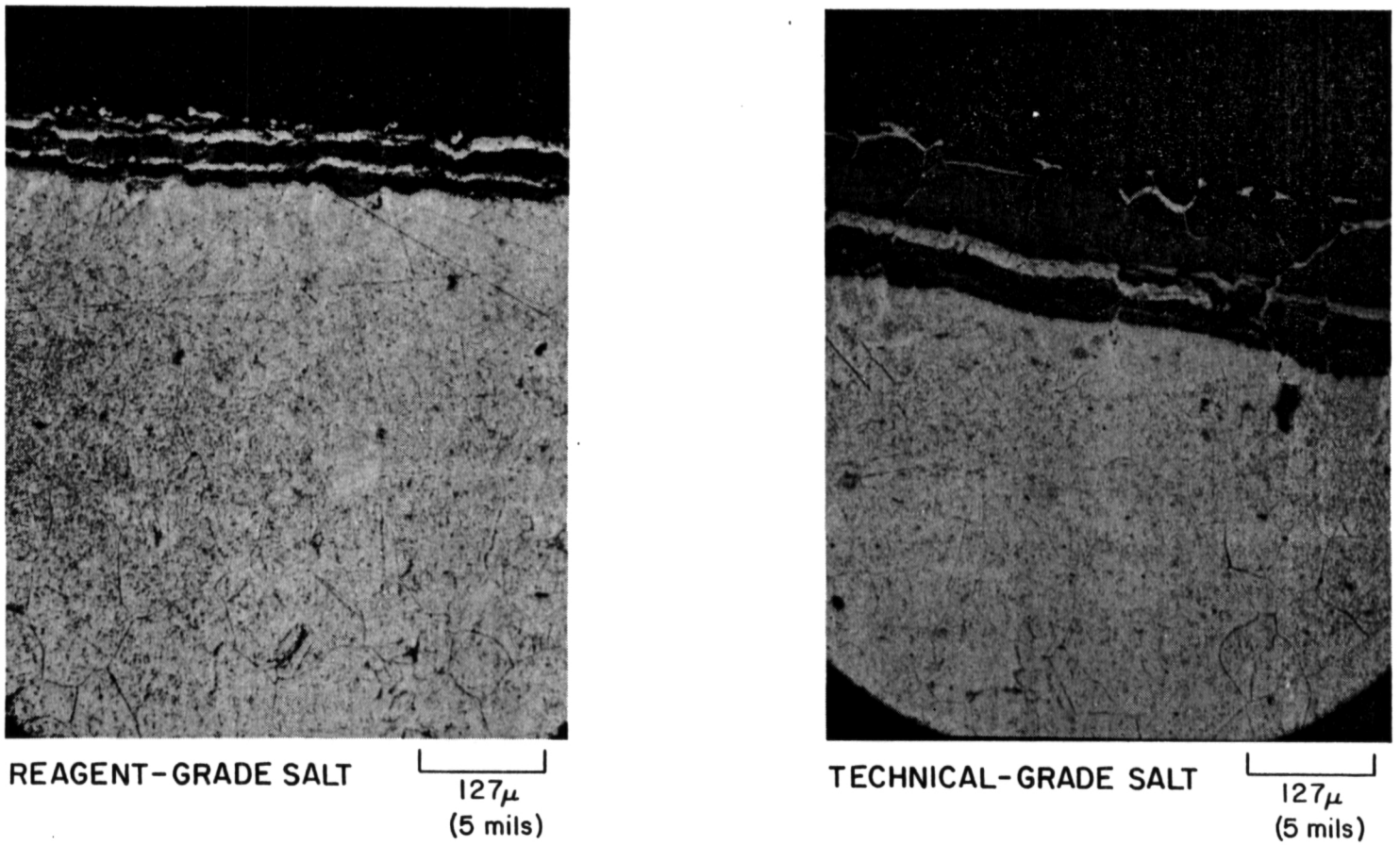

Figure 21. CORROSION LAYERS ON AISI 316 SS AFTER 1882 HOURS OF TESTING AT 750°C IN 50 wt % Na_2CO_3-50 wt % K_2CO_3 SALT (160X)

Table 18. PRE- AND POST-TEST CHEMICAL ANALYSIS OF $50Na_2CO_3$-$50K_2CO_3$ AT 750°C

Salt	Grade	In Containment	Chemical Analysis, wt %						Hours
			$CO_3^=$	Na	K	Fe	Cr	Ni	
			Pre-Test						
$50Na_2CO_3$-$50K_2CO_3$	Reagent	--	50.2	20.4	26.7	<0.01	<0.02	<0.01	--
	Technical	--	50.2	21.4	26.7	<0.01	<0.02	<0.01	
			Post-Test						
$50Na_2CO_3$-$50K_2CO_3$	Reagent	316 SS	48.7	20.1	28.3	0.38	0.06	0.09	1882
	Technical	316 SS	47.9	20.4	27.0	0.73	0.04	0.13	1882
	Reagent	Inconel 600	49.8	20.8	26.7	<0.01	<0.02	<0.01	1882
	Technical	Inconel 600	50.0	22.7	26.0	<0.01	<0.01	0.01	3106

316 SS surfaces are more dense and adherent than those formed on 304 SS, thus providing somewhat greater protection against further corrosion. Also, technical-grade 50 Na_2CO_3-50 K_2CO_3 resulted in a greater post-test iron content than its reagent counterpart (0.73% compared to 0.38% from <0.01%) when tested with 316 SS containment for 1882 hours at 750°C (Table 18).

The AISI 304 and 316 materials showed a significant amount of carbide precipitation in grain boundaries as a result of prolonged heating at 750°C. This "sensitization" effect is expected for heating of these alloys in the 450° to 900°C temperature range. However, such carbide precipitation and any associated depletion of chromium in regions near grain boundaries did not appear to have any deleterious effects on corrosion resistance to molten carbonates.

AISI 310 SS capsules generally exhibited less oxidation than 304 SS or 316 SS in 52 $BaCO_3$-48 Na_2CO_3 salts. However, at all test temperatures over the range 750° to 950°C, this alloy experienced formation of sigma phase precipitates at grain boundaries and triple points throughout the capsule specimens. The AISI 310 SS Cr/Ni composition range falls within the approximate boundary for susceptibility to sigma formation in steels as formulated by J. H. Monypenny in 1951.[50] (See Figure 22.) This precipitation effect is caused by continuous thermal exposure in this temperature regime and is not related to salt interaction effects. The presence of high concentrations of brittle inter-metallic sigma phase precipitates, as observed in these experiments, is known to significantly reduce the low-temperature ductility and strain-to-failure of the alloy structure. Thus, the usefulness of AISI 310 SS for high-temperature thermal energy storage applications may be limited primarily by the formation of sigma phase and its effect on mechanical properties. Additional work is required to more fully assess the significance of sigma phase on 310 SS structural integrity under TES service conditions.

The 310 SS material also showed good compatibility with reagent-grade 50 Na_2CO_3-50 K_2CO_3, with formation of a 1 to 2-mil-thick oxide scale after 1603 hours. However, the 310 SS capsule tested with technical-grade 50 Na_2CO_3-50 K_2CO_3 for 2947 hours experienced fairly extensive reaction with the salt, resulting in a 12 to 14-mil-thick reaction layer. The microstructure of this reaction layer was complex and appeared to be associated with several possible interaction mechanisms, which included oxidation,

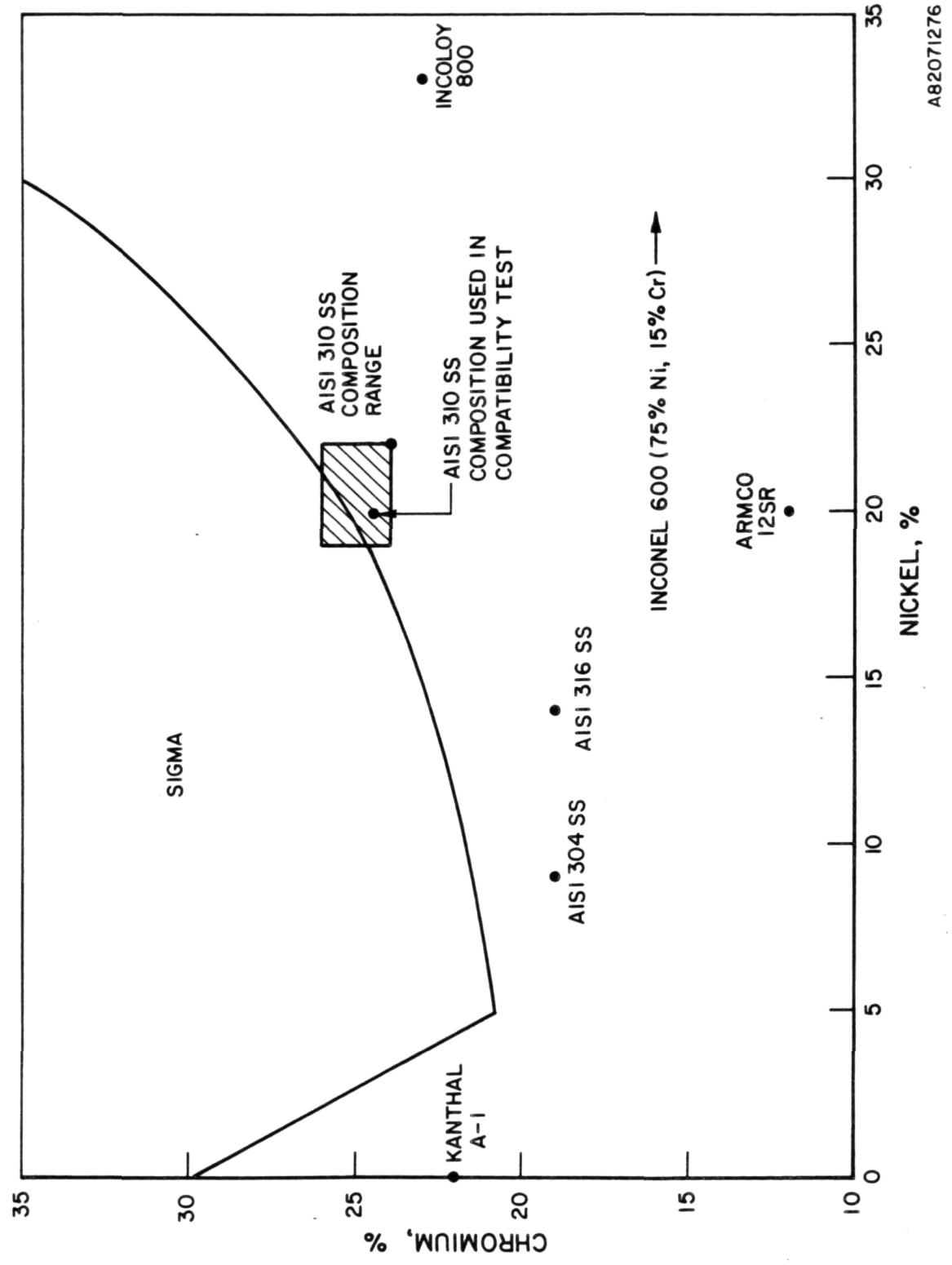

Figure 22. APPROXIMATE Cr-Ni BOUNDARY FOR SUSCEPTIBILITY TO SIGMA FORMATION IN STEELS CONTAINING 0.1% CARBON[50]

carburization, and perhaps salt penetration. The appearance of this reaction layer and the condition of the base metal are shown in Figure 23. Also evident in this figure in the base metal region are black pits left at locations where sigma phase precipitates were removed from the microstructure by oxalic acid electrolytic etching.

Alloys Inconel 600 and Incoloy 800 were found to be more corrosion resistant to molten carbonates at 750°C than any of the 300 series stainless steels (304, 316, or 310 SS). In addition, Incoloy 800 appeared to be somewhat more resistant than Inconel 600, as well as being a less expensive alloy. Although Inconel 600 did not experience excessive reaction layers at the inner surface in contact with carbonates, the underlying bulk metal appeared to be subject to extensive carburization. Figure 24 shows a typical region of subsurface carburization, showing both intergranular and very heavy intragranular carbide precipitation. Such heavy carburization extending approximately one quarter of the way through the wall thickness is expected to result in some degree of embrittlement of the alloy. The stability of both the $BaCO_3$-Na_2CO_3 and Na_2CO_3-K_2CO_3 salts in Inconel 600 and Incoloy 800 is shown in the post-test analyses of Tables 17 and 18.

Incoloy 800 showed very good compatibility with all salt compositions in the 750°C test series, forming very protective oxide scales a maximum of only 2 to 3 mils thick after 3106 hours of exposure. Representative optical micrographs of Incoloy 800 after 3106 hours of test in the technical-grade $BaCO_3$-Na_2CO_3 and Na_2CO_3-K_2CO_3 salts are shown in Figures 25 and 26. This alloy was carburized to a moderate extent, although much less so than Inconel 600 under comparable experimental conditions.

A comparative ranking of the scaling resistance of the candidate materials at 750°C is presented in Figure 27 for containment of the $BaCO_3$-Na_2CO_3 salt.

Containment/Salt Compatibility Tests at 850°C

Table 19 presents a summary of post-test metallographic examination results for the candidate containment/salt compatibility tests performed at 850°C. This series of tests was conducted with reagent and technical grades of Li_2CO_3 (723°C mp) and of 82 Na_2CO_3-18 K_2CO_3. This latter mixture melts incongruently over the temperature range 742° to 788°C. Some additional

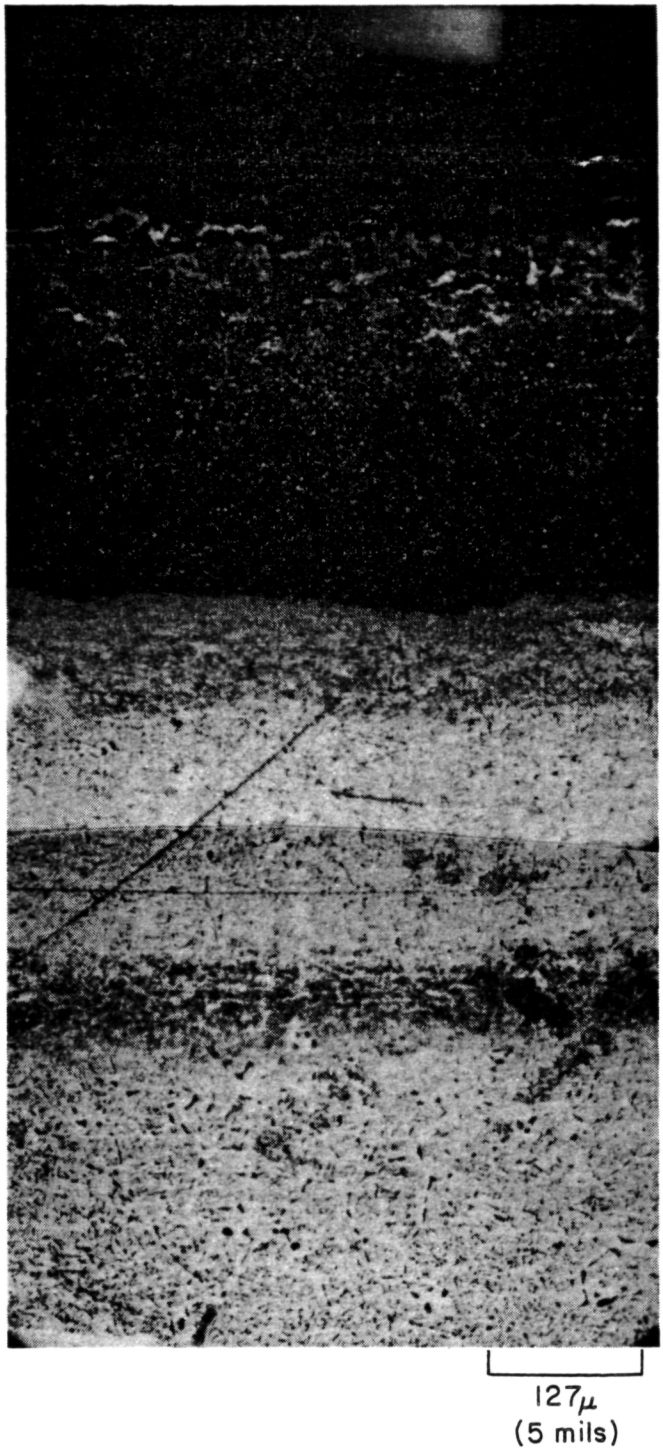

Figure 23. OPTICAL MICROGRAPH OF AISI 310 TESTED IN TECHNICAL-GRADE 50 wt % Na_2CO_3-50 wt % K_2CO_3 SALT FOR 2947 HOURS AT 750°C (160X)

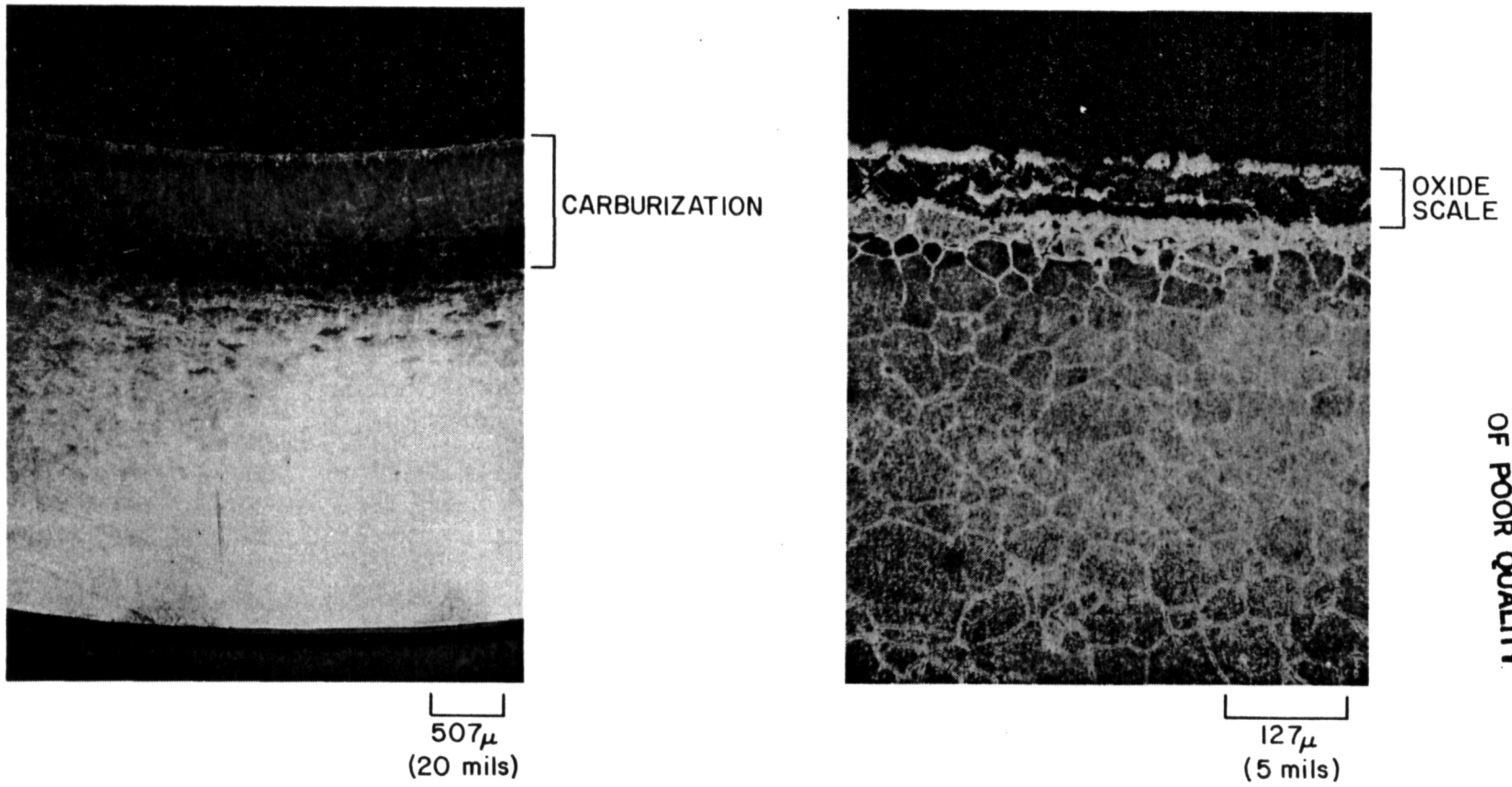

Figure 24. OPTICAL MICROGRAPHS OF INCONEL 600 TESTED IN REAGENT-GRADE 50 wt % Na_2CO_3-50 wt % K_2CO_3 FOR 1882 HOURS AT 750°C SHOWING EXTENSIVE SUB-SCALE CARBURIZATION

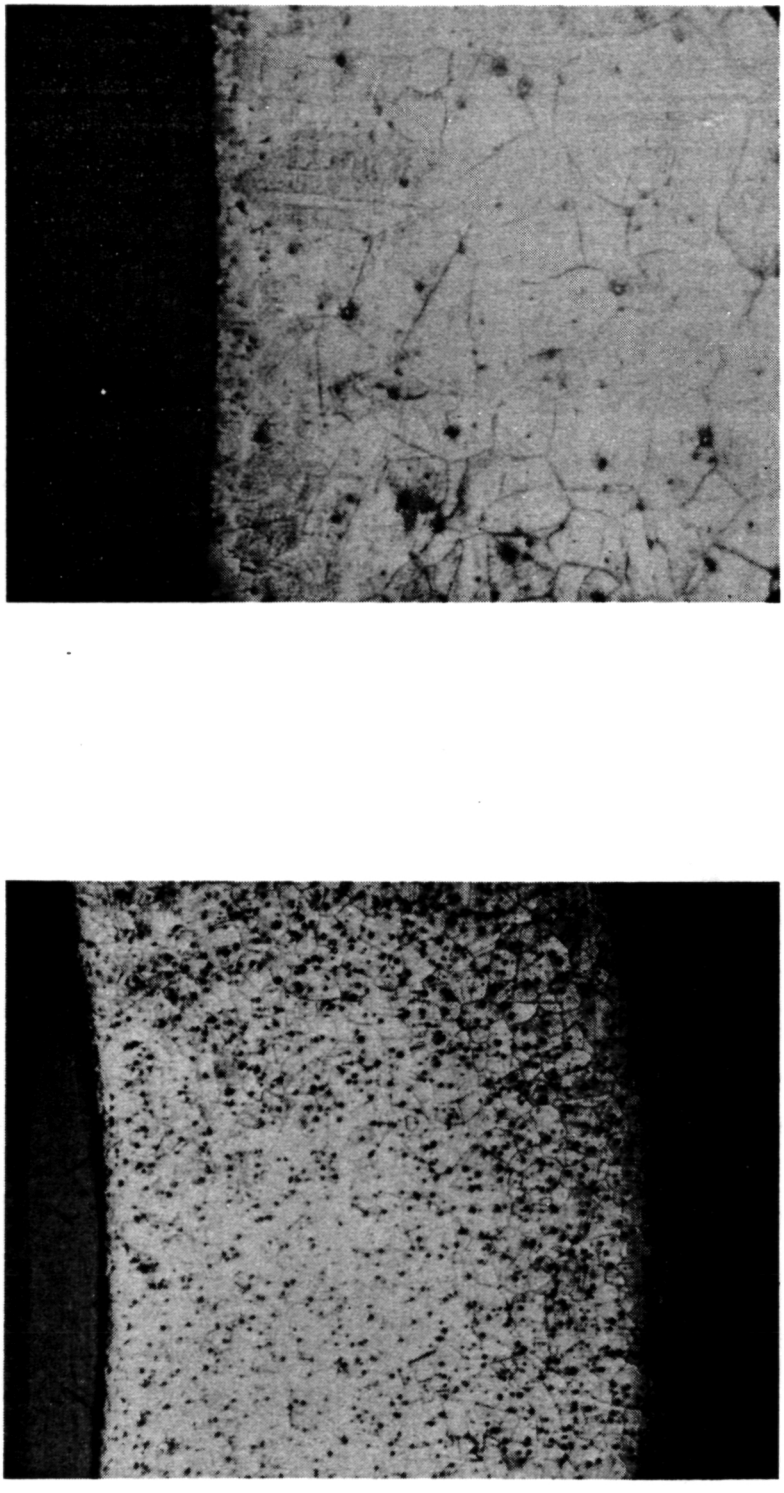

Figure 25. OPTICAL MICROGRAPHS OF INCONEL 800 TESTED IN TECHNICAL-GRADE $52BaCO_3$-$48Na_2CO_3$ FOR 3106 HOURS AT 750°C

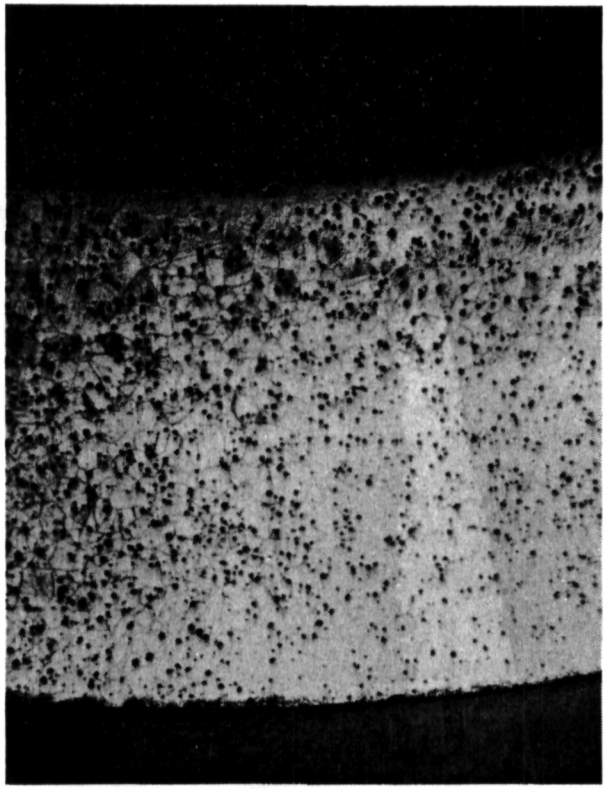

507μ
(20 mils)

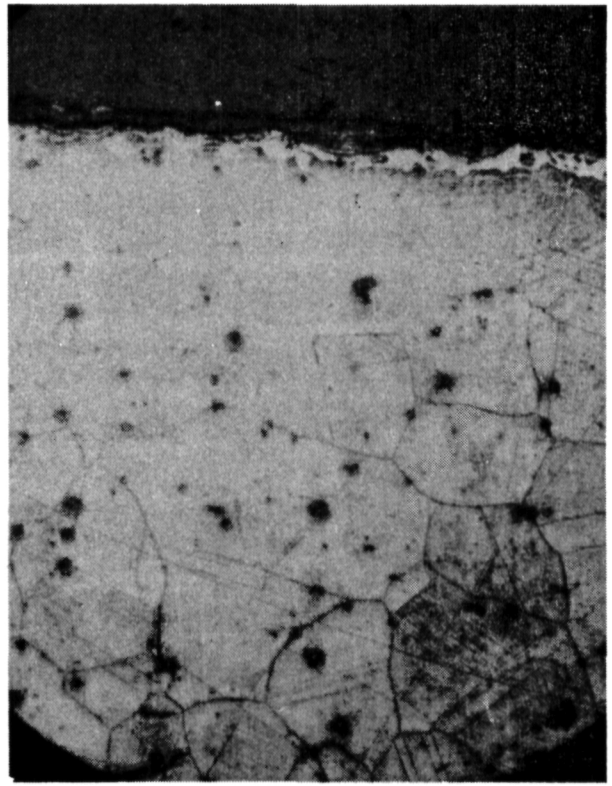

127μ
(5 mils)

Figure 26. OPTICAL MICROGRAPHS OF INCONEL 800 TESTED IN TECHNICAL-GRADE $50Na_2CO_3$-$50K_2CO_3$ FOR 3106 HOURS AT 750°C

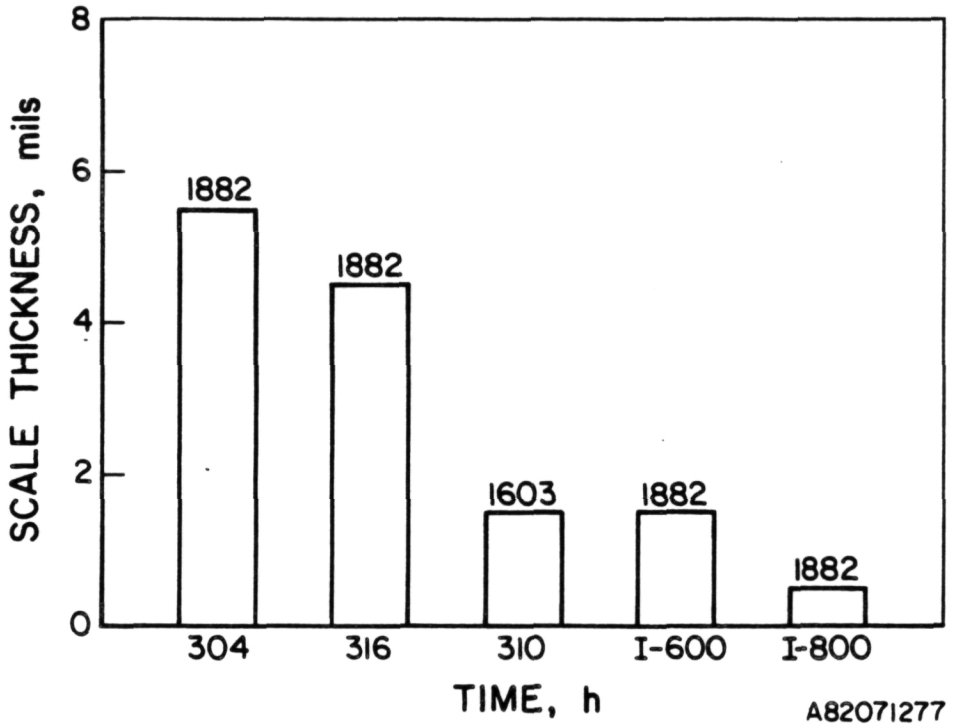

Figure 27. THICKNESS OF OXIDE SCALES FORMED ON CANDIDATE ALLOYS AFTER 1603 TO 1882 HOURS OF EXPOSURE TO REAGENT-GRADE $52BaCO_3$-$48Na_2CO_3$ AT 750°C

Table 19. RESULTS OF CONTAINMENT/SALT COMPATIBILITY TESTS AT 850°C

	Alloy	1	2	3	4	5
No.	Salt, wt %	AISI 304 SS	AISI 316 SS	AISI 310 SS	Inconel 600	Incoloy 800
5	Li_2CO_3 Reagent	1931 h 5-6 mil scale	672 h Capsule failure ~1 mil scale	1603 h 2-3 mil scale Sigma phase	288 h Capsule failure	1931 h 2 mil scale
6	Li_2CO_3 Technical	1176 h 8-9 mil scale 1931 h 10.0 mil scale	2027 h Capsule failure during last 100 h	1603 h 2 mil scale 2 mil sub-scale pitting Sigma phase 2083 h 2-3 mil scale + 4 mil sub-scale pitting Sigma phase	3106 h 1-2 mil scale + 4 mil sub-scale pitting	3106 h 5 mil scale 5 mil sub-scale intergranular penetration
7	$82Na_2CO_3$-$18K_2CO_3$ Reagent	1931 h 3-4 mil scale	1931 h 9-10 mil reaction zone	1603 h 15 mil oxidation and salt penetration	1931 h 2 mil scale Extensive carburization	1931 h 1.0 mil scale
8	$82Na_2CO_3$-$18K_2CO_3$ Technical	1931 h 4-5 mil scale + Capsule failure 65-70 mil bulk penetration	552 h 35-40 mil reaction examine zone 3083 h 65-70 mil reaction zone (Capsule failure during last 100 h)	2779 h Capsule failure 3172 h	1176 h 10 mil oxidation and salt penetration Moderate carburization	3106 h 1-2 mil scale

B83050860

results were presented in Table 16 for AISI 304 SS tested in technical-grade Li_2CO_3 with copper and graphite TCE materials at 850°C.

AISI 304 SS materials reacted with both grades of Li_2CO_3 to form banded-oxide scale structures. These scales were not highly protective because of their porous and friable nature. Scale thicknesses of up to 10 mils were observed in tests up to 1931 hours duration with air cover gas. Use of an argon cover gas appeared to result in a lower rate of oxidation than for air, as evidenced by the 7 to 8-mil oxide scale formed after 2635 hours in technical-grade Li_2CO_3 with graphite TCE's and Ar gas (Figure 28). AISI 304 SS also showed reasonable compatibility with reagent-grade 82 Na_2CO_3-18 K_2CO_3 in air, forming a 3 to 4-mil scale after 1931 hours. However, the technical grade mixture of these salts after the same period of time caused an additional 65 to 70-mil bulk penetration below the 4 to 5-mil-thick oxide scale.

Comparative evaluations of 316 SS corrosion behavior in these carbonates at 850°C were precluded by the high incidence of capsule failures. Generally the "failures" resulted in very extensive corrosion after salt had leaked from capsules because of the thin salt films formed on both inner and outer capsule surfaces after failure. The enhanced hot-corrosion rates in the presence of thin molten salt films is a well-documented phenomenon.[33,41,42] The extensive post-failure corrosion generally destroyed evidence related to the actual cause of capsule failure (for example, leakage from initial weld defects, enhanced corrosion at welds, loss of effective wall due to prior corrosion, stress corrosion, etc.). An AISI 316 SS capsule with technical-grade Li_2CO_3 failed within the last 100 hours of its 2027-hour test period. Similarly, a 316 SS capsule containing technical-grade 82 Na_2CO_3-18 K_2CO_3 failed in the last 100 hours of its 3083-hour test duration.

AISI 310 SS generally exhibited significantly improved compatibility with Li_2CO_3 at 850°C as compared to Types 304 and 316 SS. Its higher corrosion resistance is related to the more dense, adherent, and protective oxide scales formed on this alloy. The nature and extent of the scales formed on AISI 310 SS in technical-grade Li_2CO_3 after 1603 and 3083 hours illustrate their protective nature, as shown in Figure 29. As discussed for the 750°C test series, Type 310 SS specimens also experienced significant sigma phase formation throughout the capsule wall at grain boundaries and triple points.

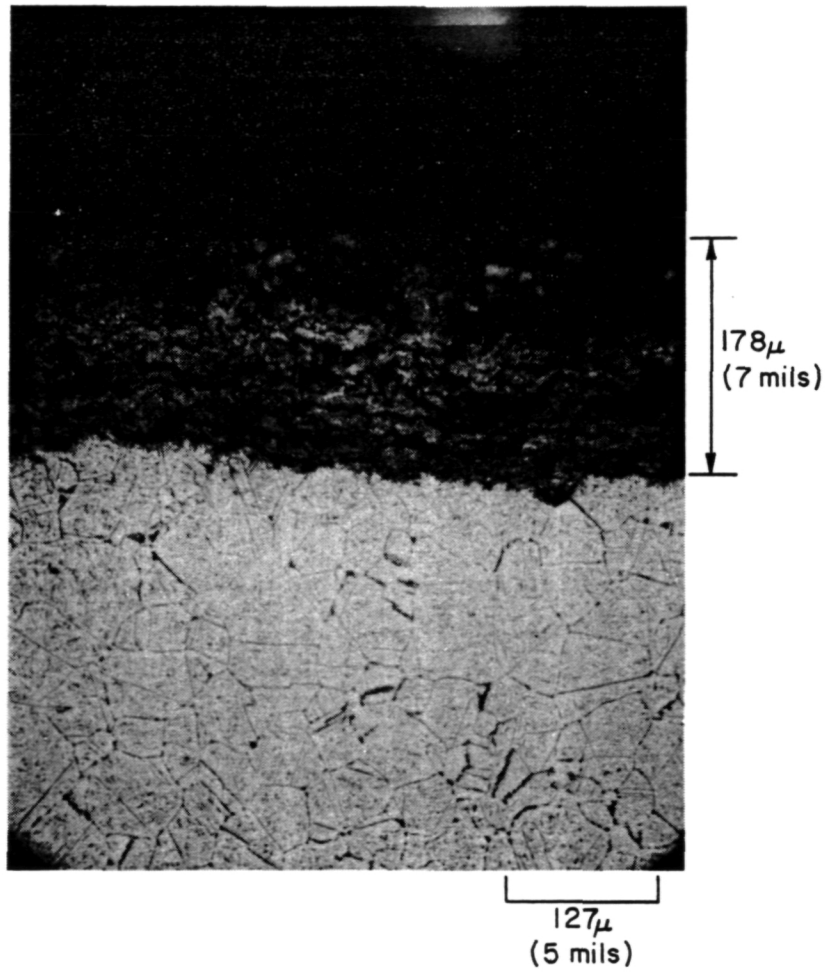

Figure 28. OPTICAL MICROGRAPH OF AISI 304 SS TESTED IN TECHNICAL-GRADE Li_2CO_3 FOR 2635 HOURS AT 850°C (With Graphite TCE Specimens/Ar Cover Gas)

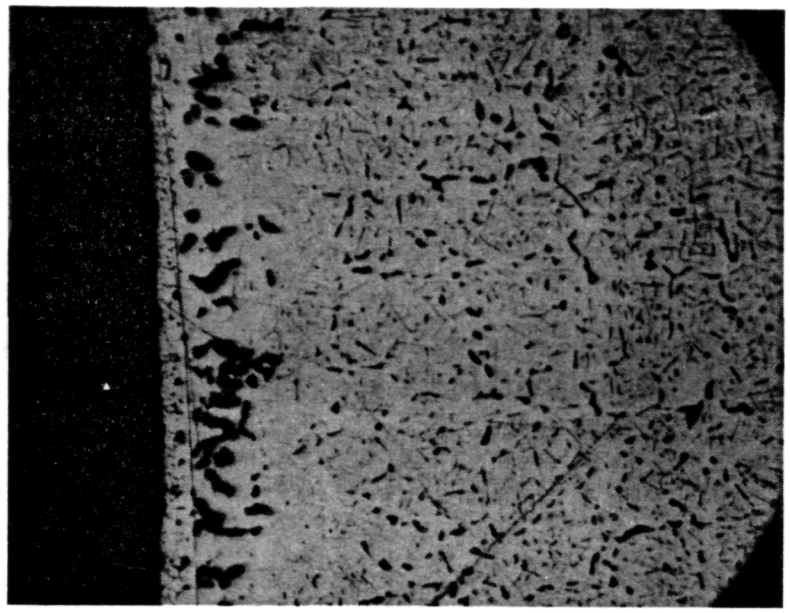

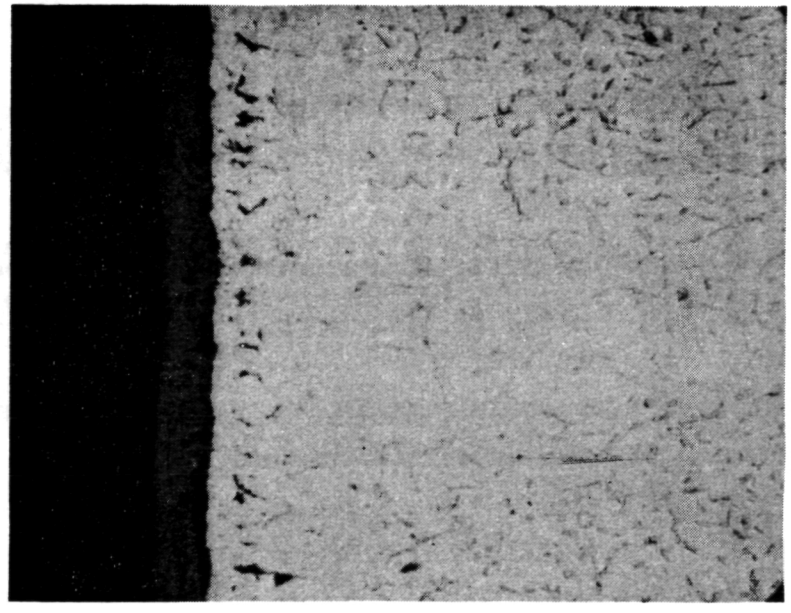

Figure 29. OPTICAL MICROGRAPHS OF AISI 310 SS TESTED IN TECHNICAL-GRADE Li_2CO_3 AT 850°C AFTER 1603 HOURS (A) AND 3083 HOURS (B)

Figure 30 shows the morphology and distribution of sigma phase precipitates at a capsule mid-wall location after 1603 hours of testing. It appears from the micrographs in Figure 29 that sigma phase particles may be undergoing preferential attack by molten Li_2CO_3, as evidenced by the 2 to 4 mil-deep subscale pitting effects. Systematic and repeated metallographic examinations of test specimens in both the as-polished and etched conditions indicated that the subscale pits were indeed associated with molten salt effects and not metallographic preparation or etching effects. (It should also be noted that the smaller grain boundary pits shown in Figure 29 (Part B) are etching effects and are unrelated to any molten carbonate interactions). The subscale leaching of sigma phase is attributed to the fact that sigma phase precipitates formed in AISI 310 SS (nominal composition of 25% Cr, 21.5% Ni, 2% Mn, 1.5% Si, balance Fe) are expected to be enriched in chromium, with an approximate composition of 46% Cr, 40% Fe, 11% Ni, and 3% Si.[51] In the presence of molten Li_2CO_3 under an oxidizing environment, metallic Cr is unstable and will be converted to Li_2CrO_4 (lithium chromate). The alkali chromates are very soluble in the corresponding molten alkali carbonates, which result in the leaching phenomenon. John[33] reported complete miscibility between Na_2CrO_4 and molten Na_2CO_3 at 900°C. Previous work at IGT related to molten carbonate fuel cell materials development also indicated extensive solubility of Li_2CrO_4 in molten Li_2CO_3-K_2CO_3 mixtures at 650°C.[39,40] Table 20 contains pre- and post-test analyses of Li_2CO_3 that demonstrate the salt's general stability, while indicating an increase in iron content of technical-grade Li_2CO_3 from <0.01% to 0.54% and an increase in chromium content from <0.02% to 0.11% after 1603 hours.

The 82 Na_2CO_3-18 K_2CO_3 composition was more aggressive toward AISI 310 SS than Li_2CO_3. The reagent-grade salt caused a 15 mil-deep reaction zone due to a combination of oxidation and apparent salt penetration along grain boundaries after 1603 hours, as shown in Figure 31. As in the Li_2CO_3 tests, the extensive amount of sigma phase precipitation and subsequent alkali chromate formation and dissolution are suspected to be the causes of this extensive reaction. An AISI 310 SS capsule containing technical-grade 82 Na_2CO_3-18 K_2CO_3 failed after 2779 hours.

Consistent with the 750°C tests, results from the 850°C series tests indicate that Inconel 600 and Incoloy 800 offer greater corrosion resistance

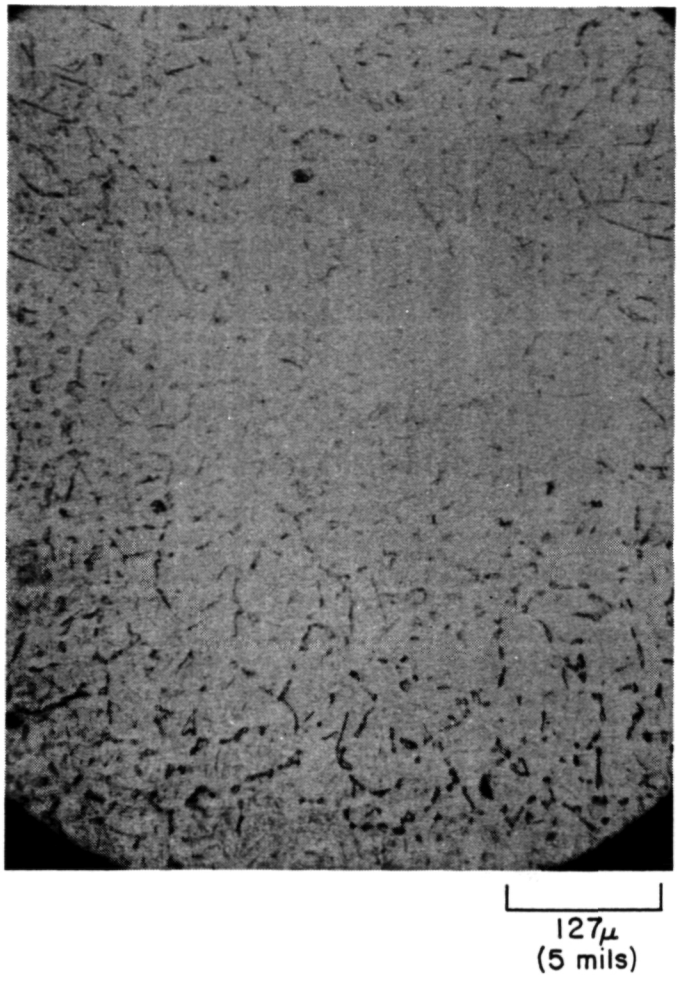

Figure 30. ETCHED MICROSTRUCTURE OF AISI 310 SS AT CAPSULE MID-WALL AFTER 1603 HOURS OF TESTING IN TECHNICAL-GRADE Li_2CO_3 AT 850°C SHOWING EXTENSIVE SIGMA PHASE FORMATION

Table 20. PRE- AND POST-TEST CHEMICAL ANALYSIS OF Li_2CO_3 AT 850°C

Salt	Grade	In Containment	Chemical Analysis, wt % $CO_3^=$	Li	Fe	Cr	Ni	Hours
			Pre-Test					
Li_2CO_3	Reagent	--	80.6	18.7	<0.01	<0.02	<0.01	--
	Technical	--	80.2	18.6	<0.01	<0.02	<0.01	--
			Post-Test					
Li_2CO_3	Reagent	310 SS	79.5	18.7	0.31	0.04	0.09	1603
	Technical	310 SS	78.5	18.7	0.54	0.11	0.17	1603
	Technical	Incoloy 800	78.3	18.2	0.66	0.18	0.24	3106

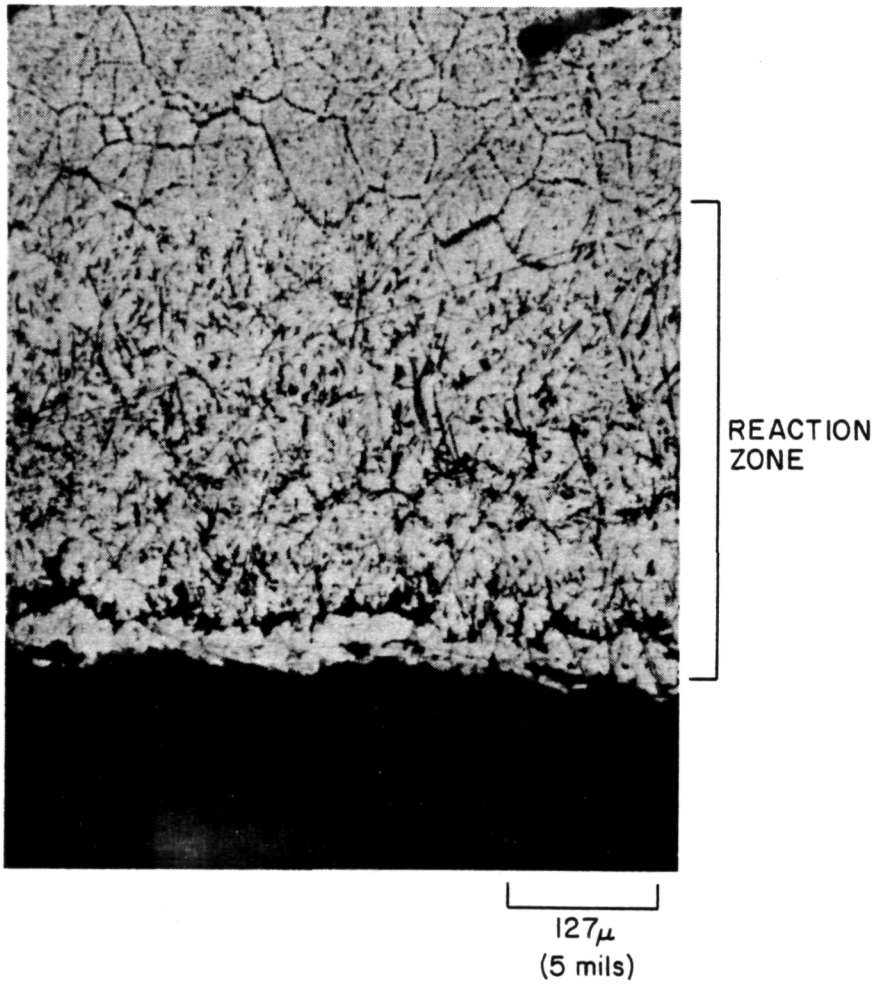

Figure 31. AISI 310 SS TESTED IN REAGENT-GRADE $82Na_2CO_3$-$18K_2CO_3$ FOR 1603 HOURS AT 850°C

than AISI 304 and 316 SS. Also, although oxide scale and surface reaction zone thicknesses in the 600 and 800 alloys were comparable to those in 310 SS, these alloys are not susceptible to sigma phase formation, which may limit the usefulness of AISI 310 SS as a containment and heat exchanger material under high-temperature thermal cycling conditions.

Figure 32 shows the microstructures of Inconel 600 and Incoloy 800 after 3106 hours of testing in molten technical-grade Li_2CO_3. Oxide scales were formed on both alloys; in addition, Inconel 600 exhibited some subscale pitting while Incoloy 800 showed intergranular attack extending ~5 mils below the scale. Both effects would be cause for some concern with respect to acting as possible points of stress concentration and crack initiation under thermal cycling conditions.

In molten 82 Na_2CO_3-18 K_2CO_3, Inconel 600 experienced a 2-mil scale formation in the reagent-grade mixture, accompanied by extensive subscale carburization after 1931 hours. As also observed with the 300-series austenitic stainless steels, the technical-grade mixture of this salt was more aggressive toward Inconel 600 than the reagent-grade, resulting in a 10-mil-thick zone of oxidation and bulk penetration after only 1176 hours of test. Incoloy 800 was determined to be the preferred containment material for technical-grade 82 Na_2CO_3-18 K_2CO_3. As revealed in the micrograph of Figure 33, this alloy formed a fairly protective 1 to 2-mil-thick oxide scale after 3106 hours with no significant subscale pitting, intergranular penetration, or carburization effects. The stability/compatibility of the technical-grade 82 Na_2CO_3-18 K_2CO_3 salt mixture was also demonstrated by no change in its pre- and post-test chemical composition and an increase in iron content from <0.01% to 0.25% after 3107 hours at 850°C. (See Table 21.)

Containment/Salt Compatibility Tests at 910° to 950°C

Results of post-test metallographic examinations of containment capsule materials tested in the 910° to 950°C temperature range are presented in Table 22. The carbonate salts tested in this series were reagent and technical grades of Na_2CO_3 (858°C mp) and K_2CO_3 (891°C mp). Phase I tests in this series were conducted at 950°C starting with undehydrated salt materials and with the original capsule weld design and fabrication procedures discussed earlier in Section 1.3, Experimental Test Components (as was the case for the 750°C and 850°C test series). The high rate of Phase I capsule failures due

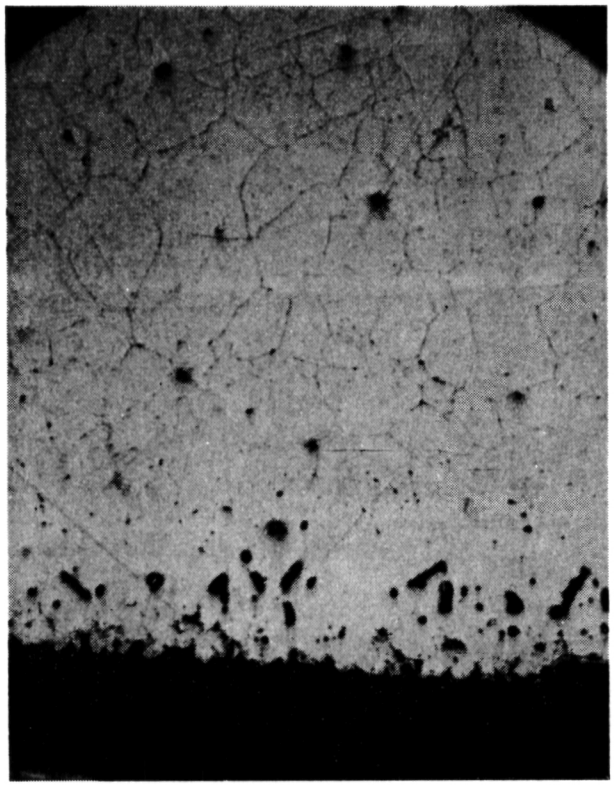

A. INCONEL 600

127μ
(5 mils)

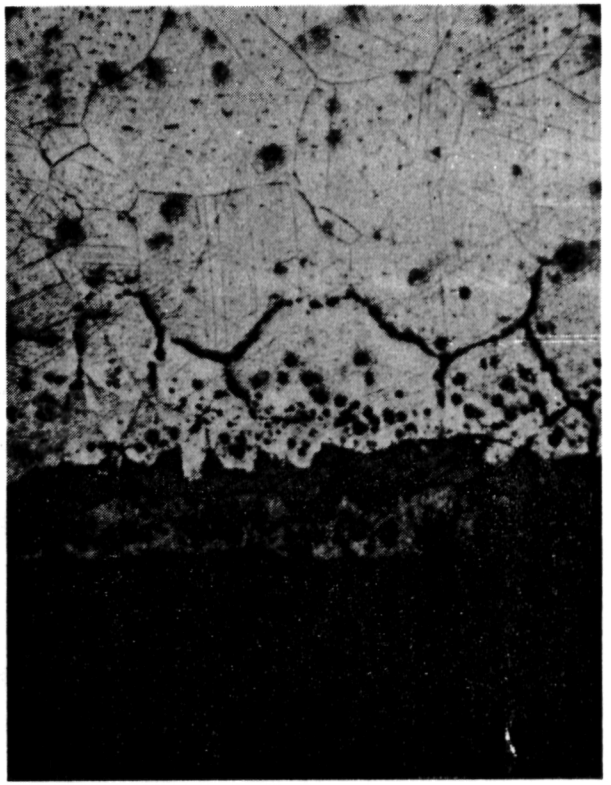

B. INCOLOY 800

127μ
(5 mils)

Figure 32. ALLOYS INCONEL 600 (A) AND INCOLOY 800 (B) AFTER 3106 HOURS OF TESTING IN TECHNICAL-GRADE Li_2CO_3 AT 850°C

Figure 33. INCOLOY 800 AFTER 3106 HOURS OF TESTING IN TECHNICAL-GRADE $82Na_2CO_3$-$18K_2CO_3$ AT 850°C

Table 21. PRE- AND POST-TEST CHEMICAL ANALYSIS OF $81Na_2CO_3$-$19K_2CO_3$ AT 850°C

Salt	Grade	In Containment	Chemical Analysis, wt %						Hours
			$CO_3^=$	Na	K	Fe	Cr	Ni	
Pre-Test									
$81Na_2CO_3$-$19K_2CO_3$	Technical	--	54.0	30.8	8.1	<0.01	<0.02	<0.01	--
Post-Test									
$81Na_2CO_3$-$19K_2CO_3$	Technical	Incoloy 800	53.9	34.4	9.8	0.25	<0.01	<0.012	3107

Table 22. RESULTS OF CONTAINMENT/SALT COMPATIBILITY TESTS AT 910° TO 950°C

	Alloy	1	2	3	4	5
No.	Salt, wt %	AISI 304 SS	AISI 316 SS	AISI 310 SS	Inconel 600	Incoloy 800
9	Na_2CO_3 Reagent	288 h at 950°C Capsule failure	288 h at 950°C Capsule failure	763 h at 950°C Capsule failure	288 h at 950°C Capsule failure	816 h at 950°C 25 mil oxidation and salt penetration
10	Na_2CO_3 Technical	552 h at 950°C Capsule failure 816 h at 910°C Capsule failure	288 h at 950°C Capsule failure 960 h at 910°C Capsule failure	763 h at 950°C Capsule failure	288 h at 950°C Capsule failure 1272 h at 910°C 8-9 mil oxidation and salt penetration 230 h at 910°C 21 mil oxidation and salt penetration	816 h at 950°C 17 mil oxidation and salt penetration 1656 h at 910°C 20 mil oxidation and salt penetration
11	K_2CO_3 Reagent	288 h at 950°C Capsule failure	288 h at 950°C Capsule failure	1490 h at 950°C 50 mil oxidation and salt penetration Sigma phase	1803 h at 910°C 40 mil reaction zone	816 h at 950°C 11 mil oxidation and salt penetration
12	K_2CO_3 Technical	552 h at 950°C Capsule failure 984 h at 910°C 16 mil scale	816 h at 910°C 4-5 mil scale Minor carburization	1490 h at 950°C 37 mil oxidation and salt penetration Sigma phase	816 h at 950°C 28 mil oxidation and salt penetration Moderate carburization 1056 h at 910°C 20 mil oxidation and salt penetration Extensive carburization	816 h at 950°C 15 mil oxidation and salt penetration 1152 h at 910°C 11 mil oxidation and salt penetration

B83050861

to salt leakage was attributed to inadequate weld design, insufficient depth of weld penetration, and internal gas pressure buildup due to evolution of adsorbed water (primarily from K_2CO_3-containing compositions). The failure rate of Phase I capsules at 950° was higher than at 750°C or 850°C, especially for the 300-series stainless steels. In addition to these welding and moisture-related problems, the significant loss of strength of the austenitic stainless steels undoubtedly also contributed to their high rate of failures early in life at 910°C to 950°C. Fabrication procedures for Phase II capsule tests were modified to provide improved design and integrity of capsule welds. In addition, the test temperature for this series was reduced from 950° to 910°C to provide a more realistic assessment of alloy corrosion resistance in the most cost-effective alkali carbonate heat storage medium available, Na_2CO_3. This 910°C test temperature used in Phase II evaluations was selected because it was approximately 50°C above the 858°C melting point of Na_2CO_3.

The test results in Table 22 indicate a significant failure rate of AISI 304 and 316 SS capsules in Phase II, in spite of the lower test temperature of 910°C and modified capsule fabrication procedures. All six 304 or 316 SS capsules tested in Na_2CO_3 failed before 1000 hours of testing had been attained. One 304 SS capsule survived 984 hours of testing in technical-grade K_2CO_3 at 910°C and experienced oxide scale formation to a depth of 16 mils. A 316 SS capsule tested successfully in the same salt for 816 hours at 910°C was found to be oxidized to a depth of 4 to 5 mils.

Two capsules of 310 SS tested with Na_2CO_3 (reagent and technical) both failed during 763-hour tests at 950°C. The 310 SS capsules containing reagent-and technical-grade K_2CO_3 formed reaction zones from oxidation and bulk penetration to depths of 50 mils and 37 mils, respectively, after 1490 hours at 950°C. The significant extent and nature of 310 SS corrosion in technical-grade K_2CO_3 is illustrated in Figure 34. As in the 750° and 850°C tests discussed above, 310 SS suffered from extensive precipitation of sigma phase at grain boundaries, apparently contributing to the significant intergranular penetration and grain boundary separations observed at 950°C.

The alloys Inconel 600 and Incoloy 800 were also more badly corroded at 910° to 950°C than at the lower test temperatures. Inconel 600 experienced salt reaction layers ranging from 8 to 40 mils in thickness, depending on salt

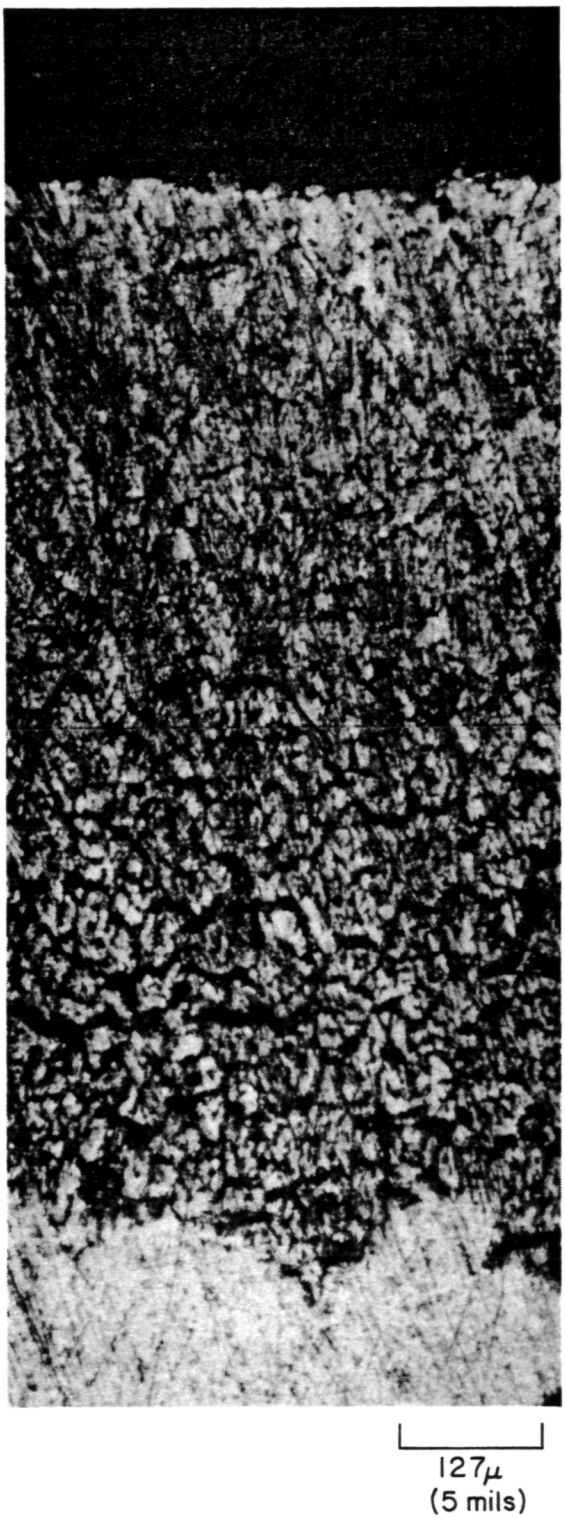

Figure 34. EXTENSIVE CORROSION OF AISI 310 SS AFTER 1490 HOURS IN TECHNICAL-GRADE K_2CO_3 AT 950°C

composition and exposure time and temperature. The microstructures of the reaction zones on Inconel 600, whether caused by Na_2CO_3 or K_2CO_3, were very similar; a typical reaction layer, formed in technical-grade Na_2CO_3 after 2304 hours at 910°C, is shown in Figure 35. Table 23 presents some additional experimental data for Inconel 600 tested with copper or graphite TCE materials in Na_2CO_3 and K_2CO_3 with Ar cover gas.

The corrosion behavior of Incoloy 800 in molten Na_2CO_3 and K_2CO_3 was not significantly different from that of Inconel 600. Salt reaction zones formed on inner capsule walls to depths of 11 to 25 mils, depending on the particular experimental conditions employed, as summarized in Table 22. The appearance of a typical reaction zone formed on Incoloy 800 in molten Na_2CO_3 (technical grade) after 816 hours at 950°C is shown in Figure 36. Technical-grade Na_2CO_3 pre- and post-test chemical analysis data show its good stability and an increase in iron content from <0.01% to 0.32% (Table 24), when in contact with Incoloy 800 for 816 hours at 950°C.

A representative micrograph showing the nature and extent of Incoloy 800 reaction with technical-grade K_2CO_3 is shown in Figure 37. In this case, exposure at 950°C for 816 hours has resulted in a 15-mil-deep surface reaction zone of oxidation and salt penetration. Some intergranular cracks were observed in this salt-affected surface zone. Both intragranular and grain-boundary carbides that formed during prolonged heating at the test temperature can be seen below this surface zone.

Adequate long-term containment of molten Na_2CO_3 and K_2CO_3 at temperatures of 900°C and above represents a significant materials challenge, as evidenced by the high rate of capsule failures and the inability of the commercial alloys tested to form protective oxide films or scales. The lack of any protective scale formation is indicated by the nearly linear rate of increase in depth of surface reaction zone between 1200 and 2700 hours of exposure of Inconel 600 to technical-grade Na_2CO_3 at 910°C, as shown in Figure 38. Significant additional alloy materials and/or coatings development efforts will be required to satisfy long-term containment and heat exchanger requirements for such high-temperature molten carbonate TES systems.

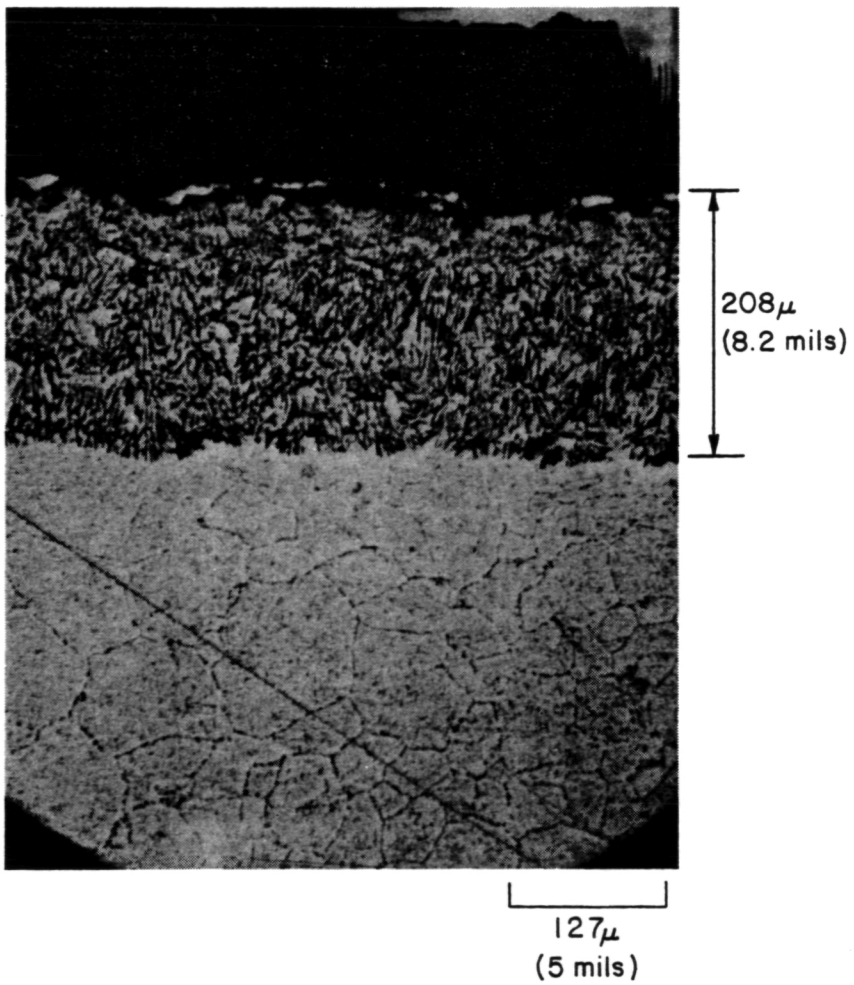

Figure 35. TYPICAL CORROSION LAYER FORMED ON INCONEL 600 AFTER 2304 HOURS OF TESTING IN TECHNICAL-GRADE Na_2CO_3 AT 910°C

Table 23. INCONEL 600/SALT COMPATIBILITY TESTS CONDUCTED WITH TCE MATERIALS
(Argon Cover Gas)

Containment Material	Salt*	TCE Materials**	Exposure	Results
Inconel 600	Na_2CO_3	PG, ATJ	2714 hr at 910°C	13-14 mil reaction zone - Intergranular penetration
Inconel 600	Na_2CO_3	Cu	2714 hr at 910°C	27-28 mil reaction zone
Inconel 600	K_2CO_3	PG, ATJ	2714 hr at 910°C	15-16 mil reaction zone - Intergranular penetration
Inconel 600	K_2CO_3	Cu	2714 hr at 910°C	19-20 mil reaction zone - Intergranular penetration

* Technical-grade salts.

** PG: Pyrolytic graphite
ATJ: Union Carbide ATJ graphite
Cu: Porous reticulated and tubular copper.

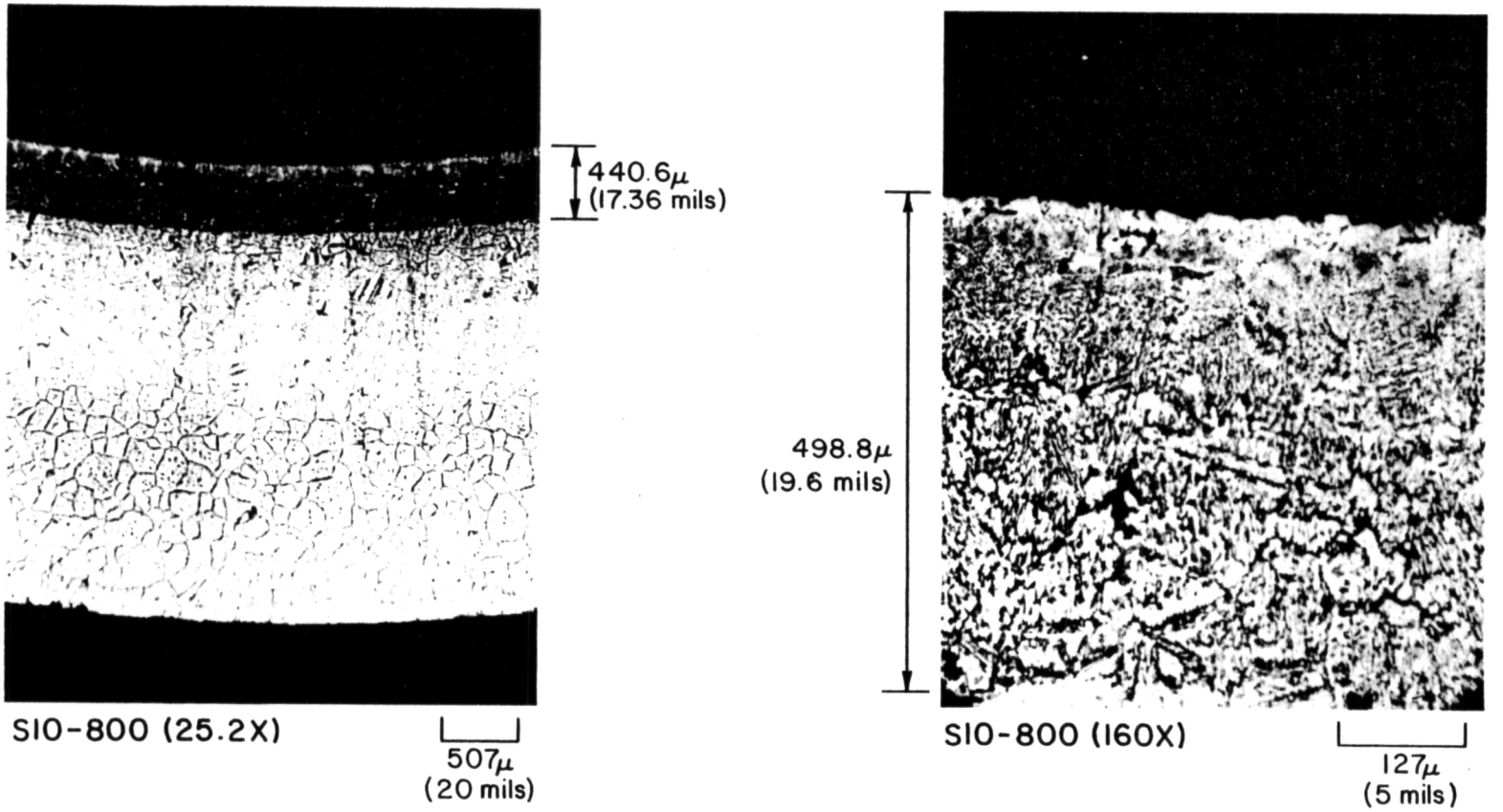

Figure 36. APPEARANCE OF INCOLOY 800 AT MID-SALT LOCATION AFTER 816 HOURS OF TESTING IN TECHNICAL-GRADE Na_2CO_3 AT 950°C

Table 24. PRE- AND POST-TEST CHEMICAL ANALYSIS OF Na_2CO_3 AT 910° TO 950°C

Salt	Grade	In Containment	$CO_3^=$	Na	Fe	Cr	Ni	Hours
			Pre-Test					
Na_2CO_3	Technical	--	56.3	39.0	<0.01	<0.02	<0.01	--
			Post-Test					
Na_2CO_3	Technical	Incoloy 800	54.6	40.1	0.32	<0.05	<0.012	816

Figure 37. APPEARANCE OF INCOLOY 800 AFTER 816 HOURS OF TESTING IN TECHNICAL-GRADE K_2CO_3 AT 950°C

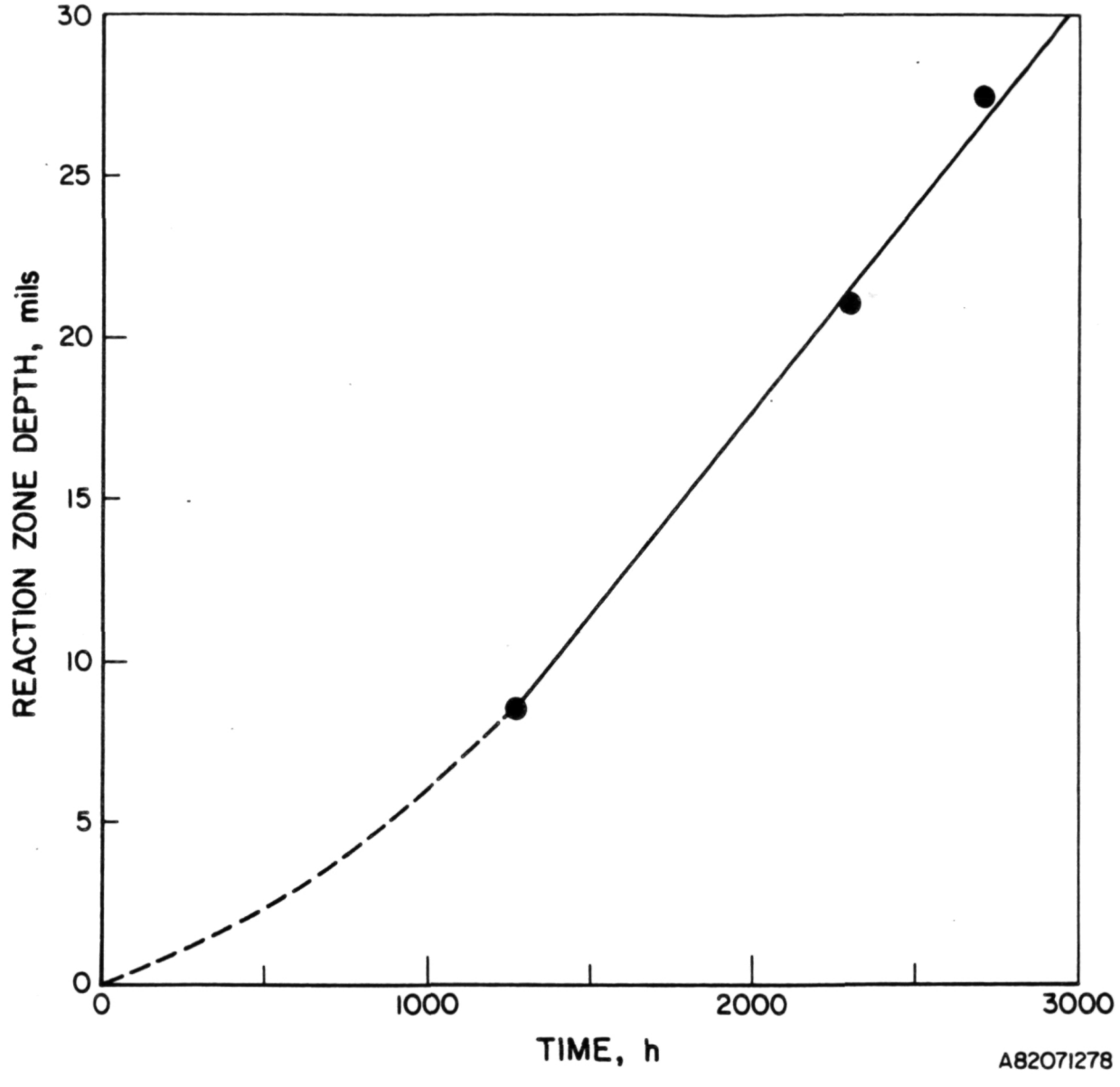

Figure 38. DEPTH OF SURFACE REACTION ZONES FORMED ON INCONEL 600 IN TECHNICAL-GRADE Na_2CO_3 AT 910°C

Evaluation of Aluminum-Containing Alloys as Containment Materials

The objective of this work element was to conduct a preliminary assessment of the feasibility of using aluminum-containing alloys as containment and heat exchanger materials for improved corrosion resistance in high-temperature molten carbonates. This activity included a limited experimental fabrication and compatibility study of commercially available alloys containing aluminum and AISI 304 and 316 SS specimens that were surface aluminized by a commercial process. The experimental study was intended to provide an initial indication of potential advantages and limitations of these approaches to containment of molten carbonates. A comprehensive corrosion behavior study of such materials was outside the scope of the program.

The commercial alloys included in the experimental study included Armco 12SR (1.25 wt % Al) and Kanthal A-1 (5.5 wt % Al). Complete nominal compositions of these alloys were presented earlier in Table 7. Alloy Kanthal A-1 wires have been used extensively in woven-screen form as reinforcement for molten carbonate fuel cell electrolyte structures and have demonstrated reasonably good compatibility in molten Li_2CO_3-K_2CO_3 at 650°C for greater than 10,000 hours of testing.

During the course of this investigation, discussions were conducted with researchers at the Products Research and Development Laboratories of Nippon Steel Corporation, Sagamihara, Japan, who are developing a family of high-aluminum austenitic stainless steels for high-temperature use. These experimental alloys, which contain 4 to 6 weight percent aluminum, form thin protective Al_2O_3 films which are claimed to provide superior air oxidation and hot corrosion resistance compared to that of commercially available heat-resisting stainless steels at temperatures above 850°C. Unfortunately, no specimens of the experimental Nippon alloys could be obtained for evaluation of molten carbonate corrosion resistance under this program. However, because these alloys appear to possess significant promise for containment of high-temperature molten salts, a brief summary of their possible advantages for molten carbonate TES applications is presented.

The Nippon experimental alloys are of nominal composition 17Cr-24Ni-5Al-balance Fe and are austenitic. A minimum aluminum content of 5 weight percent and chromium contents of 15 to 22 weight percent have been found to provide a

very protective Al_2O_3 film, which is non-spalling and yields greater oxidation resistance than typical stainless steels such as AISI 310 or Incoloy 800. Additions of cerium (~0.5%) and/or titanium (0.06%) further enhance the film's non-spalling characteristics under thermal cycling conditions and also improve hot-workability. Because chromium and aluminum tend to stabilize the ferrite phase, the nickel content must be adjusted in relation to the aluminum and chromium contents to assure stability of the austenite structure. Tests at Nippon show —

- Superior air oxidation resistance at 1200°C as compared to Incoloy 800
- Greater resistance to hot corrosion by Na_2SO_4 + 10% NaCl at 1000°C than AISI 310 SS and Incoloy 800
- Improved resistance in cyclic air oxidation tests (1200°C to room temperature) over AISI 310 SS
- Tensile and creep rupture strengths at 800° to 1000°C as compared to those of Incoloy 800.

Based on these promising indications, these Nippon alloys should be experimentally evaluated for corrosion compatibility with molten carbonate storage media. In addition, alloy weldability should be evaluated because of the known effect of moderate levels (~5%) of aluminum in reducing fluidity of molten weld metal. Also, the effect of long-term exposure at high temperatures on alloy phase stability and mechanical properties should be investigated.

The possible use of aluminized stainless steels or nickel-base alloys for corrosion protection was suggested by the successful long-term stability (>10,000 hours) demonstrated by aluminized 316 SS hardware in molten carbonate fuel cell applications at 650°C. Aluminizing treatment studies were focused on the Alon* commercial process. Alloys of AISI 304 and 316 SS, Inconel 600, and Incoloy 800 were aluminized by the Alon process, although only the AISI 304 and 316 SS materials were experimentally tested in molten carbonate environments. Alonizing is a high-temperature (900° to 1000°C) pack-cementation process in which aluminum is diffused into the surface of the metal parts being treated. The process may be applied to a rather broad range

---

*Alon Processing, Inc., Grantham St., Tarentum, Pa. 15084

of iron- and nickel-base alloys. This vapor-phase diffusion process results in a metallurgically modified surface zone containing a high concentration of aluminum. The concentration and depth of aluminum in this surface zone depends upon time and temperature of treatment and upon the chemical composition of the alloy being treated. Depending on alloy composition, the surface zone generally consists of aluminum-containing alloys or intermetallic phases formed in the Fe-Al, Ni-Al, or Fe-Ni-Al systems. Subsequent use of these aluminized materials in even slightly oxidizing environments at high temperature results in formation of Al_2O_3-rich protective oxide layers, which afford enhanced resistance against oxidation, sulfidation, and carburization. The "alonizing" process is used to protect heat exchanger and process equipment in numerous petroleum refining, petrochemical, and chemical applications requiring duty in severe environments.[52,53]

Adequate long-term stability of aluminum-containing or aluminized alloys will depend largely on their ability to form dense, adherent, and non-spalling reaction layers that are essentially insoluble in molten carbonate environments. In molten carbonate fuel cell applications, such corrosion protection is afforded by formation of $LiAlO_2$-rich corrosion layers, which have very low solubilities in the Li_2CO_3-K_2CO_3 eutectic electrolyte at 600° to 700°C use temperatures. Similar protection would be expected in Li_2CO_3-containing TES melts at higher temperatures provided that the $LiAlO_2$-rich scales possess adequate physical and mechanical integrity to withstand thermal stresses generated during thermal charge/discharge cycling of the TES system.

In addition, there is significant interest in the use of Na_2CO_3-based carbonates for storage applications because of its relatively high heat of fusion (114 Btu/lb) and availability at a very low materials cost ($0.03/lb). In the case of pure Na_2CO_3 (858°C mp) and lower-melting Na_2CO_3-based mixtures containing K_2CO_3 or $BaCO_3$, corrosion protection of aluminum-containing alloys would be dependent on the stability of $NaAlO_2$-rich scales. The solubility of $NaAlO_2$ in molten Na_2CO_3 has been determined by two investigators[33,54] and has been found to be very low, as shown in Figure 39. The solubility is also very insensitive to temperature (activation energy of only -25.3 kcal/g-mol $NaAlO_2$) from 21.15 molar ppm at 878°C to 24.5 ppm at 1028°C. Thus, the low-solubility requirement for $NaAlO_2$-rich scale protection of alloys in Na_2CO_3-base melts is apparently satisfied.

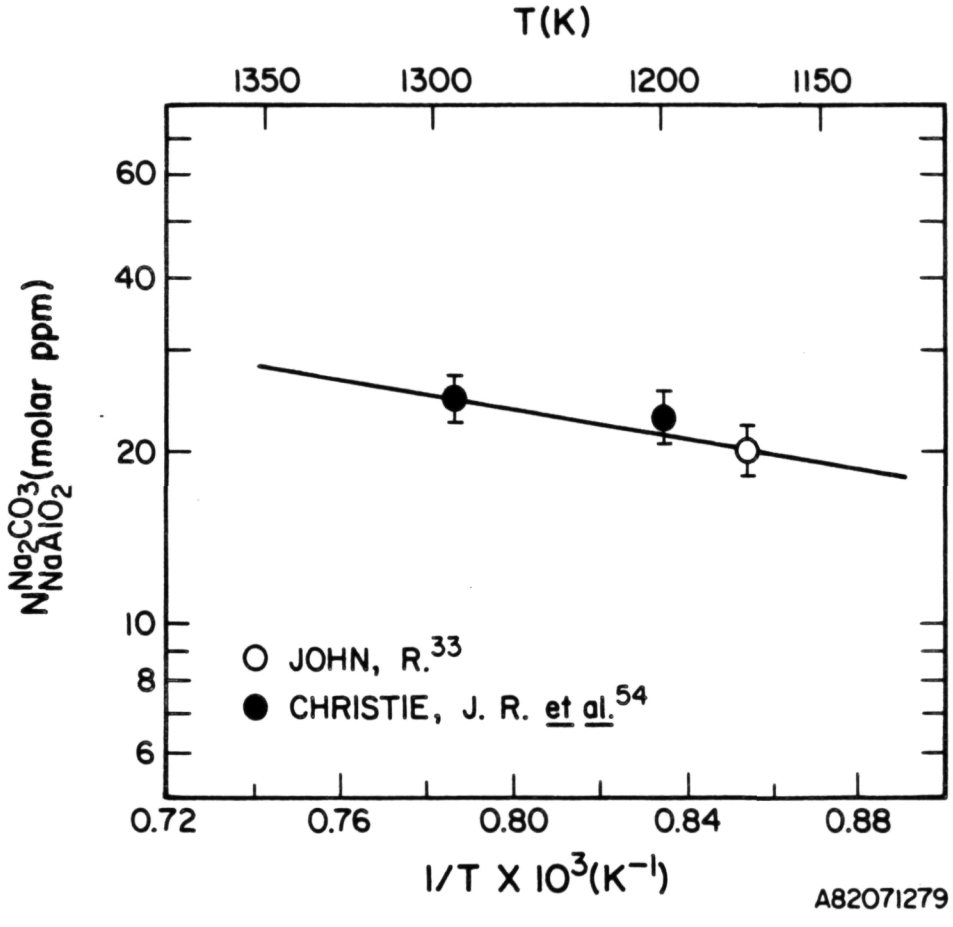

Figure 39. SATURATION SOLUBILITY OF $NaAlO_2$(s) IN Na_2CO_3(l) AS A FUNCTION OF RECIPROCAL TEMPERATURE

Experimental results obtained for the aluminum-containing alloys and aluminized (alonized) AISI 304 and 316 SS capsule materials are summarized in Table 25.

The carbonate salts employed for these tests were technical grades of the core salt mixtures, which spanned operating test temperatures from 750° to 910°C.

Surface aluminizing and testing was conducted on AISI 304 and 316 SS capsules identical in design to those in the core testing matrix (Figure 7). Fabrication/aluminizing of the capsules was completed in a five-step process:

1. Initial welding of one capsule end cap to its capsule body

2. Surface pack aluminizing of capsule body with one end weld and a separate "second" end cap. The threads of the "second" end cap and capsule body were "masked" by threading on sacrificial open-both-ends nipples and end caps (respectively) prior to aluminization. This would ensure final threaded fit of the "second" end-cap to its mate-capsule body after final salt loading.

3. Final salt-loading

4. Machining removal of aluminized coating at two key weld-contact areas (to facilitate final welding of capsule). This "unalonized" weld and mated thread end of the capsule was orientated as the "top" portion of any capsule in the test furnaces, opposite from the molten salt mixture during actual operation.

5. Final welding of unalonized "second" end cap to the capsule body.

The photomicrographs of Figures 40 and 41 reveal the pre-test structure of AISI 304 and 316 SS that have been pack vapor diffusion aluminized. In stainless steels that undergo this process, distinct diffusion zones typically result. Over 50% aluminum is present in the outer surface layer. The amount of aluminum decreases through the intermetallic zone to the alloy/substrate interface, at which point the aluminum content drops to zero. This diffusion zone (~29 and 23 mils in the AISI 304 and 316 SS samples, respectively) possesses the integrity of a true metallurgical alloy, with no holidays or voids.

750°C Tests: The alonized AISI 304 SS capsules generally exhibited more superior resistance to corrosion than the untreated samples in technical grades of both $52BaCO_3$-$48Na_2CO_3$ and $50Na_2CO_3$-$50K_2CO_3$. In each of these salts, alonized AISI 304 SS appeared relatively unaffected after 1344 hours of

Table 25. RESULTS OF ALUMINUM-CONTAINING ALLOYS/SALT COMPATIBILITY TESTS

Salt, wt %	Grade	Temp, °C	Alonized AISI 316 SS	Alonized AISI 316 SS	Alloy Armco 12SR	Alloy Kanthal A-1
$52BaCO_3$-$48Na_2CO_3$	Technical	750	1344 h 0 mil reaction scale 11 mil aluminized layer		2616 h 6-8 mil dense oxide layer Subscale localized carbide ppt.	2616 h 3-6 mil dense oxide layer Heavy subscale localized carbide ppt.
$50Na_2CO_3$-$50K_2CO_3$	Technical	750	1344 h 0 mil corrosion reaction scale 9.2 mils of Al reaction layer		1056 h 10-15 mil oxide slightly spalled Subscale g.b. ppt.	1056 h 1-2 mils oxide Bulk-slight localized carbide ppt at g.b. junction
Li_2CO_3	Technical	850	1608 h Failed in unalonized weld 17.5 mil sclae	50 h Failed in unalonized weld 6-7 mil Al reaction layer	2620 h 23-24 mil porous oxide scale Little bulk metal effects	2620 h 8-9 mil oxide layer Subscale 4 mils localized carbide ppt.
$80Na_2CO_3$-$20K_2CO_3$	Technical	850	1344 h Failed in unalonized weld	696 h Failed in unalonized weld		
Na_2CO_3	Technical	910	648 h Failed in last 100 h in unalonized weld 13-15 mil oxide scale	552 h 12-15 mils of Al reaction layer 2-3 mil top crusted scale subscale g.b. ppt.	1034 h 26-28 mil coarse oxide scale Heavy subscale g.b. ppt. especially at triple-points	1034 h 1-2 mil dense oxide Lightly pitted subscale
K_2CO_3	Technical	910	648 h Failed in unalonized weld 17-18 mil oxide scale Subscale g.b. ppt	648 h Failed in unalonized weld		

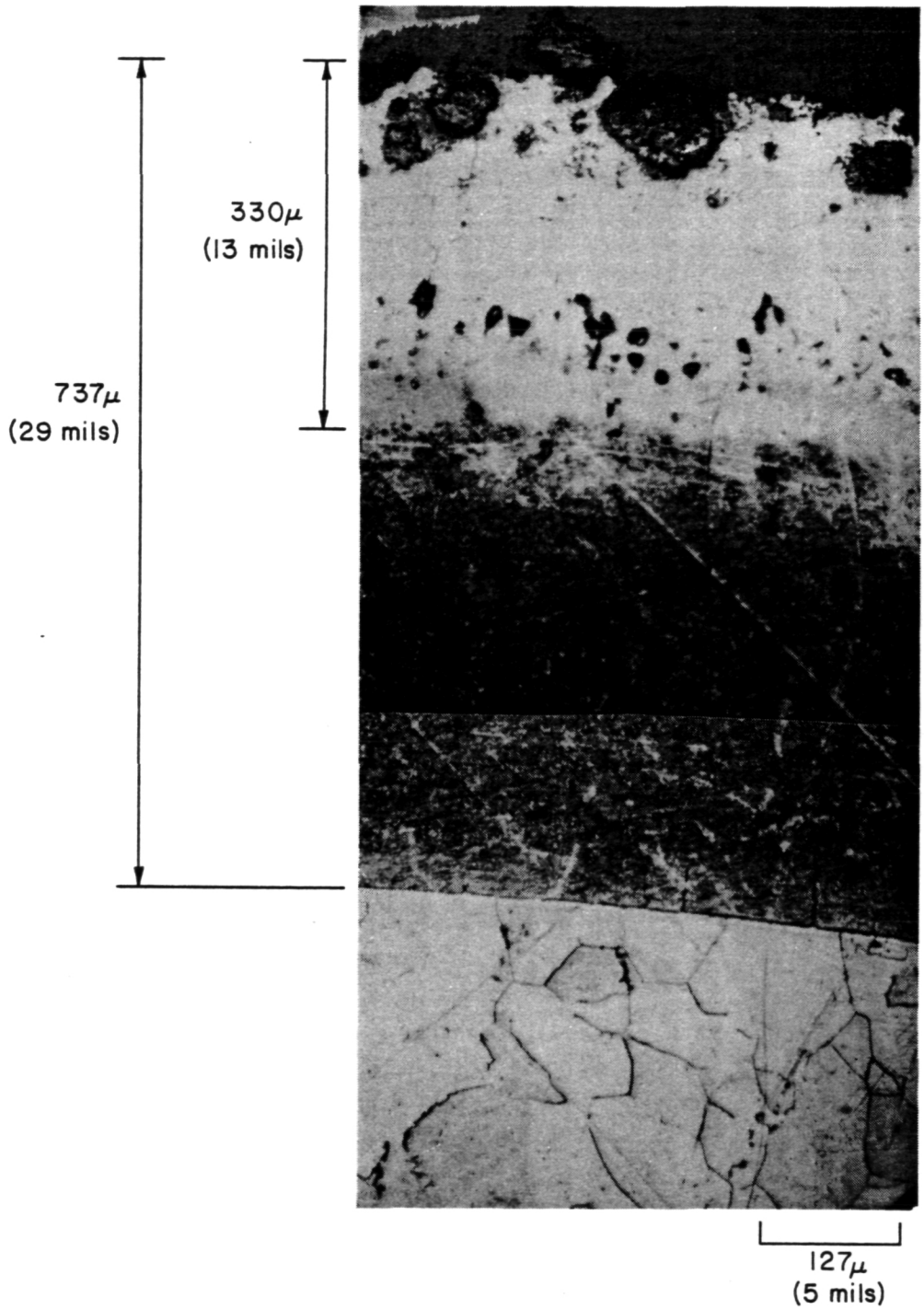

Figure 40. PRETEST PHOTOMICROGRAPH OF ALONIZED AISI 304 SS (160X)

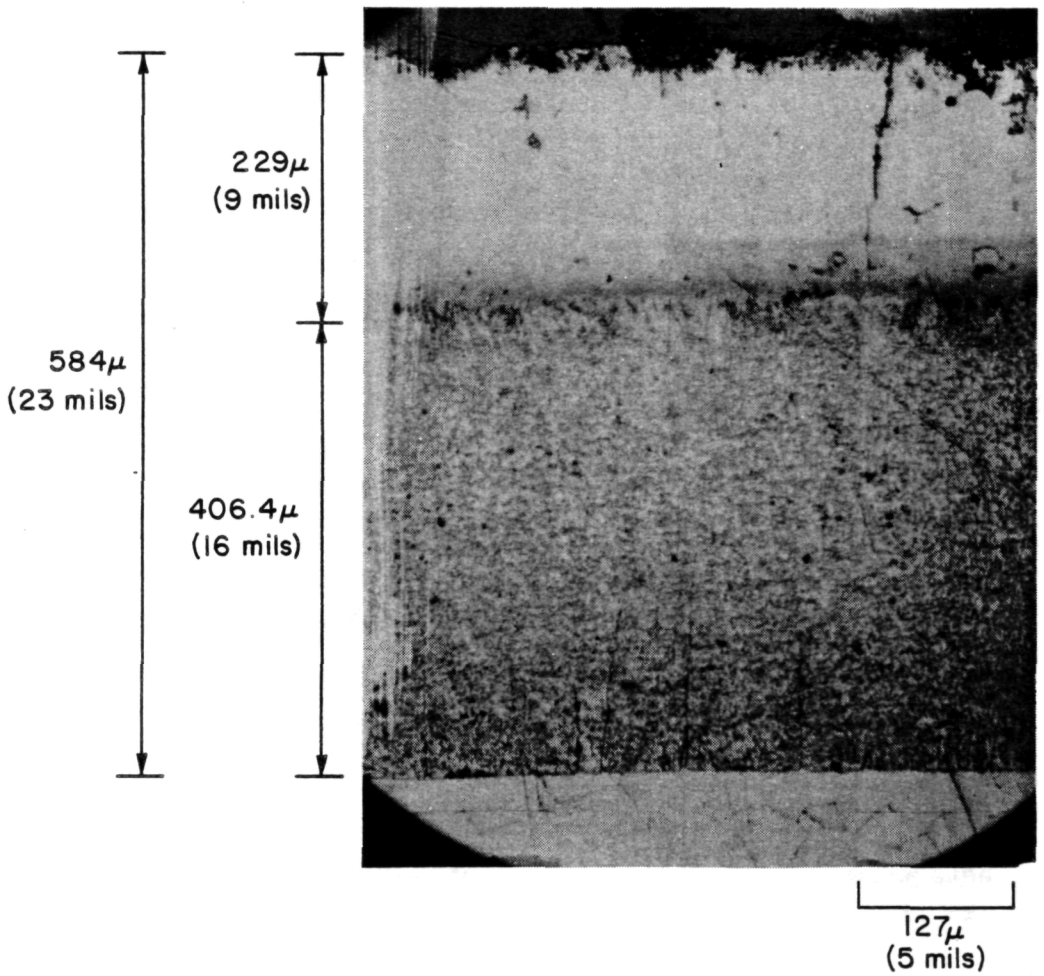

Figure 41. PRETEST PHOTOMICROGRAPH OF ALONIZED AISI 316 SS (160X)

testing. Figure 42 exhibits the undisturbed 11-mil aluminum intermetallic layer over a 304 SS substrate. The comparative advantages of aluminizing are shown in the micrograph of Figure 43 and the bar chart of Figure 44. The unprotected 304 SS resulted in a slightly porous oxide scale with a significant amount of carbide precipitation in the grains and grain boundaries. Although the alonized samples' outermost (higher Al) layer (3.6 mils) did fissure slightly, the remaining 60% (5.5 mils) of the 9.2-mil diffusion zone remained intact and undisturbed. The slight carbide precipitation in the bulk grain boundaries is solely the result of heat "sensitization."

The alloy Armco 12SR capsule bodies tested with technical-grade $52BaCO_3$-$48Na_2CO_3$ resulted in a 3 to 7-mil scale with some areas of very dense gray oxide and others with holidays and voids (Figure 45) after 2616 hours. The $50Na_2CO_3$-$50K_2CO_3$ salt mixture, however, exhibited an enhanced corrosive attack to Armco 12SR, with a 14 to 18-mil slightly spalled and porous oxide scale and carbide grain boundary precipitation (Figure 46) after 1050 testing hours.

An optical micrograph of sectioned as-received one-half inch diameter Kanthal A-1 rod is shown in Figure 47. The difference in characteristic grain structure between surface and midsample is possibly due to fabrication-related working effects.

Kanthal A-1 generally demonstrated excellent compatibility with carbonates from 750° to 910°C. After 2616 hours at 750°C, testing with technical-grade $52BaCO_3$-$48Na_2CO_3$ resulted in a dense Al_2O_3-rich 3 to 4-mil scale. There were voids observed in the as-polished condition that became more prominent on etching as clustered heat-affect carbide precipitation and pick-out at the grain-boundary triple-point junctions, which decreased from subsurface to midsample (Figure 48). It is uncertain whether this difference in grain structure from edge- to mid-sample was nucleated from the observed disparate pretest fabrication/work-induced stresses or a salt-related effect. Testing in $50Na_2CO_3$-$50K_2CO_3$ for 1056 hours revealed a uniform 1-mil reaction layer with 10 mils of a lightly pitted subscale region (Figure 49).

A comparative ranking of the scaling/corrosion resistance of the core- and aluminum-containing alloys at 750°C is presented in Figure 44 for containment of technical-grade $50Na_2CO_3$-$50K_2CO_3$.

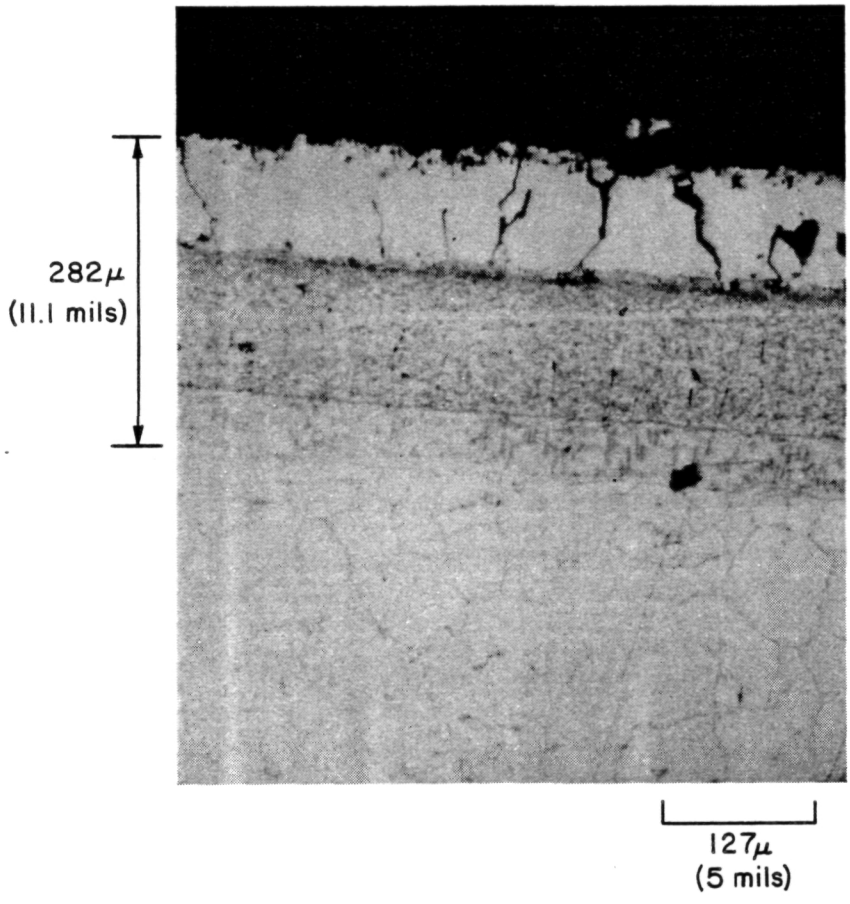

Figure 42. OPTICAL MICROGRAPH OF ALUMINIZED AISI 304 SS IN TECHNICAL-GRADE $52BaCO_3$-$48Na_2CO_3$ FOR 1344 HOURS AT 750°C (160X)

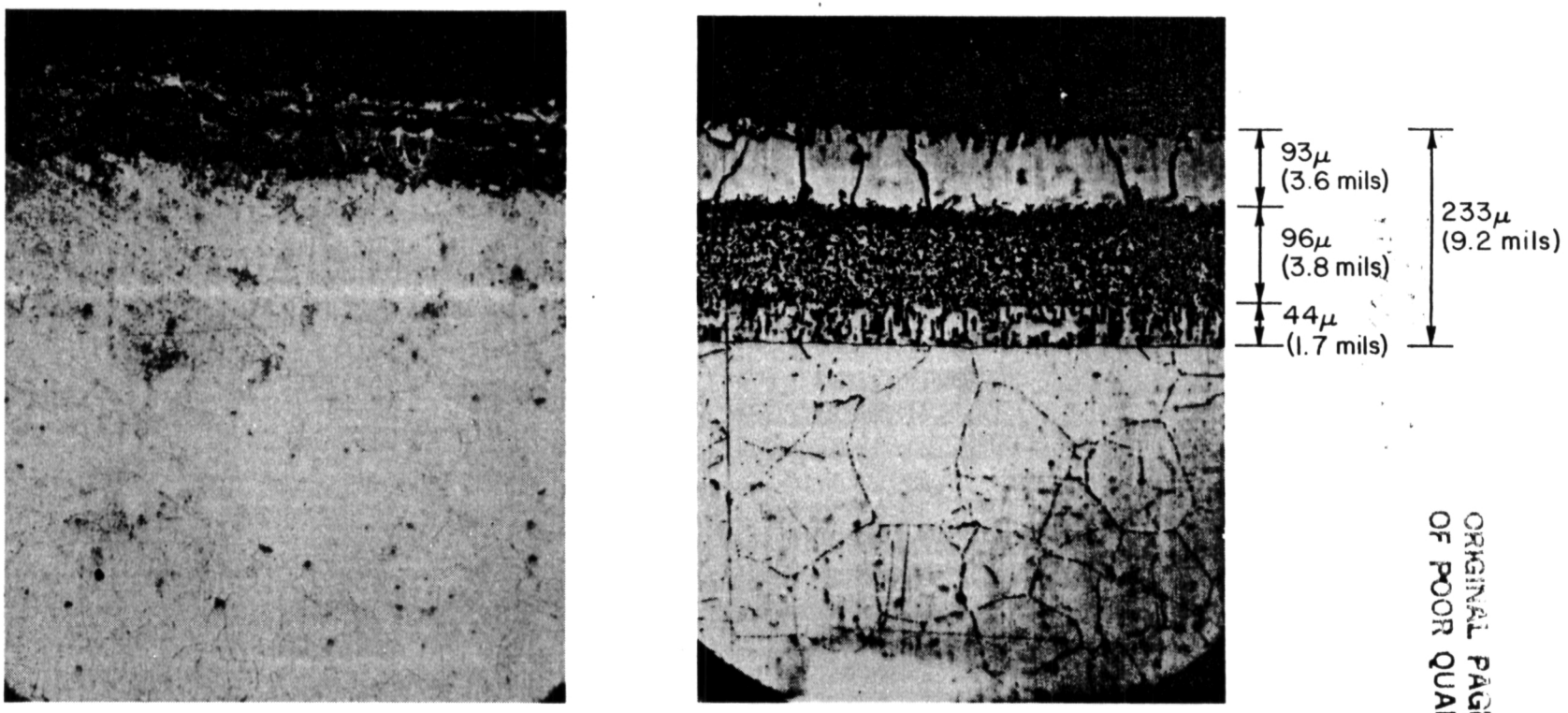

Figure 43. COMPARATIVE CORROSION LAYERS ON UNPROTECTED AND ALONIZED AISI 304 SS AFTER 1882 AND 1344 HOURS, RESPECTIVELY, IN TECHNICAL-GRADE $50Na_2CO_3$-$50K_2CO_3$ AT 750°C (160X)

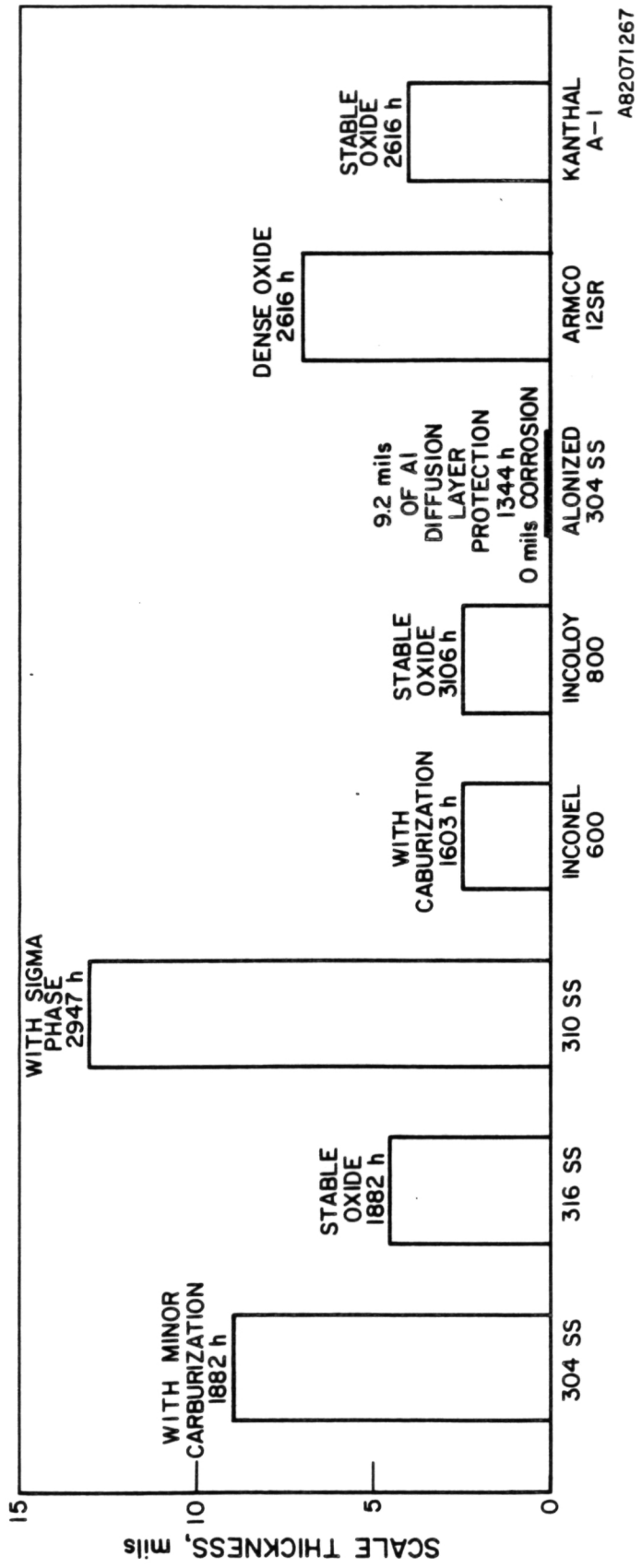

Figure 44. THICKNESS OF OXIDE SCALES FORMED ON CORE AND ALUMINUM-CONTAINING ALLOYS AFTER 1344 TO 3106 HOURS OF EXPOSURE TO TECHNICAL-GRADE $50Na_2CO_3$-$50K_2CO_3$ AT 750°C

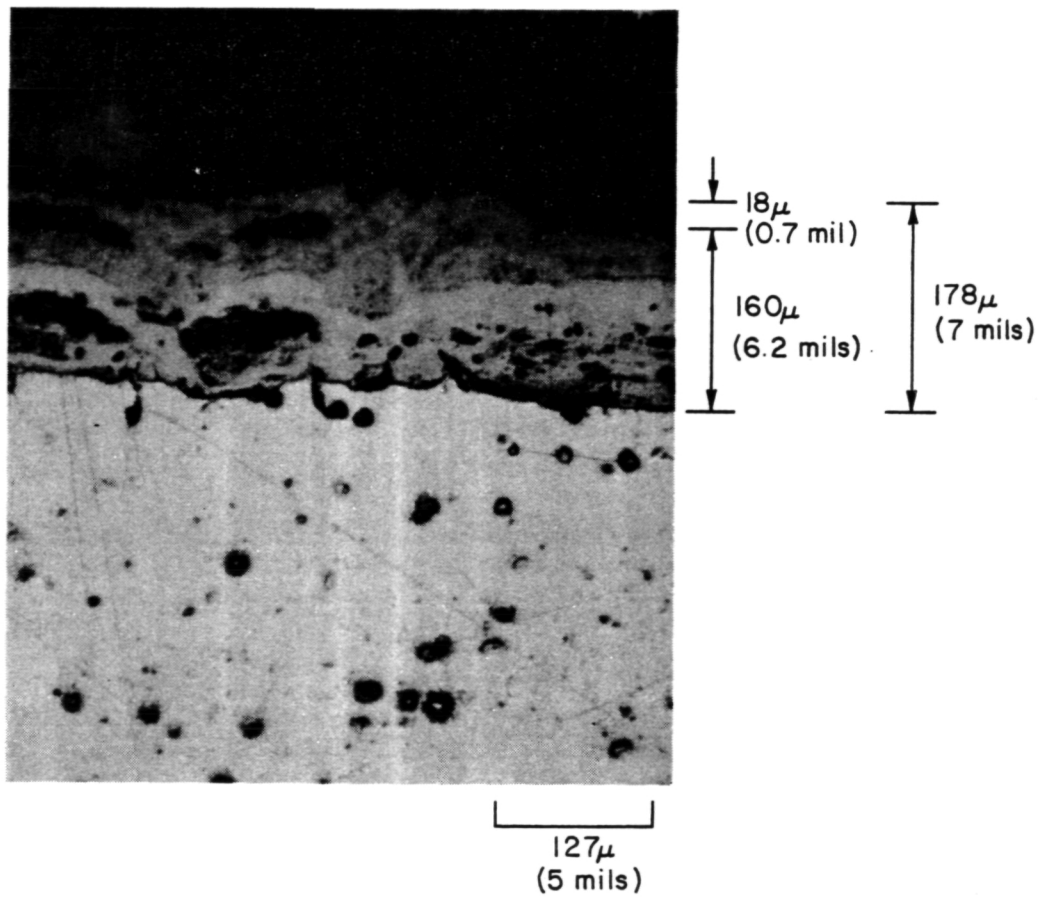

Figure 45. OPTICAL MICROGRAPH OF ALLOY ARMCO 12SR IN TECHNICAL-GRADE $52BaCO_3$-$48Na_2CO_3$ FOR 2616 HOURS AT 750°C (160X)

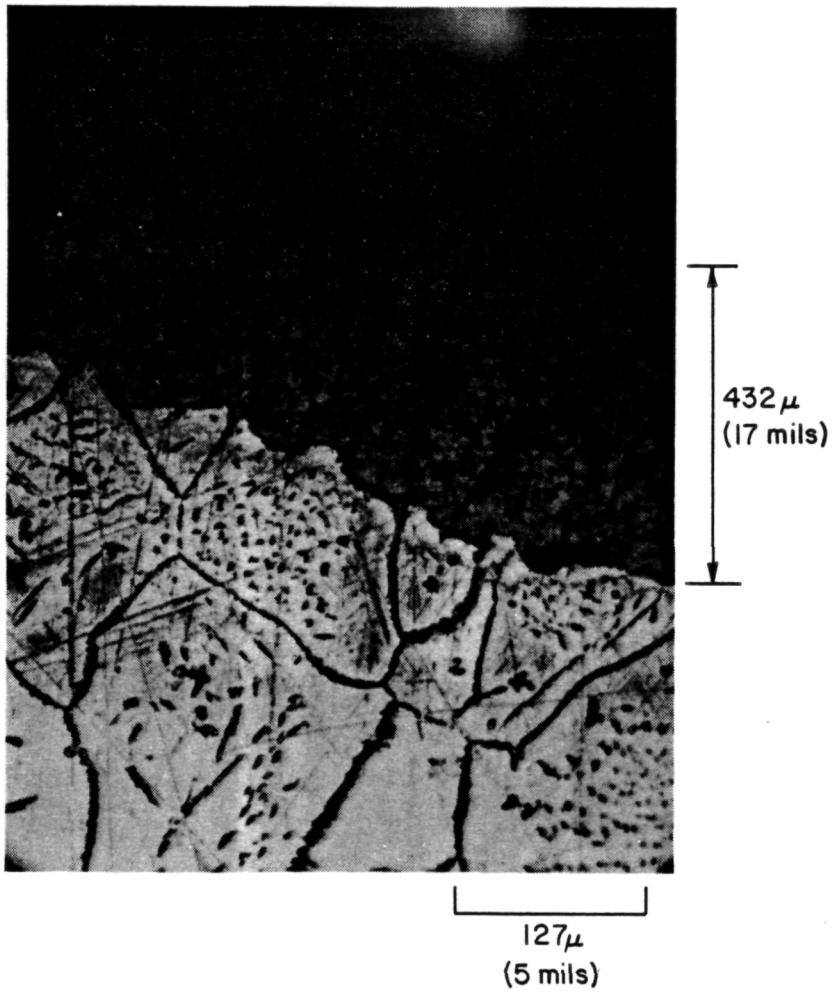

Figure 46. PHOTOMICROGRAPH OF ALLOY ARMCO 12SR IN TECHNICAL-GRADE $50Na_2CO_3$-$50K_2CO_3$ FOR 1056 HOURS AT 750°C (160X)

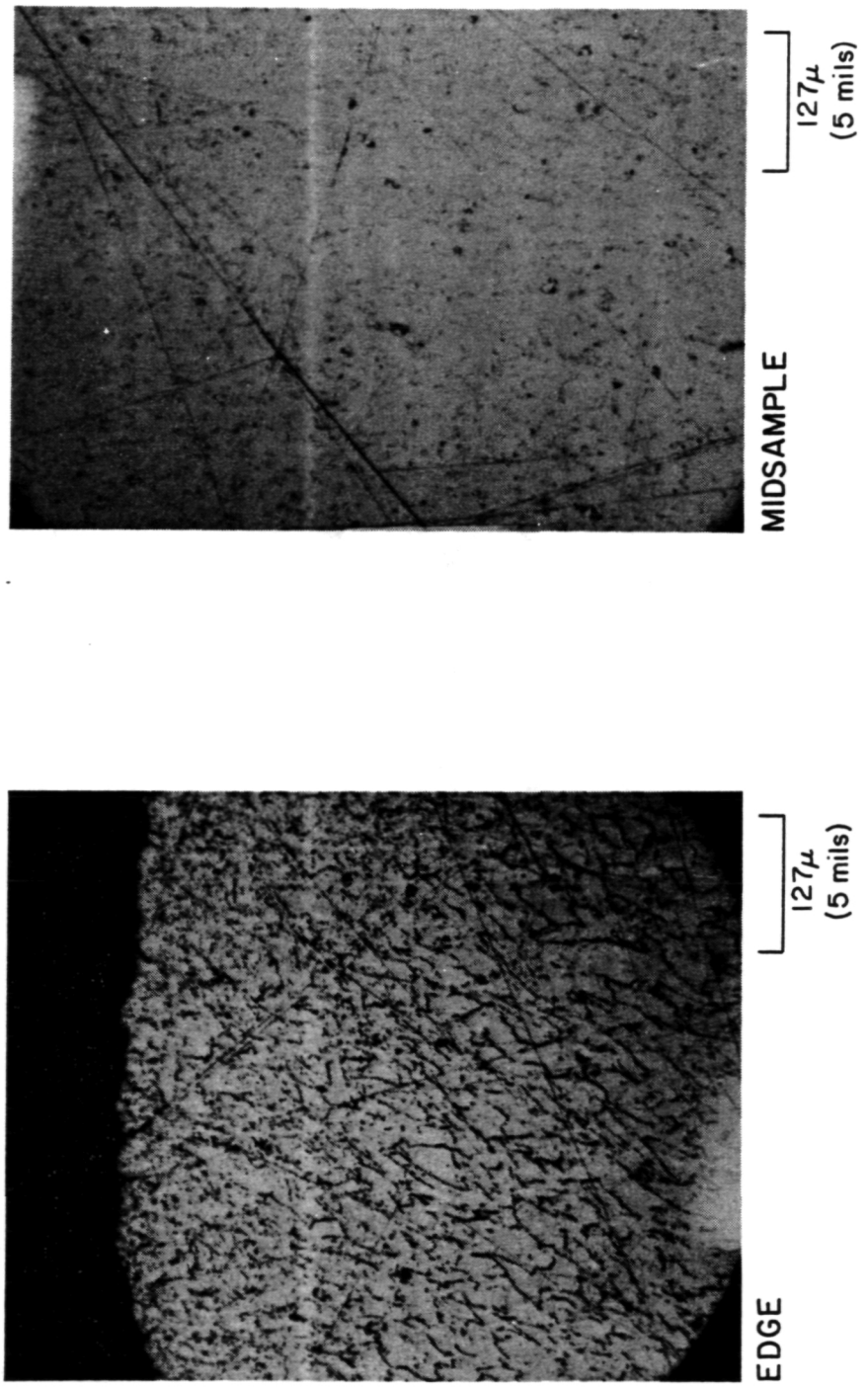

Figure 47. PHOTOMICROGRAPH OF SECTIONED AS-RECEIVED 1/2-INCH-DIAMETER KANTHAL A-1 "WIRE"/BAR (160X)

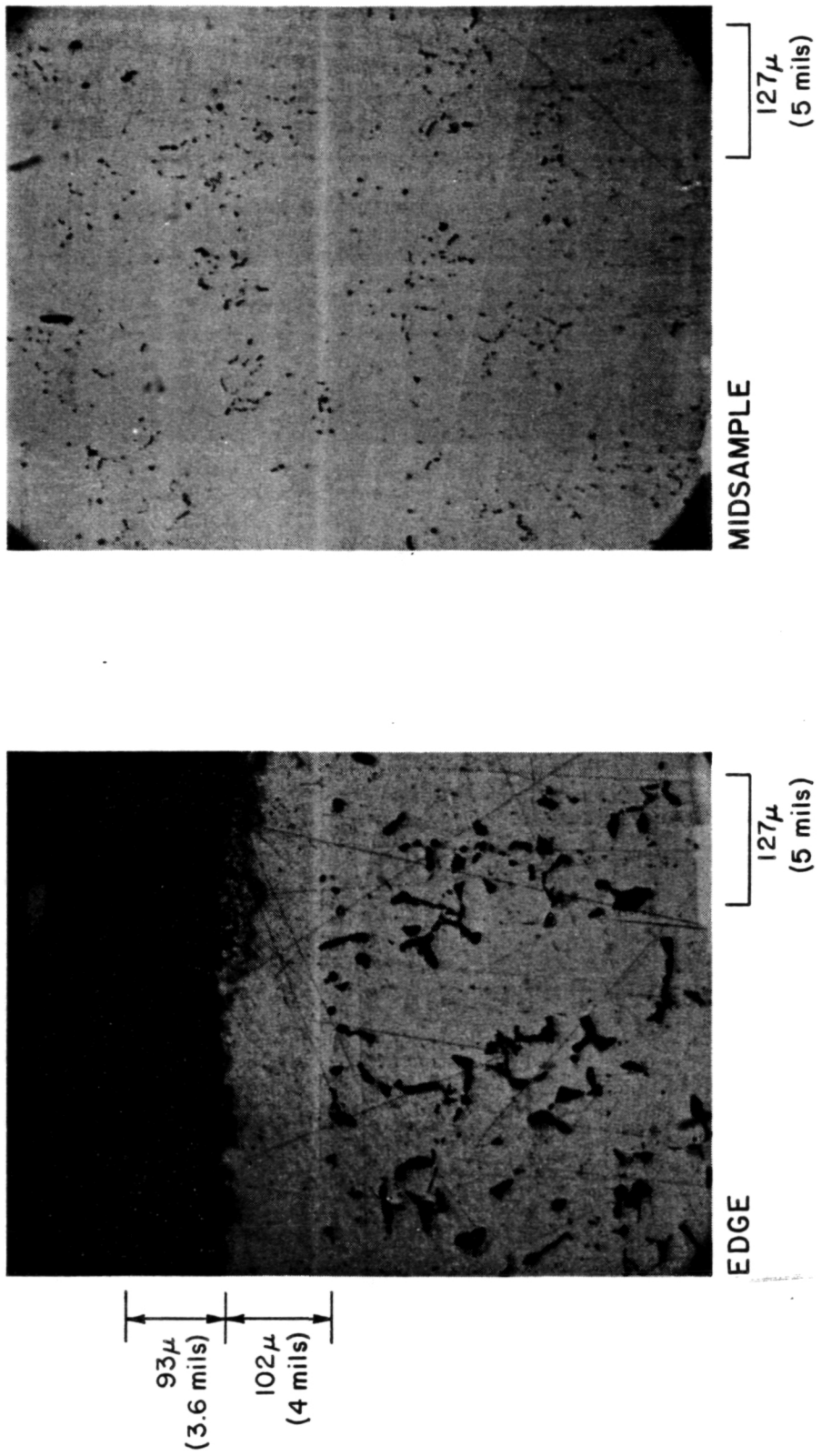

Figure 48. OPTICAL MICROGRAPH OF KANTHAL A-1 IN TECHNICAL-GRADE $52BaCO_3$-$48Na_2CO_3$ FOR 2616 HOURS AT 750°C (160X)

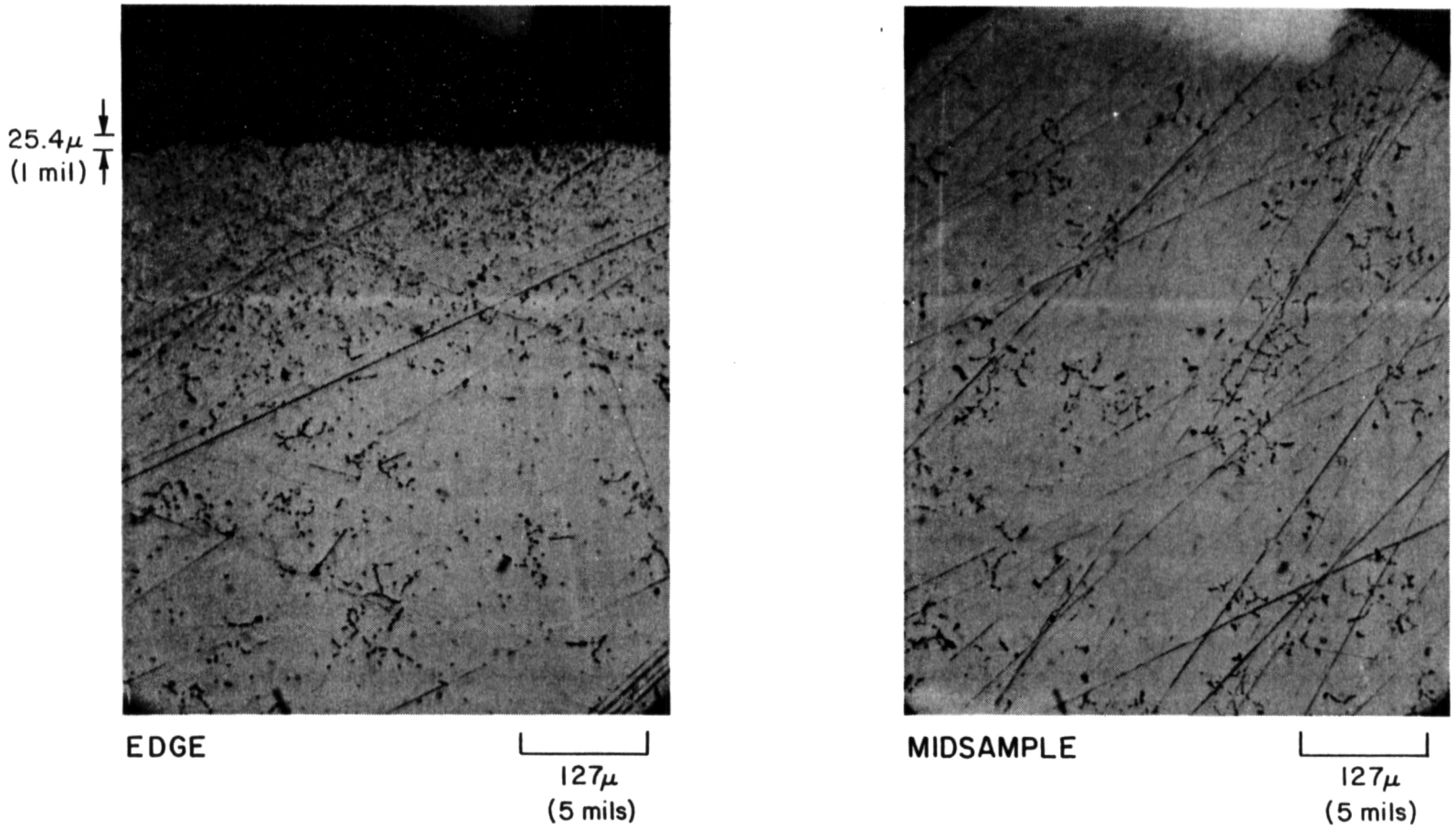

Figure 49. OPTICAL MICROGRAPH OF ALLOY KANTHAL A-1 IN TECHNICAL-GRADE $50Na_2CO_3$-$50K_2CO_3$ FOR 1056 HOURS AT 750°C (160X)

850°C Tests: Analysis of both alonized AISI 304 and 316 SS was obviated by a high incidence of capsule failures at 850°C. Capsule breaches consistently occurred at the previously described, top, "un-alonized" weld, in spite of following machining and welding procedures recommended for alonized structures. The failures appear to be attributed to a combination of aggressive corrosion mechanisms at the alonized SS/unalonized SS weld interface, possibly including —

- Wetted, thin salt film crevice corrosion in the inner, unalonized threads
- Inferior weld integrity related to decreased flowability of aluminum-containing molten weld metal
- Galvanic coupling between the Fe-Cr-Ni-rich stainless steel weld and the surrounding aluminum-rich capsule metal.

These weld "failures" resulted in very extensive attack after salt had leaked from the capsules because of the thin salt films formed on both the inner and outer capsule surfaces after leakage. This post-failure corrosion generally destroyed evidence related to actual material/salt compatibility. Alonized AISI 304 SS in $52BaCO_3$-$48Na_2CO_3$ and $50Na_2CO_3$-$50K_2CO_3$ failed after 1608 and 1344 hours, respectively, at 850°C in the above mentioned weld area.

One sample of alonized AISI 316 SS in technical-grade Li_2CO_3 failed in its weld after 48 hours at 850°C. The dense, protective nature of the aluminum-rich oxide coating (4 to 5 mils) can nonetheless be seen from Figure 50, with little discernible subscale or bulk effects. Another alonized AISI 316 SS capsule failed in its weld after 696 hours in technical-grade $81Na_2CO_3$-$19K_2CO_3$ at 850°C.

Aluminized coatings for high-temperature carbonate TES containment do show definite promise of increased corrosion resistance, however, avoidance of unalonized final welds or far greater weld-washing times (to allow for diminished weld flowability in aluminum-rich alloys) should be seriously considered.

Figure 51 shows alloy Armco 12SR after 2620 hours in technical-grade Li_2CO_3 at 850°C. Although the oxide scale was adherent and non-spalled, it was relatively porous and non-protective, resulting in a 23 to 25-mil-thick scale.

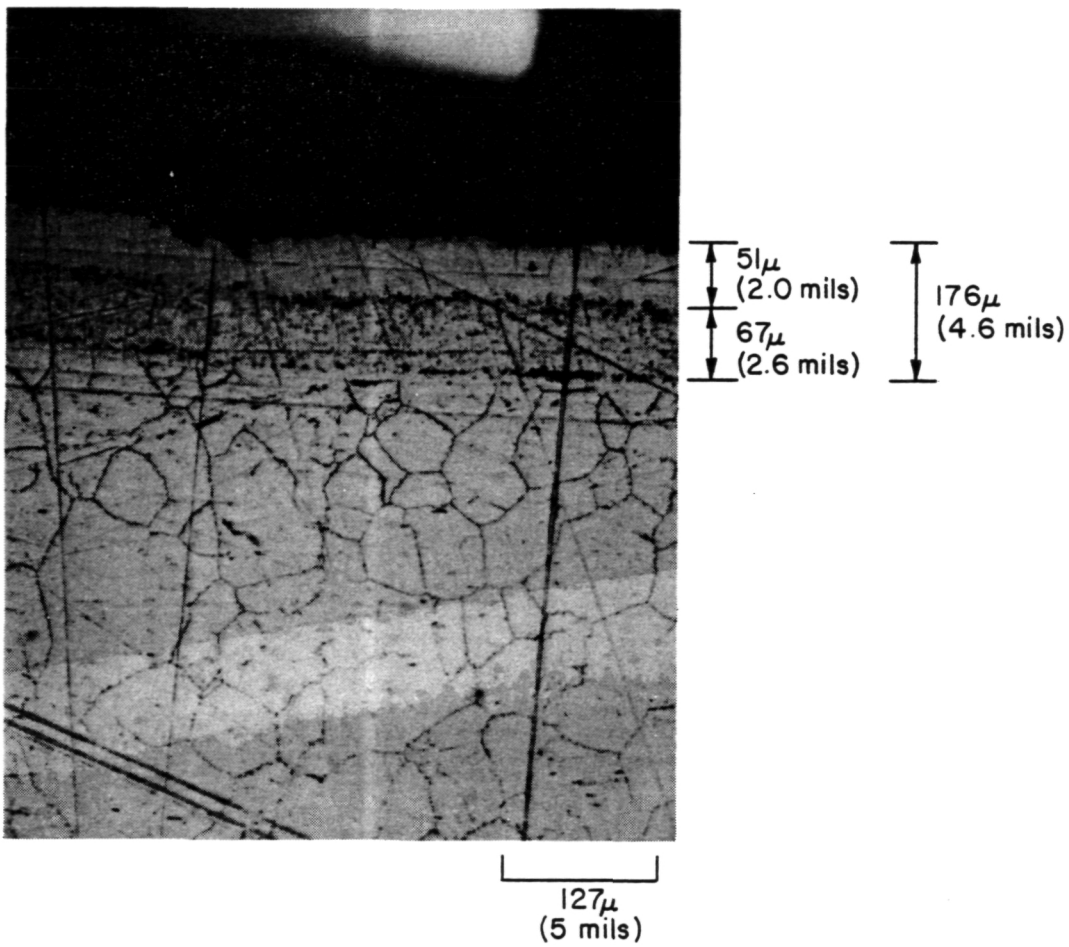

Figure 50. PHOTOMICROGRAPH OF ALONIZED AISI 316 SS IN TECHNICAL-GRADE Li_2CO_3 FOR 48 HOURS AT 850°C (160X)

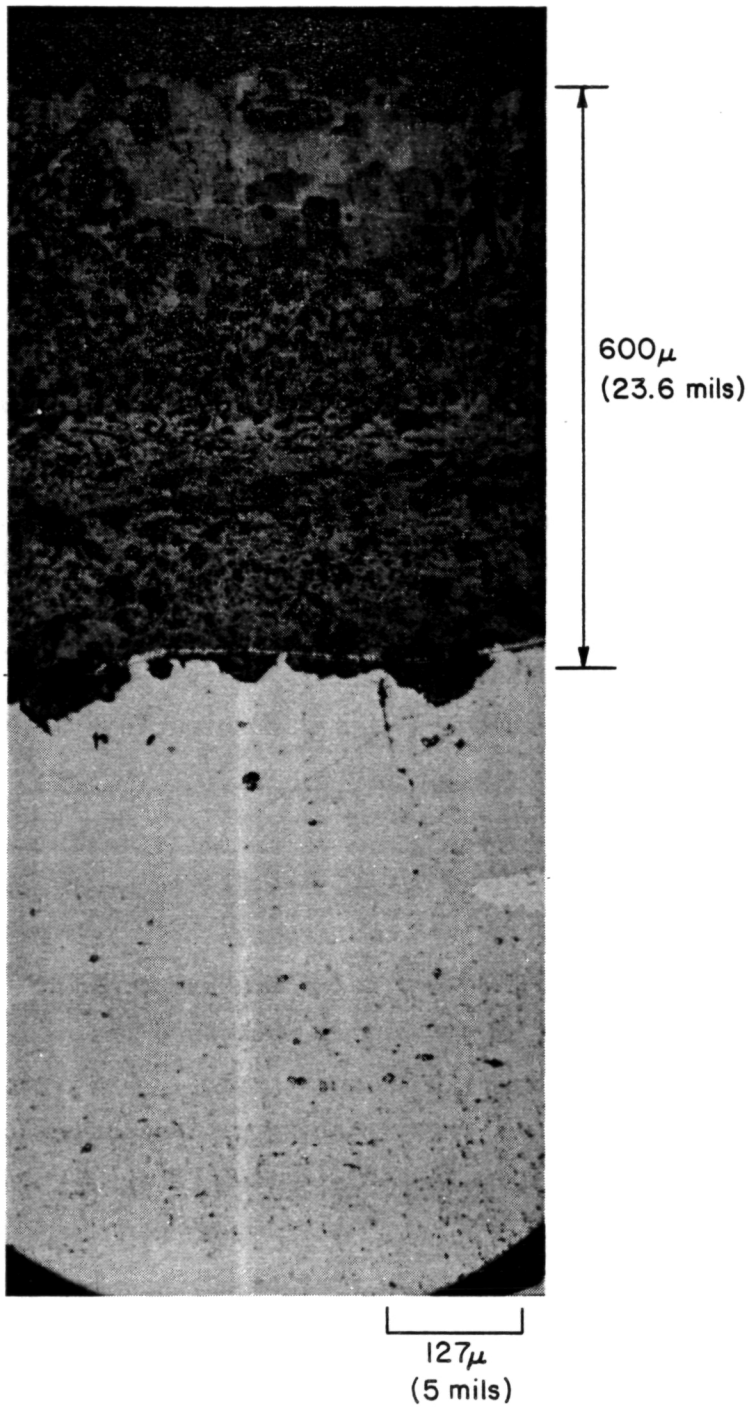

Figure 51. PHOTOMICROGRAPH OF ALLOY ARMCO 12SR IN TECHNICAL-GRADE Li_2CO_3 FOR 2620 HOURS AT 850°C

Screening with alloy Kanthal A-1 again resulted in a protective dense, dark gray 8 to 9-mil oxide layer when tested with technical-grade Li_2CO_3 for 2620 hours. As seen from Figure 52, this layer was followed by a 2 to 4-mil clean unreacted subscale and 4 to 5 mils of localized carbide pick-out. This isolated carbide pitting may be a residual effect of the edge-grain deformation resulting from the wire/bar stock processing steps (observed in the pretest wire/bar stock from Figure 46) compounded by continued service in the thermal sensitization region. This is supported by the fact that pick-out is edge-localized, with a relatively undisturbed bulk metal (midsample) region. A general corrosion resistance ranking of the core- and aluminum-containing alloys appears in Figure 53 for containment of technical-grade Li_2CO_3 salt.

910°C Tests: Analysis of alonized AISI 304 and 316 SS in salts at 910°C was again hindered by failures in the "unalonized" weld, with extensive attack after salt had leaked from the capsules. A capsule containing technical-grade Na_2CO_3 failed during the last 100 hours of testing (total of 648 hours). Alonized AISI 304 SS in technical-grade K_2CO_3 failed after 650 hours at 910°C.

As shown in Figure 54, alonizing offers improved corrosion protection with AISI 316 SS in technical-grade Na_2CO_3 at 910°C. After 550 hours of testing, the 14 to 15-mil-thick alonized layer remained adherent and dense. When compared to a pretest photomicrograph of alonized AISI 316 SS (Figure 41), the Na_2CO_3 sample's top region (2 to 3 mils) appears to have become further oxidized (darker) or slightly carburized, although the remaining diffusion zone appears intact and relatively undisturbed. The sensitized bulk metal contains carbide grain boundary precipitation with no observable salt-related effects. Alonized AISI 316 SS in K_2CO_3 failed after 648 hours at 910°C.

Examination of alloy Armco 12SR in technical-grade Na_2CO_3 revealed a 26 to 28-mil slightly spalled oxide scale after 1034 hours at 910°C (Figure 55). The sensitized bulk matrix contained enhanced grain boundary carbide precipitation and no evidence of salt penetration.

Kanthal A-1 in technical-grade Na_2CO_3 resulted in a 1 to 3-mil protective, dense oxide with the previously mentioned edge-localized subscale pitting and a clean, undisturbed bulk metal matrix in 1034 hours at 910°C. The comparative advantages of aluminum-containing alloys at this elevated

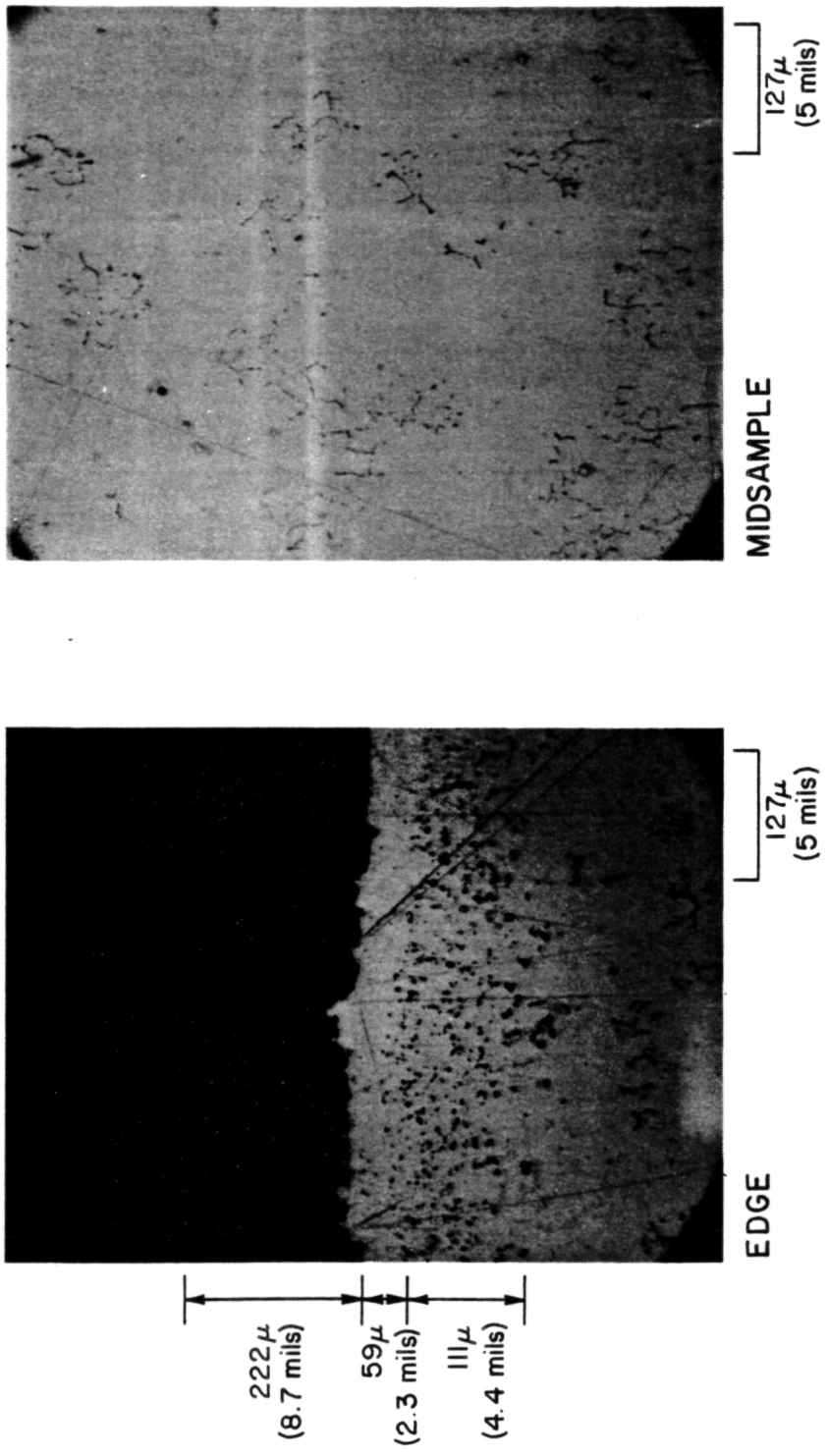

Figure 52. OPTICAL MICROGRAPH OF ALLOY KANTHAL A-1 IN TECHNICAL-GRADE Li_2CO_3 FOR 2620 HOURS AT 850°C

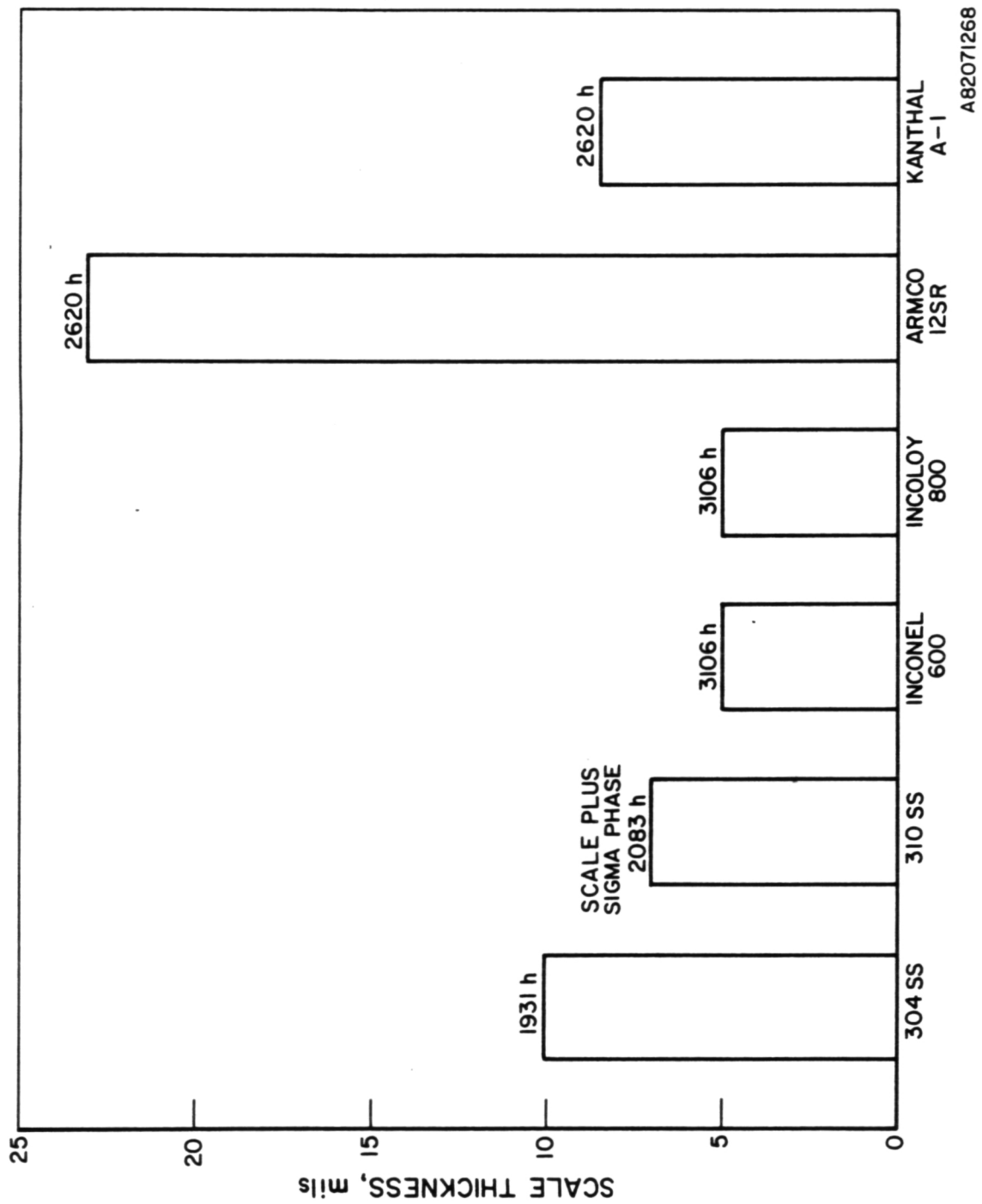

Figure 53. THICKNESS OF SCALES FORMED ON CANDIDATE ALLOYS AFTER 1931 TO 3106 HOURS OF EXPOSURE TO TECHNICAL-GRADE Li_2CO_3 AT 850°C

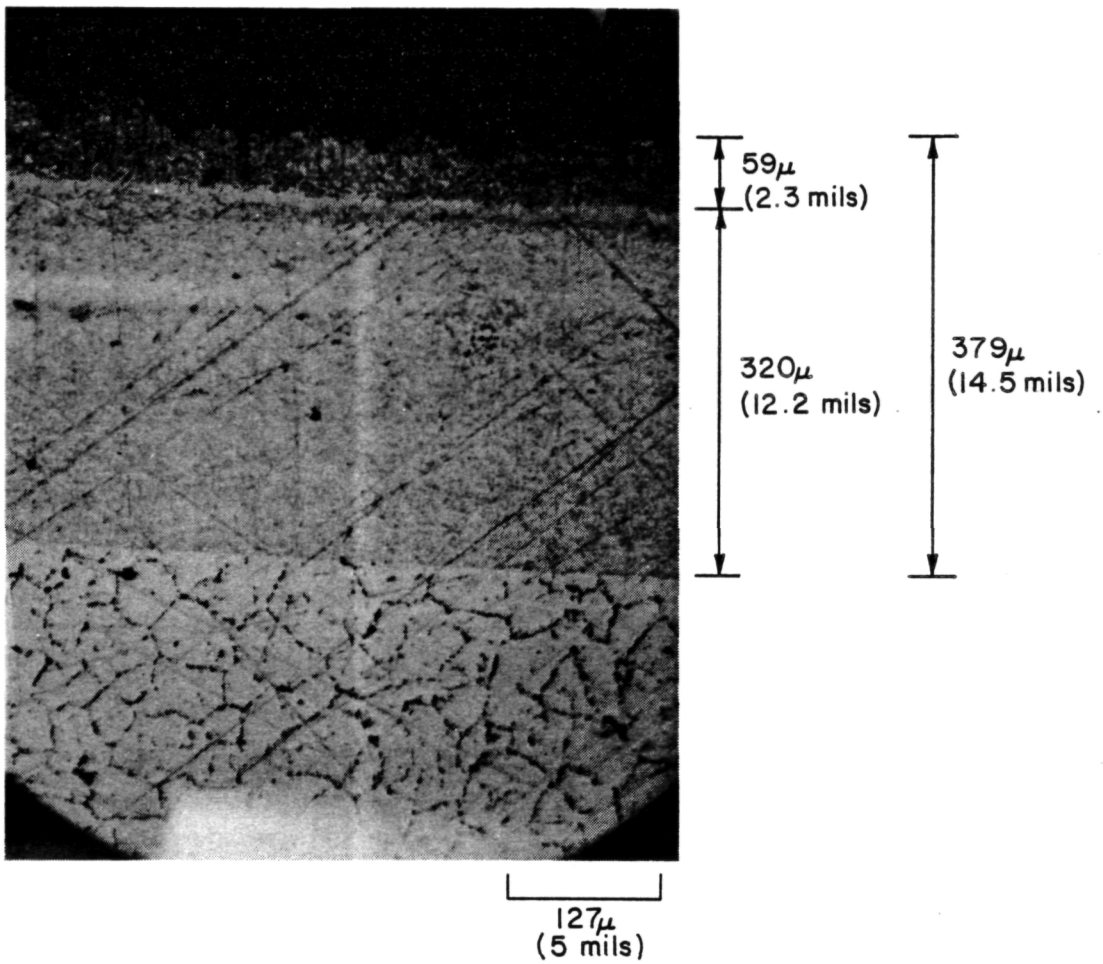

Figure 54. PHOTOMICROGRAPH OF POST-TEST ALONIZED AISI 316 SS IN TECHNICAL-GRADE Na_2CO_3 FOR 552 HOURS AT 910°C (160X)

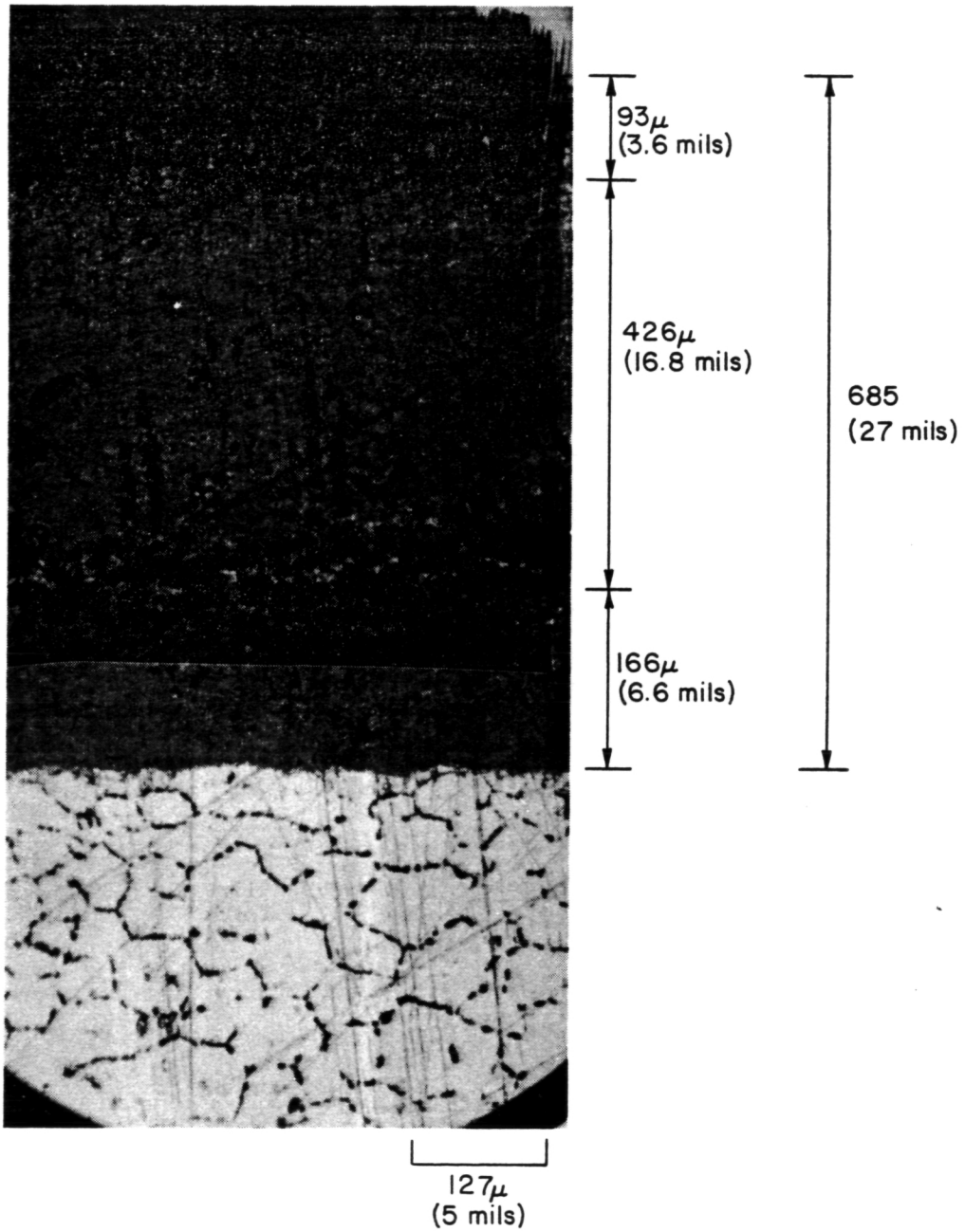

Figure 55. OPTICAL MICROGRAPH OF ALLOY ARMCO 12SR IN TECHNICAL-GRADE Na_2CO_3 FOR 1034 HOURS AT 910°C (160X)

temperature are illustrated in the overall corrosion resistance rankings of Figure 56 for containment of technical-grade Na_2CO_3 salt.

The generally enhanced high-temperature (750° to 910°C) compatibility of especially Kanthal A-1 (5.5 wt % Al-containing alloy) and alonized (in unfailed capsules) AISI 304 and 316 SS (aluminum diffusion coating) is consistent with the demonstrated long-term (>10,000 hours) stability of aluminized stainless steels in 650°C fuel cell applications. Aluminum-alloying and/or -coating are, indeed, two promising methods of attaining improved high-temperature stability and corrosion protection at 750° to 910°C. The high-temperature mechanical strength (sagging) and current availability of Kanthal A-1 (produced in Sweden) in suitable fabricated configurations (plate and tube) are areas of question. Also, determination of an incremental cost increase factor for alloy aluminizing is primarily related to the volume a given piece occupies in a furnace retort and is therefore neither simplistic nor easily generalized. Evaluation of the economics of alloy coating is consequently a matter of future inquiry. Concentrated investigation into these two elements (alloying and/or coating) of our screening test matrix may further define the metallic-component/processing/weldability requirements and long-term compatibility/strength limitations associated with carbonate containment in this high-temperature regime.

Thermal Conductivity Enhancement Materials

The objective of this subtask involved compatibility screening and evaluation of graphite and copper as potential TCE materials in the high-temperature solar thermal application range. Solid and reticulated copper and pyrolytic and ATJ graphite were screened in technical-grade $52BaCO_3$-$48Na_2CO_3$, $50Na_2CO_3$-$50K_2CO_3$, Li_2CO_3, Na_2CO_3, and K_2CO_3 with an argon cover-gas. (See Section 1.1.) A summary of the experimental results obtained for these materials compatibility tests conducted from 750° to 910°C is given in Table 26.

Pyrolytic graphite was found to have reacted significantly with carbonate salt in every test. This may have been due to inherent weaknesses of its directionally oriented crystal structure (which results in a preferentially high thermal conductivity in one plane). ATJ graphite, however, was found

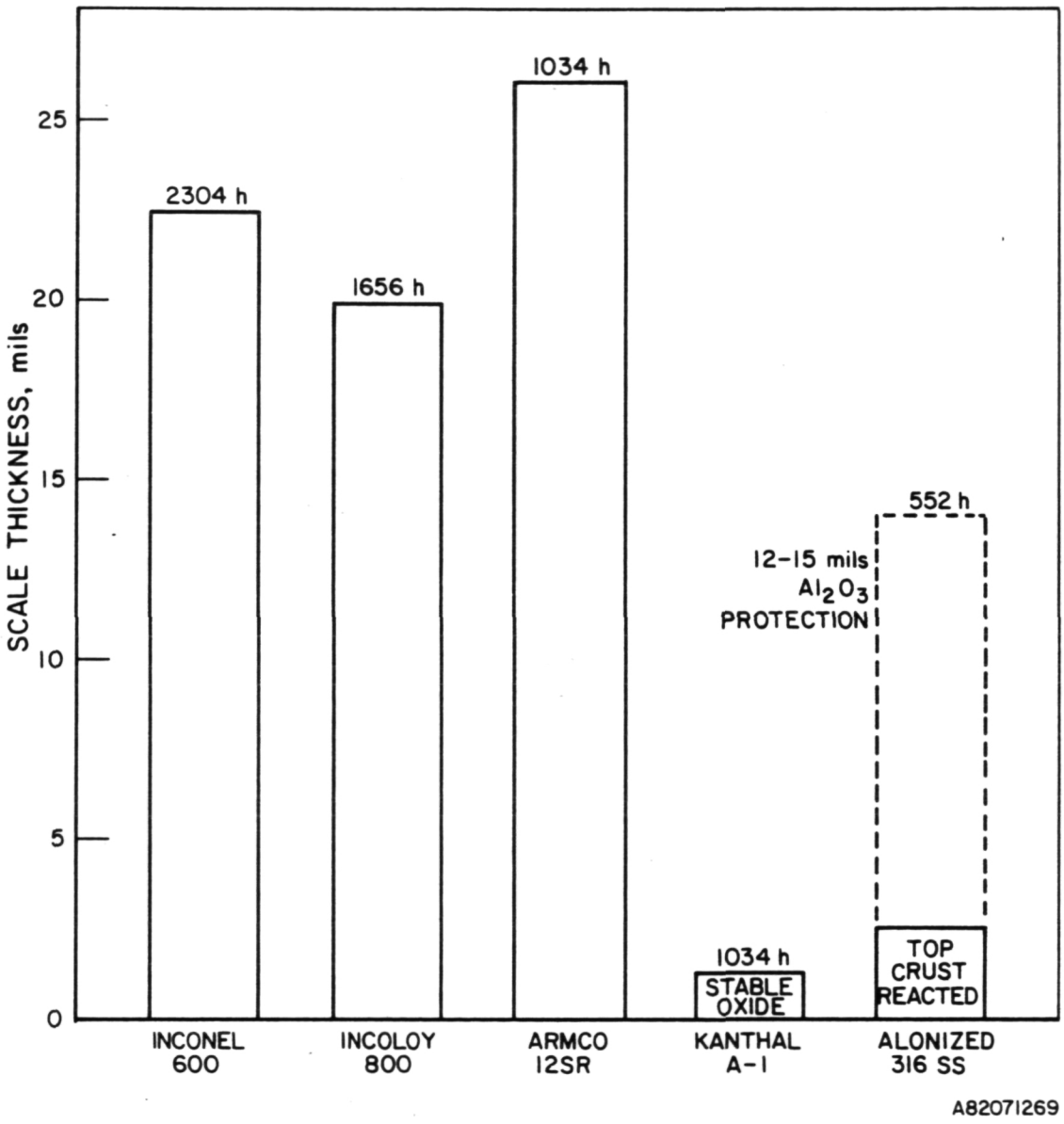

Figure 56. THICKNESS OF OXIDE SCALES FORMED ON CANDIDATE ALLOYS AFTER 550 TO 2300 HOURS OF EXPOSURE TO TECHNICAL-GRADE Na_2CO_3 AT 910°C

Table 26. RESULTS OF TCE MATERIALS COMPATIBILITY TESTS

Salt, wt %	Containment	Temp, °C	Pyrolytic Graphite	ATJ Graphite	Copper Solid	Copper Reticulated Matrix
$52BaCO_3$-$48Na_2CO_3$ Technical grade	304 SS	750	Significantly reacted	Qualitatively reacted	2635 hours 4-5 mil reaction zone Bulk unaffected	2635 hours 4 mil reaction zone Non-metallic inclusions or pits
$50Na_2CO_3$-$50K_2CO_3$ Technical grade	304 SS	750	Significantly reacted	Qualitatively reacted	2635 hours 4 mil reaction zone Clean	2635 hours 4 mil reaction zone 0.6 mil pits (enhanced) through entire ligament wall
Li_2CO_3 Technical grade	304 SS	850	Significantly reacted	Qualitatively reacted	2635 hours <1 mil reaction zone Clean	2635 hours <1 mil reaction zone Clean
Na_2CO_3 Technical grade	Inconel 600	910	Significantly reacted	Qualitatively reacted	2714 hours 2-5 mil reaction zone Metal silver-grey in color Localized inclusions	2714 hours 1 mil reaction zone Metal silver-grey in color Large (1 mil) inclusions
K_2CO_3 Technical grade	Inconel 600	910	Significantly reacted	Qualitatively reacted	2714 hours 1-2 mil oxide scale Subscale enhance cuprous oxide	2714 hours <1 mil reaction zone Localized cuprous oxide in bulk

through qualitative inspection to be relatively unaffected and compatible with carbonates from 750° to 910°C.

A pretest optical micrograph of the reticulated matrix copper used in these tests appears in Figure 57. As mentioned in Section 1.1, the reticulated copper matrix was a high-porosity [96% porosity, 25 pores per cm (10 pores per inch)], thick [508 (20 mils)], hollow ligament powder metallurgy (PM) product from Rocket Research Inc. Figure 57 contains a cross section of one of the hollow ligaments of the matrix. It contains typical PM equiaxed, radially oriented, twinned grains of copper with a slight dispersion of particles of oxide.

750°C: Generically, copper-in-argon environment demonstrated excellent compatibility with carbonate salts from 750° to 910° to 950°C. In both technical-grade $52BaCO_3$-$48Na_2CO_3$ and $50Na_2CO_3$-$50K_2CO_3$, the copper solid samples especially were found relatively unaffected (after 2635 hours at 750°C in $50Na_2CO_3$-$50K_2CO_3$). The reticulated copper matrix was subject to oxide precipitation within the hollow ligament walls after 2635 hours in $52BaCO_3$-$48Na_2CO_3$.

850°C: Testing of copper in technical-grade Li_2CO_3 resulted in a 0.3 to 0.7-mil reaction layer with a clean, unaffected subscale and bulk metal region after 2635 hours (Figure 58).

910° to 950°C: An unusual reaction product formed on copper in technical-grade Na_2CO_3 at 910° to 950°C. The copper (solid and reticulated)/salt samples were contained within an Inconel 600 capsule with an argon environment. Post-test examination of both copper specimens revealed a silver-gray reaction zone, which inhibited delineation with a standard copper etchant (ammonium hydroxide/hydrogen peroxide/water 1:1:1). X-ray fluorescence and chemical analyses indicated that the layer contained high amounts of nickel. Analytical determinations of percent Na, $CO_3^=$, Ni, Cr, Fe by atomic adsorption are contained in Table 27 for both the pre- and post-test Na_2CO_3 salt, revealing a 32% loss in carbonate and an increase in iron, chromium, and nickel from <0.02% pretest to 0.25%, 0.26%, and 0.10%, respectively. In this test environment, Ni from the Inconel 600 alloy capsule dissolved in the molten Na_2CO_3, and the soluble species diffused through the melt and into the Cu matrix to form a Cu-Ni alloy.

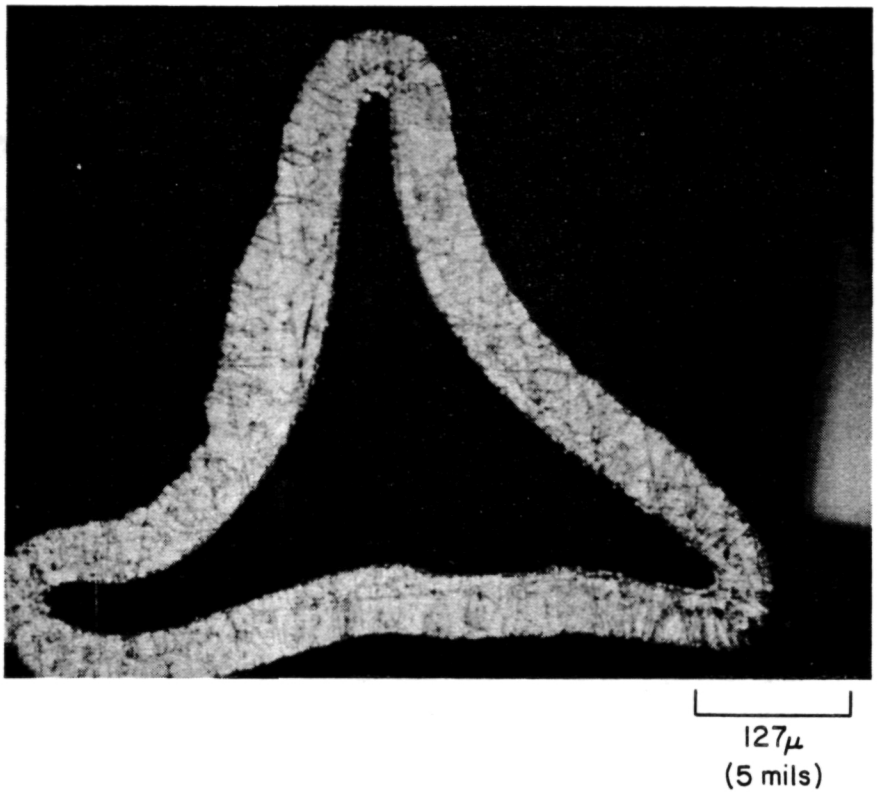

Figure 57. PRETEST OPTICAL MICROGRAPH OF RETICULATED COPPER TCE MATRIX (Cross Section of One Ligament, 160X, Etchant: Ammonium Hydroxide/Water/Hydrogen Peroxide 1:1:1 by Volume)

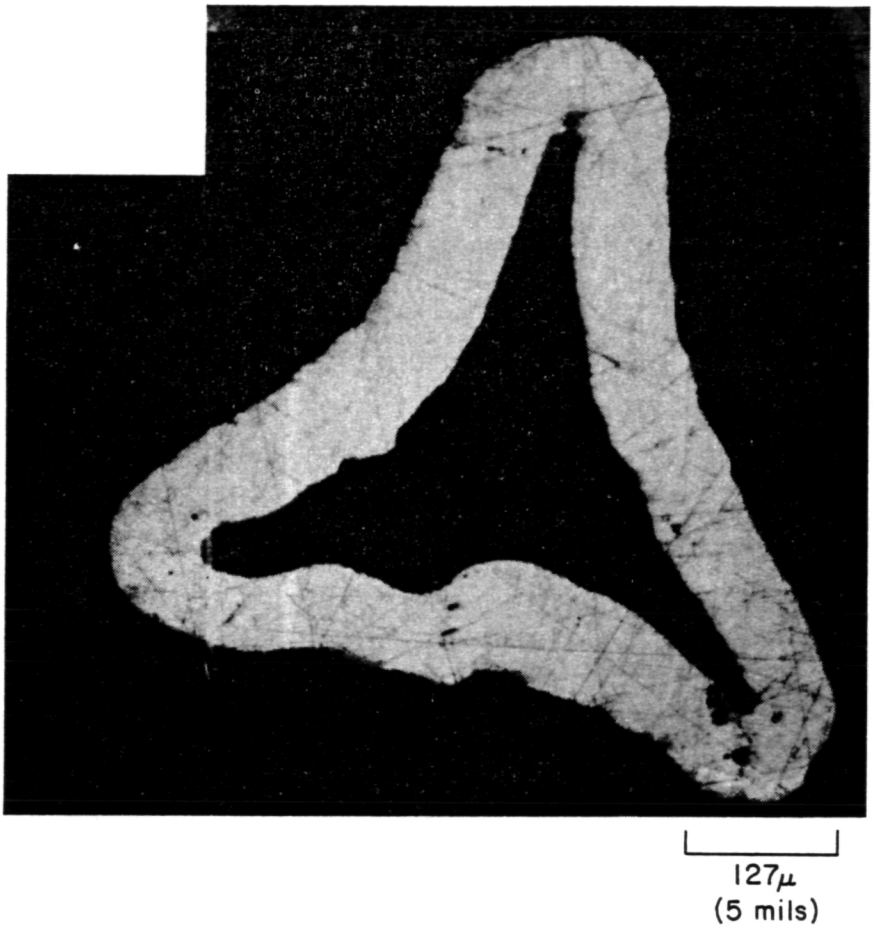

Figure 58. OPTICAL MICROGRAPH OF RETICULATED COPPER LIGAMENT (Hollow) IN TECHNICAL-GRADE Li_2CO_3 FOR 2635 HOURS AT 850°C (Argon Environment, 160X, Etchant: Ammonium Hydroxide/Water/Hydrogen Peroxide 1:1:1 by Volume)

Table 27. PRE- AND POST-TEST CHEMICAL ANALYSIS OF Na_2CO_3 AT 910°C

Salt	Grade	In Containment	Chemical Analysis, wt % $CO_3^=$	Na	Fe	Cr	Ni	Hours
			Pre-Test					
Na_2CO_3	Technical	--	56.3	39.0	<0.01	<0.02	<0.01	--
			Post-Test					
Na_2CO_3	Technical	Inconel 600 Capsule Argon Environment Copper Inside	38.2	40.5	0.25	0.26	0.101	2714

Task 2. Carbonate Salt Property Measurements

Introduction

Accurate salt property data (for example, heat of fusion, specific heat, melting point, volumetric expansion, and thermal conductivity) are required for adequate design and engineering of high-temperature latent-heat thermal energy storage systems. A review of available data for molten carbonates in the 700° to 900°C temperature range revealed some critical data gaps, as well as some apparent inconsistencies in existing data.

In particular, the carbonate mixture 47.8 wt % Na_2CO_3-52.2 wt % $BaCO_3$ is reported[55] to melt congruently at 686°C. However, in lab-scale TES module experiments using this salt,[4] thermal arrests were observed to occur in the 712° to 717°C temperature range, indicating a slightly higher melting point than that reported. No other thermophysical property data for this salt have been reported. Its enthalpy and heat of fusion are needed to further assess its potential use as a TES storage medium. The incongruently melting mixture 81.3 wt % Na_2CO_3-18.7 wt % K_2CO_3, which was estimated to melt over the range 740° to 790°C, contains a large amount of Na_2CO_3, which is low cost and has a high specific heat. This mixture forms a "slush" composition during thermal cycling, thus reducing the formation of solid salt layers on the heat exchanger surface, which particularly impedes heat transfer during thermal discharge. The magnitude of heat effects associated with melting/solidification of this interesting mixture have never been measured.

The melting point, heat capacity, and heat of fusion of the above salts were measured at Dynatech R/D Company* under a subcontract from IGT. The carbonate salt samples were prepared by fusion of Fisher reagent-grade materials.

Melting Point Measurements

Measurements of salt melting points were performed on a Netzsch Differential Thermal Analyzer (DTA) Model 404, which employs an alumina measuring head and alumina cups centered inside a closed-end alumina tube 24 mm in diameter. Thermocouples [28-gauge platinum, 10% rhodium (ANSI

*Dynatech R/D Company, 99 Erie St., Cambridge, Mass. 02139

Type S)] led to the measuring head through double bore alumina tubes. The two tubes containing the differential thermocouple fit inside and supported the sample and reference cups. The differential thermocouple thus sensed the difference between temperatures at the bottom centers of the cups. The third thermocouple, for readout of temperature, was in contact with the outside of the sample cup near the bottom of the sample. This thermocouple was referenced to 0°C and was connected to a Newport 2400 Digital Voltmeter with a resolution of ±1 μV. This thermocouple voltage was also displayed on the chart recorder for correlation of reactions with temperature.

The Netzsch system was equipped with an automatic temperature controller that could sweep the temperature of the furnace from room temperature to 1550°C at selected rates. The samples were run in a flowing helium atmosphere from RT to ~900°C, then back to RT. In the region 650° to 900°C, the heating and cooling rate was 10°C/min; some of the samples were heated to 650°C at a rate of 20° to 50°C/min and allowed to stabilize at that temperature for a few minutes before proceeding.

All runs employed reagent-grade ignited Al_2O_3 powders as reference material; this material was run initially against an empty cup to ensure that no transitions occurred in the temperature range of interest. The system was then calibrated against NBS Standard Reference Material 759, K_2CrO_4, and against 99.9% nickel powder obtained from Alfa/Ventron. The former material exhibits a transition between 665° and 673°C, and the nickel melts at approximately 1453°C.*

Results of the DTA measurements are presented in Table 28. As a check for the melting point measurements, Li_2CO_3 and Na_2CO_3 samples were also tested and acceptable results were obtained as shown in this table. The Na_2CO_3-$BaCO_3$ carbonate mixture showed a melting point of 716°C consistent with the thermal arrests (712°C to 717°C) observed in the TES module experiments.[4] The Na_2CO_3-K_2CO_3 mixture melted between 742° and 813°C, with the liquidus temperature slightly higher than that estimated from the Na_2CO_3-K_2CO_3 phase diagram. (See Figure E-1 in Appendix E.)

---

*Touloukian, Y. S. and Buyco, E. H., Thermophysical Properties of Matter 4, "Specific Heat," IFI/Plenum: New York, 1970.

Table 28. THERMOPHYSICAL PROPERTY MEASURMENTS OF SELECTED CARBONATE SALTS*

Salt**	Melting Point, °C		Effective Heat of Fusion, J/g (Btu/lb)		Specific Heat at Melting Point, J/g-K(Btu/lb-°F)		Melting to Slush Region (742° to 813°C)		
	Measured	Literature	Measured	Estimated	Measured	Estimated	Contribution Due to Specific Heat Assuming Avg cp = 1.71 J/g-K (0.41 Solid/Liquid Btu/lb-°F) Btu/lb	Heat of Fusion Measured	Heat of Fusion Estimated
Li_2CO_3	730	723	--	--	--	--	--	--	--
Na_2CO_2	860	858	--	--	--	--	--	--	--
81.3 Na_2CO_3-18.7 K_2CO_3	742-813	740-790	332 (143)	375 (161)	1.75 (0.42)	1.67 (0.40)	52	91	109
52.2 $BaCO_3$-47.8 Na_2CO_3	716	686	185 (80)	--	1.32 (0.32)	--	--	--	--

* Measurements performed by Dynatech R/C Company, Cambridge, MA.

** Samples prepared from Fisher reagent-grade carbonates.

B83050862

Heat of Fusion and Specific Heat Measurements

A high-temperature calibrated copper drop calorimeter was used to determine the heats of fusion and specific heats. The samples were dropped in an AISI 304 SS container from three temperaures below and three temperatures above their melting point. From the drops, after subtracting out the container enthalpy change, the enthalpy change curve for the samples in the solid and liquid phase was determined.

From the ΔH curve and a knowledge of the melting temperature of the samples from the DTA measurements, the enthalpy change (heat of fusion) between the solid and liquid phase at T_m could be determined:

$$\Delta H_F = [\Delta H_L - \Delta H_S]_T = T_m \qquad (4)$$

where,

ΔH_F = heat of fusion

ΔH_L = enthalpy change from the melting temperature to RT for the liquid phase

ΔH_S = enthalpy change from the melting temperature to RT for solid phase.

Results of these measurements are presented in Table 28, along with previous estimates of heat of fusion and specific heat of the Na_2CO_3-K_2CO_3 mixture based on molar additivity and the rule-of-mixtures.

Heat capacities and heats of fusion were determined by using a copper drop calorimeter, which involved enthalpy change measurements between room and various temperatures and at the melting point, respectively. The results are shown in Table 28. Because heat of fusion data are not available for $BaCO_3$, predictions of this property for the Na_2CO_3-$BaCO_3$ carbonate mixture cannot be made. For the Na_2CO_3-K_2CO_3 mixture, the specific heat determined experimentally from the measured enthalpy changes is higher than that estimated from literature values for pure Na_2CO_3 and K_2CO_3. The differences may be attributed to limited data points in the present measurements or to possible heat effects associated with solid-state phase transformations occurring within the experimental temperature range. Additional data are required in order to establish a more precise enthalpy curve for the solid phases of the

Na_2CO_3-K_2CO_3 system. The measured heat of fusion for this salt mixture appears to be reasonable. The experimental value is well below that predicted from the rule-of-mixtures, with the difference being due to the heat-of-mixing effects.

CONCLUSIONS

In this project, we —

- Screened 100 material/salt combinations for containment/HX/TCE compatibility with carbonate salts in the high-temperature solar-thermal application range of 704° to 871°C. (Summary of material/salt combination number versus time appears in Figure 59.)

- Tested nine potential containment/HX alloy materials and two TCE materials with six candidate solar thermal carbonate storage salts.

Containment/HX Materials

- AISI 304 and 316 SS — Reasonable good compatibility with carbonates to 850°C. AISI 304 SS exhibited an approximately parabolic corrosion rate in technical-grade $52BaCO_3$-$48Na_2CO_3$ at 750°C extrapolated to 9 mils after 1 year and 30 mils after 10 years exposure. AISI 316 SS exhibited somewhat better corrosion resistance in carbonates to 850°C, although its service at temperatures greater than 900°C should be limited to short-term testing only.

- AISI 310 — Exhibited less oxidation (greater corrosion protection potential) than 304 SS or 316 SS, with dense stable scale formation, although it was susceptible to intermetallic sigma-phase precipitation at 750°C and above. Testing at 910° to 950°C indicated more complex and severe corrosive attack, possibly related to sigma-phase dissolution. Further work is required to assess the significance of sigma phase on 310 SS structural integrity under cyclic and steady-state TES service conditions.

- Inconel 600 — More corrosion resistant (along with Incoloy 800) to molten carbonates from 750° to 950°C than AISI 304 or 316 SS. Although it contains 75% nickel and represents the highest priced "core" containment material tested ($12/lb of bar stock compared to $9/lb for Incoloy 800 and $1/lb for 304 SS), there was little gained in corrosion resistance to carbonates in this temperature range over Incoloy 800, with the exception, perhaps, of containing specifically technical-grade Li_2CO_3 (850°C) or Na_2CO_3 (910°C). Nevertheless, its apparent linear corrosion rate in Na_2CO_3 at 910°C indicates a need for further materials development efforts for TES containment and operations activities above 900°C.

- Incoloy 800 — Exhibited the best overall corrosion resistance from 800 to 3000 hours in molten carbonates from 750° to 910° to 950°C (although effective medium-term containment may be more economically achieved with 316 SS or a modified, sigma-phase-free 310 SS: $2 and $3/lb of bar stock, respectively, compared to ~$9/lb for Incoloy 800). It is the preferred, economical containment for short- to mid-term work over Inconel 600 in carbonates to 910°C.

- Pack Vapor Diffusion Aluminized AISI 304 and 316 SS — Aluminized AISI 304 SS demonstrated superior corrosion resistance over uncoated AISI 304 SS in carbonates from 600 to 1300 hours at 850°C. Although the

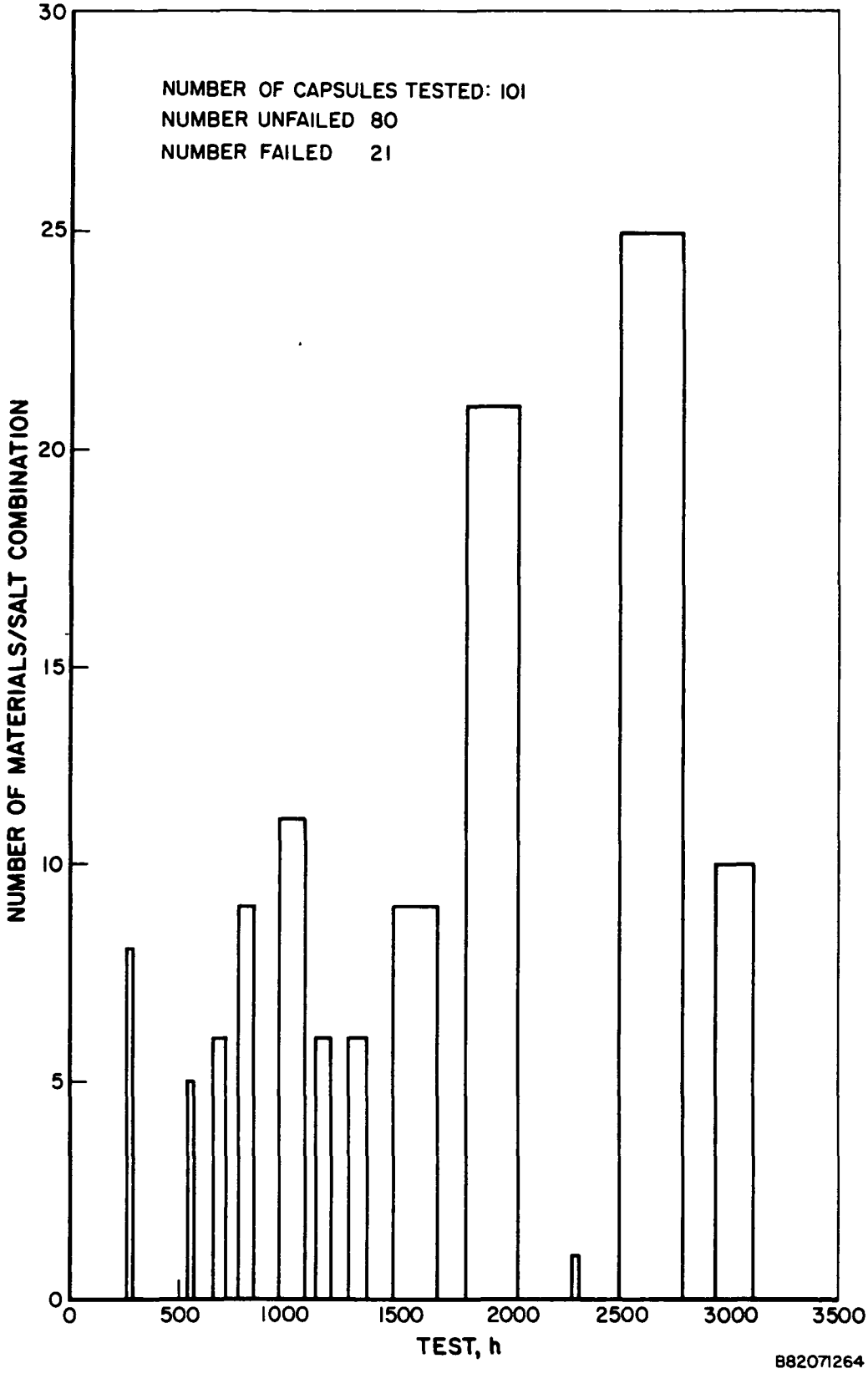

Figure 59. SUMMARY OF MATERIALS/SALTS COMPATIBILITY TEST MATRIX
(Number of Materials/Salt Combinations Tested vs. Time)

aluminized 304 SS test capsules failed in an "unaluminized" weld at 910°C, there is indication that aluminized coatings will remain dense and adherent and offer improved corrosion resistance over 304 SS at this highest temperature regime in carbonates. Although testing with aluminized 316 SS was likewise greatly hindered by capsule failure in an "unaluminized" weld, the enhanced corrosion protection and compatibility of aluminized 316 SS in carbonates was indicated by 550 hours in technical-grade Na_2CO_3 at 910°C with minimal degradation of the 15-mil diffusion aluminized layer.

- Armco Alloy 12SR — This ferritic stainless alloy exhibited adequate compatibility with carbonates to 750°C, and may be considered preferred over AISI 304 or 316 SS for mid-term testing from an economic ($1.03/lb Armco 12SR, $1.07/lb 304 SS, and $1.86/lb of 316 SS bar stock) and corrosion resistance viewpoint. Above 850°C, this metal's oxidation rates were found to be unacceptably high.

- Kanthal A-1 — This Al_2O_3-forming material is attractive for containment of molten carbonates for the high-temperature, solar-thermal power application range of 704° to 871°C. It demonstrated satisfactory short- to mid-term corrosion resistance and compatibility with carbonate salts for 1000 to 2600 hours at 750° to 910°C, especially with technical-grade Na_2CO_3 (for 1034 hours at 910°C). However, its high-temperature strength properties are questionable, and it is presently available only in wire, ribbon, and rod stock, therefore, limiting its potential practical application in TES systems.

TCE Materials

- Graphite —
  - Pyrolytic: Found to react significantly in carbonates under an argon environment from 750° to 910°C, precluding its use in these applications.
  - ATJ: Observed to be compatible with and unaffected in carbonates with an argon environment above melt for 1320 to 2710 hours at 750° to 910°-950°C.

- Copper — Both solid and porous reticulated matrix forms of copper are attractive in molten carbonates with an argon environment above the melt at 750° to 910°-950°C. Demonstrated excellent compatibility in this range for ~2700 hours in five tests.

Salts

- Carbonate salts are extremely attractive thermal energy storage media candidates for the high-temperature, solar-thermal power application range of 704° to 871°C.
  - Possess excellent thermal, chemical, and physical properties and stabilities

- Safe and simple handling, transportation, and operating procedures can be used.

- Carbonates can be melted, loaded, and container-welded in an air environment safely and acceptably.

- High-temperature, steady-state testing with one to five free-cool thermal cycles did not affect physiochemical properties of any of the carbonate salts studied for up to 3100 hours at 750° to 910°C.

- Technical-grade versions of the six salts tested generally exhibited a slightly higher corrosive attack with time than their reagent-grade counterparts. This salt-chemistry/corrosion difference does not, however, become the sole life-limiting aspect of any one compatibility scenario.

General Considerations for Containment of High-Temperature Carbonate Salts

- Long-term containment of molten Na_2CO_3 and K_2CO_3 and storage applications at temperatures above 900°C, in general, represents a considerable materials challenge requiring additional development and testing.

- Welds for high-temperature molten carbonate TES applications require extremely low porosity.

- In applications of coatings, uncoated weld areas should be minimized and far greater weld-washing times should be implemented to allow for diminished weld flowability in aluminum-rich alloys.

- Al_2O_3-forming alloys are attractive for containment of molten carbonates from 750° to 910°C because of the protective nature of alkali aluminate corrosion products formed.

RECOMMENDATIONS FOR FUTURE RESEARCH

- Chemical alloying modifications of AISI 310 SS should be investigated to produce a 310 SS-like material that is less susceptible to brittle, intermetallic sigma-phase precipitation in high-temperature (750° to 910°C) applications. This may possibly be achieved through variation of chromium or nickel composition or by additions of aluminum, which may further result in an attractive Al_2O_3-forming family of alloys.

- Pursue high-temperature materials research of aluminum-oxide forming materials through alloy and/or coatings development efforts to define the metallic-component/processing/weldability requirements and long-term (>8000 hour lab tests) compatibility/strength limitations for carbonate containment and TES applications in the 750° to 910°C temperature range.

- Maintain integrated programs that assess and analyze the systems cost/benefit trade-offs involved in tube-intensive TES subsystem HX concepts and use of TCE materials in these tube-intensive HX applications in the 750° to 910°C temperature range.

- Pursue generic research and development into other (that is, non-tube-intensive) TES media, insulation, working fluid, HX, and resultant containment schemes that may potentially offer further cost and performance benefits over current, state-of-the-art sensible and/or latent heat TES systems for solar/industrial-related applications in the elevated temperature regime of 750° to 910°C.

176/RPE/ms-tes

REFERENCES

1. Copeland, R. J., "Preliminary Requirements for Thermal Storage Subsystems in Solar Thermal Applications." DOE report prepared under Contract No. EG-77-C-01-4042. Golden, Colorado: Solar Energy Research Institute, April 1980.

2. Manvi, R., "Dish Mounted Latent Heat Buffer Storage." Paper presented at DOE Thermal and Chemical Storage Branch Annual Contractors' Review Meeting, McLean, Virginia, October 14-16, 1980.

3. Maru, H. C., Dullea, J. F., Karda, A. and Paul, L., "Molten Salt Thermal Energy Storage Systems." Report prepared under Contract No. EV-76-C-02-2888 for the U.S. Energy Research and Development Administration, Chicago: Institute of Gas Technology, March 1978.

4. Petri, R. J., Claar, T. D., Tison, R. R. and Marianowski, L. G., "High-Temperature Molten Salt Thermal Energy Storage Systems." IGT Project 9100 Final Rep. DOE report prepared under Contract No. NAS3-20806. Chicago, February 1980.

5. Rapp, R. A., Professor of Materials Engineering, Ohio State University, Janz, G. J., Professor of Chemistry, Rensselaer Polytechnic Inst., and Walker, W. W., Director, Molten Salts Data Center. Personal program consultations.

6. Rapp, R. A., Professor of Materials Engineering, Ohio State University. Personal consultations, 1981.

7. Airey, G. P., "Effect of Processing Variables on the Caustic Stress Corrosion Resistance of Inconel Alloy 600," Corrosion NACE, Vol. 36, No. 1, Pittsburgh: Westinghouse R&D, January 1980.

8. Airey, G. P., "Microstructural Aspects of the Thermal Treatment of Inconel Alloy 600." Metallography, 21-41 (1980).

9. Ambegaonkar, M. S., "Corrosion in Austenitic Stainless Steel Under Chemical Conditions." Chemical Age of India, Vol. 30, No. 3, March 1979.

10. Andresen, R. E., "Solubility of Oxygen and Sulfur Dioxide in Molten Sodium Sulfate and Oxygen and Carbon Dioxide in Molten Sodium Carbonate." J. Electrochimica Soc., Vol. 126, No. 2, 328-34, February 1979.

11. Metals Properties Council, Inc., "A Program to Discover Materials Suitable for Service Under Hostile Conditions Obtaining in Equipment for the Gasification of Coal and Other Solid Fuels," Annual Progress Report of Contract No. EX-76-C-01-1784, 1977.

12. Appleby, A. J. and VanDrunen, C., "Solubilities of Oxygen and Carbon Monoxide in Carbonate Melts." J. of the Electrochemical Society, Chicago: Institute of Gas Technology, August 1980.

13. Cable, M. and Martlen, D., "The Corrosion of Silica by Sodium Carbonate and Carbonate Rich Melts," Glass Technology, Vol. 12, No. 6, Sheffield, England: Dept. of Glass Technology, December 1971.

14. Davis, H. J. and Kinnibrugh, D. R., "Passivation Phenomena and Potentiostatic Corrosion in Molten Alkali Metal Carbonates," J. of the Electrochemical Society, 392-96, Toronto: Ferranti-Packard Limited, March 1970.

15. DeVan, J. H., "Molten Salt Compatibility," Oak Ridge, Tenn.: Oak Ridge National Laboratory.

16. Devereux, D. F., "Electrode Polarization Studies in Hot Corrosion Systems." DOE report prepared under Contract No. EY-76-S-02-2960A001. Storr, Conn.: University of Conn., May 1978.

17. Drugli, J. M. and Bardal, E., "A Short Duration Test Method for the Prediction of Crevice Corrosion Rates on Stainless Steels," Corrosion NACE, Vol. 34, No. 12, December 1978.

18. Institute of Gas Technology, "Fuel Cell Research on Second Generation Molten Carbonte Systems, Volume II: Task II, Characteristics of Carbonate Melts, Task IV, Corrosion Studies." Argonne National Laboratory Contract No. 31-109-3552. Chicago, 1977.

19. Grantham, L. F. and Ferry, P. B., "Corrosion in Alkali Metal Carbonate-Based Melts," in Proceedings of the International Symposium on Molten Salts. Canoga Park, Calif.: Atomics International Corporation, n.d.

20. Heine, D., Heess, F. and Groll, M., "Investigation of the Corrosion and Melting/Freezing Behavior of High Temperature Latent Heat Storage Materials." American Chemical Soc. No. 799096, Stuttgart, Germany: Universitat Stuttgart, 1979.

21. AISI, Committee of Stainless Steels Producers, "High Temperature Characteristics of Stainless Steels — A Designer's Handbook Series," Washington, D.C., 1979.

22. Huntington Alloys Inc., "Huntington Alloys Handbook," Huntington, West Virginia, 1979.

23. Huntington Alloys Inc., "Huntington Alloys, Incoloy Alloys," Huntington, West Virginia, 1979.

24. Huntington Alloys Inc., "Huntington Alloys, Inconel 600," Huntington, West Virginia, 1979.

25. Huntington Alloys Inc., "Huntington Alloys — Resistance to Corrosion," Huntington, West Virginia, 1979.

26. Ingram, M. D. and Janz, G. J., "The Thermodynamics of Corrosion in Molten Carbonates: Application of E/pCO_2 Diagrams," Electrochimica Acta 10, 783-92 (Pergammon Press Ltd., printed in Northern Ireland), Troy, N.Y.: Dept. of Chem., Rensselaer Polytechnic Inst., 1965.

27. Janz, G. J. and Conte, A., "Corrosion of Gold-Palladium, Nickel and Type 347 Stainless Steel in Molten Alkali Carbonates." Corrosion-NACE 20, 237-38, 1963.

28. Janz, G. J. and Conte, A., "Potentiostatic Polarization Studies in Fused Carbonates — I. The Noble Metals, Silver and Nickel," Electrochimica Acta 9, 1269-78 (Pergammon Press Ltd., Printed in Northern Ireland), Troy, N.Y.: Dept. of Chem., Rensselaer Polytechnic Inst., 1964.

29. Janz, G. J. and Conte, A., "Potentiostatic Polarization Studies in Fused Carbonates — II. Stainless Steels," Electrochimica Acta 9, 1279-87, Troy, N.Y.: Dept. of Chem., Rensselaer Polytechnic Inst., 1964.

30. Janz, G. J., Conte, A. and Neuenschwander, E., "Corrosion of Platinum, Gold, Silver and Refractories in Molten Carbonates." Paper presented at 19th Annual Conference of the National Association of Corrosion Engineers, New York, (1963) March.

31. Janz, G. J., Neuenschwander, E. and Conte, A., "Corrosion of Silver in Molten Alkali Carbonates," Corrosion Science 3, 177-80 (Pergammon Press Ltd., Printed in G.B.), Troy, N.Y.: Dept. of Chem., Rensselaer Polytechnic Inst., 1963.

32. Janz, G. J., Neuenschwander, E. and Kelly, F. J., "High Temperature Heat Content and Related Properties for Li_2CO_3, Na_2CO_3, K_2CO_3 and the Ternary Eutectic Mixture." Troy, N.Y.: Dept. of Chem., Rensselaer Polytechnic Inst., 1962.

33. John, R., "Corrosion of Metals by Liquid Na_2CO_3," Ph.D. Dissertation, Ohio State University, 1979.

34. Jones, R. L. and Stern, K. H., "New Eras in Molten Salt Corrosion Research," in V. 15th State of the Art Symposium, ACS-I&EC Division, National Symposium on Wear and Corrosion, Washington, D.C., June 1979.

35. "The Kanthal Handbook," Bethel, Conn.: The Kanthal Corp., 1966.

36. May, W. R. et al., "High Temperature Corrosion in Gas Turbines and Steam Boilers by Fuel Impurities, I. Measurement of Nickel Alloy Corrosion Rate in Molten Salts by Linear Polarization Technique." Ind. Eng. Chem. Prod. Res. Develop, Vol. 11, No. 4, St. Louis: Corporate Research Laboratories, 1972.

37. Institute of Gas Technology, "Development of Molten Carbonate Fuel Cell Power Plant." DOE Contract No. DE-AC01-80ET17019. Chicago, April 1981.

38. "Armco 18SR Stainless Steel Sheet and Strip," Product Data Report. Advanced Materials Division of Armco Steel Corp., 1977.

39. Institute of Gas Technology, "Fuel Cell Research on Second Generation Molten Carbonate Systems, Volume II — Characteristics of Carbonate Melts." Argonne National Laboratory Contract No. 31-109-38-3552. Chicago, 1976.

40. Institute of Gas Technology, "Fuel Cell Research on Second Generation Molten Carbonate Systems." Argonne National Laboratory Contract No. 31-109-38-3552. Chicago, 1977.

41. Rapp, R. A., "Materials Selection and Problems for Molten Carbonate Fuel Cells," in Oak Ridge Molten Carbonate Fuel Cell Proceedings. Columbus: Dept. Metallurgical Engineering, Ohio State University, 1978.

42. Rapp, R. A. and Goto, K. S., "The Hot Corrosion of Metals by Molten Salts." Paper presented at Symposium on Fused Salts, Pittsburgh, October 1978.

43. Selman, J. R. and Maru, H. C., "Physical Chemistry and Electrochemistry of Alkali — Carbonate Melts," Advances in Molten-Salt Chemistry 4, New York: Plenum Press, 1978.

44. Simmons, W. F., "Compilation of Chemical Compositions and Rupture Strengths of Superalloys." Issued under the auspices of ASTM Committee A-10 and the Defense Metals Information Center.

45. Stern, K. H. and Weise, E. L., "High Temperature Properties and Decomposition of Inorganic Salts — Part 2. Carbonates." National Bureau of Standards NSRDS-NBS-30, November 1969.

46. Strond, W. P. and Rapp, R. A., "The Solubilities of Cr_2O_3 and α-Al_2O_3 in Fused Na_2SO_4 at 1200K." Paper presented at ECS Symposium on Metal Halide Reactions, Atlanta, October 1977.

47. Venatasetty, H. V. and Seathoff, D. J., "Corrosion Studies of Alloys in Molten Eutectic Mixtures," Honeywell Corporate Research Center, Bloomington, Minn., 1975.

48. Gray, A. G., "Four Metals at Top of Critical List," Metal Progress, November 1979.

49. Huntington Alloy's Laboratory Data and Manufacturers Published Data, High Temperature Alloy Hot Performance Guide, 1979.

50. Monypenny, J. H. G., Stainless Iron and Steel 1, 3rd Ed. London: Chapman and Hall, 1951.

51. Peckner, D. and Bernstein, I. M., Handbook of Stainless Steels. New York: McGraw-Hill Book Company, 1977.

52. McGill, W. A. and Weinbaum, M. J., "Alonized Heat Exchangers Give Good High Temperature Service," National Association of Corrosion Engineers-Materials Performance, Along Processing, Tarentum, Pennsylvania, January 1978.

53. McGill, W. A. and Weinbaum, M. J., "The Selection, Application and Fabrication of Alonized Systems in the Refinery Environment." Paper presented at API, Refining 40th Midyear Meeting, Chicago, May 18, 1975.

54. Christie, J. R., Darnell, A. J. and Dustin, D. F., J. Phys. Chem. 82, 33 (1978).

55. Janz, G. J. et al., "Eutectic Data: Safety, Hazards, Corrosion, Melting Points, Compositions and Bibliography." Report presented under Contract No. TID-27163-P1 for U.S. Energy Research and Development Administration, Troy, N.Y.: Rensselaer Polytechnic Inst., July 1976.

APPENDIX A. Suppliers of Specific Technical-Grade Carbonate Salts

Table A-1, Part 1. SUPPLIERS OF SPECIFIC TECHNICAL-GRADE CARBONATE SALTS

Company	Location
Lithium Carbonate, Li_2CO_3	
Atomergic Chemetals Co.	Plainville, NJ
J T Baker Chem. Co.	Phillipsburg, NJ
Ceramic Color & Chem. Co.	New Brighton, PA
Chicago Vitreous Corp.	Chicago, IL
Foote Mineral Co.	Philadelphia, PA
General Color & Chem. Co.	Minerva, OH
Lithium Corp. of America	Gastonia, NC
United Mineral & Chem. Co.	New York, NY
U.S. Borax & Chemical Corp.	Los Angeles, CA
Sodium Carbonate, Na_2CO_3	
BASF Wyandotte Corp.	Wyandotte, MI
J T Baker Chem. Co.	Phillipsburg, NJ
Ceramic Color & Chem. Mfg. Co.	New Brighton, PA
Chicago Vitreous Corp.	Chicago, IL
Diamond Shamrock Chem. Co.	Cleveland, OH
FMC Corporation	Exton, PA
Harshaw Chem. Co.	Chicago, IL
Kaiser Chemicals	Oakland, CA
Kerr-McGee Chemical Corp.	Oklahoma City, OK
Stauffer Chemical Co.	Westport, CT
United Mineral & Chem. Corp.	New York, NY

Table A-1, Part 2. SUPPLIERS OF SPECIFIC TECHNICAL-GRADE CARBONATE SALTS

Company	Location
Potassium Carbonate, K_2CO_3	
Chicago Vitreous Corp.	Chicago, IL
General Color & Chem. Co.	Minerva, OH
Hooker Chemicals and Plastics Corp.	Niagara Falls, NY
IMC Chem. Group. Inc.	Boston, MS
Kaiser Chemicals	Oakland, CA
Shepard Chem. Ind. Inc.	New York, NY
Barium Carbonate, $BaCO_3$	
J T Baker Chem. Co.	Phillipsburg, NJ
Barium & Chem. Inc.	Slenlenville, OH
Chemical Products Corp.	Cantersville, GA
FMC Corp.	Exton, PA
General Color & Chem. Co.	Minerva, OH
Hammill & Gillespie, Inc.	Livingston, NJ
Harshaw Chem. Compnay	Chicago, IL
IMC Chem.	Boston, MA
Shepard Chemical Ind. Inc.	New York, NY
Sherwin Williams Chem.	Toledo, OH
United Mineral & Chem. Corp.	New York NY
Calcium Carbonate, $CaCO_3$	
American Pelletizing Corp.	DesMoines, Iowa
Anglo-Amer. Clays Corp.	Atlanta, GA
J T Baker Chem. Co.	Phillipsburg, NJ
Barium Chem. Inc.	Steubenville, OH

Table A-1, Part 3. SUPPLIERS OF SPECIFIC TECHNICAL-GRADE CARBONATE SALTS

Company	Location
Calcium Carbonate (Cont'd)	
Calcium Carbonate Co.	Quincy, IL
Diamond Shamrock Chem. Co.	Dallas, TX
General Color & Chem. Co.	Minerva, OH
General Electric Co.	Schenectady, NY
Harrisons & Crossfield	
Ohio Lime Co.	Woodville, OH
Pzier Minerals	New York, NY
United Mineral & Chem. Corp.	New York, NY
Ventron Corp. Alpha Prods.	Danvers, Mass.
Magnesium Carbonate, $MgCO_3$	
Aremco Prods. Inc.	Ossining, NY
J T Baker	Phillipsburg, NJ
General Color & Chem. Co.	Minerva, OH
General Electric Co.	Schenectady, NY
Harshaw Chem. Corp.	Cleveland, OH
Michigan Chem. Corp.	St. Louis, MI
United Mineral & Chem. Corp.	New York, NY

APPENDIX B. Suppliers of Alloy Containment Materials

Table B-1. SUPPLIERS OF ALLOY CONTAINMENT MATERIALS

Company	Location
Aeromet Inc.	Englewood, NJ
Allegheny Ludlum Steel Corp.	Palatine, IL
Armco, Eastern Steel Division	Middletown, OH
Carpenter Technology	Reading, PA
Climax Molybdenum Co.	Greenwich, CT
Huntington Alloys, Division of International Nickel Co.	Huntington, WV
J L Steel and LTV Co., Specialty Steels Division	Pittsburgh, PA
Kanthal Corporation	Bethal, CT
Republic Steel	Cleveland, OH
Rolled Alloys	Detroit, MI
Sandmeyer Steel	Philadelphia, PA
Sandvik, Inc.	Fairlawn, NJ
Special Metals	Wheaton, IL
Stellite Division, Cabot Corp.	Elmsford, NY
Universal Cyclops	Melrose Park, IL
Wisconsin Centrifugal	Waukasha, WI

APPENDIX C. Suppliers of Thermal Conductivity Enhancement Materials

Table C-1. SUPPLIERS OF TCE MATERIALS

- Astromet Associates, Incorporated; (Cincinnati, OH) porous, sintered and impregnated powder metallurgical structures
- Foametal Incorporated; (Willoughby, OH) low density, sintered reticulated cellular powder metal products
- Rocket Research Company (WA); open cell foams prepared by electroplating, powder metallurgy, or casting
- Union Carbide (NY); pyrolytic and ATJ graphite, and pyrolytic boron nitride
- Vicarb Corporation; impregnated graphite heat exchangers

In addition, the following companies were contacted as potential suppliers of specially configured, high-performance heat exchange products.

- APV Processing Equipment, Tonawanda, N.Y.
- Astro Metallurgical Corporation, Wooster, OH
- Bastex Corporation, Indianapolis, IN
- Berdell Industries, Inc., Long Island City, N.Y.
- Brown Fintube Company, Tulsa, OK
- Escoa Corporation, Elk Grove Village, IL
- John Zink Process Systems Comapny, Tulsa, OK
- Myren Multicoil Company, Oslo, Sweden
- Noranda Metal Industries, Newtown, CT
- Panelcoil Company, Brooklyn, N.Y.
- Rome Turney Radiator Comapny, Rome, N.Y.
- Slant/Fin Heating, Greenvale, N.Y.
- Tranter Corp., Tulsa, OK
- Vogt Machine Comapny, Louisville, KY
- Voss Finned Tube Products, Medina, OH
- Young Radiator Company, Racine, WI

APPENDIX D. Conversion Factors

Table D-1. CONVERSION FACTORS

Non-SI Unit	Operation	SI Unit
atm	X 1.013×10^5	Pa
Btu	X 1055.06	J
Btu/lb	X 2326.00	J/kg
Btu/lb-°F	X 4186.80	J/kg-K
Btu/hr-ft-°F	X 1.731	W/m-K
Btu/hr-ft^2-°F	X 5.678	W/m^2-K
Btu/hr-ft^2	X 3.154	W/m^2
Cal	X 4.18	J
°C	+ 273.15	K
cP	X 0.001	Pa-s
°F	(5/9) (°F-32)	°C
ft	X 0.3048	m
ft^2	X 0.0929	m^2
ft^2/hr	X 0.0000258	m^2/s
ft^3	X 0.0283	m^3
in.	X 0.0254	m
$in.^2$	X 0.00064516	m^2
lb	X 0.4536	kg
lb/ft^3	X 16.018	kg/m^3
lbm/ft^2-s	X 4.882	kg/m^2-s
mil	X 0.0000254	m
psia	X 6894.8	Pa

APPENDIX E. Carbonate Phase Diagrams

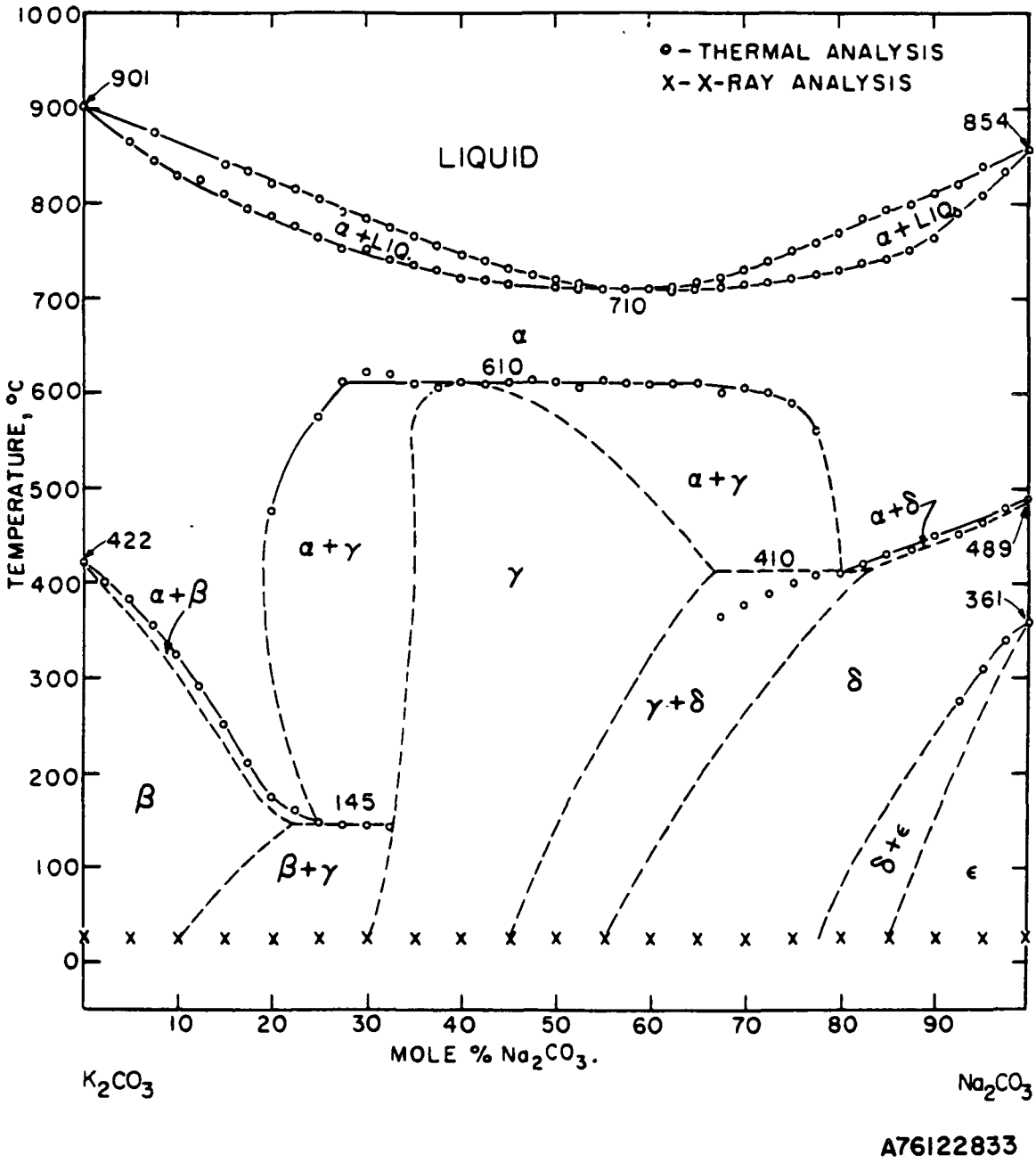

Figure E-1. PHASE DIAGRAM OF THE $(Na-K)_2CO_3$ SYSTEM[30]

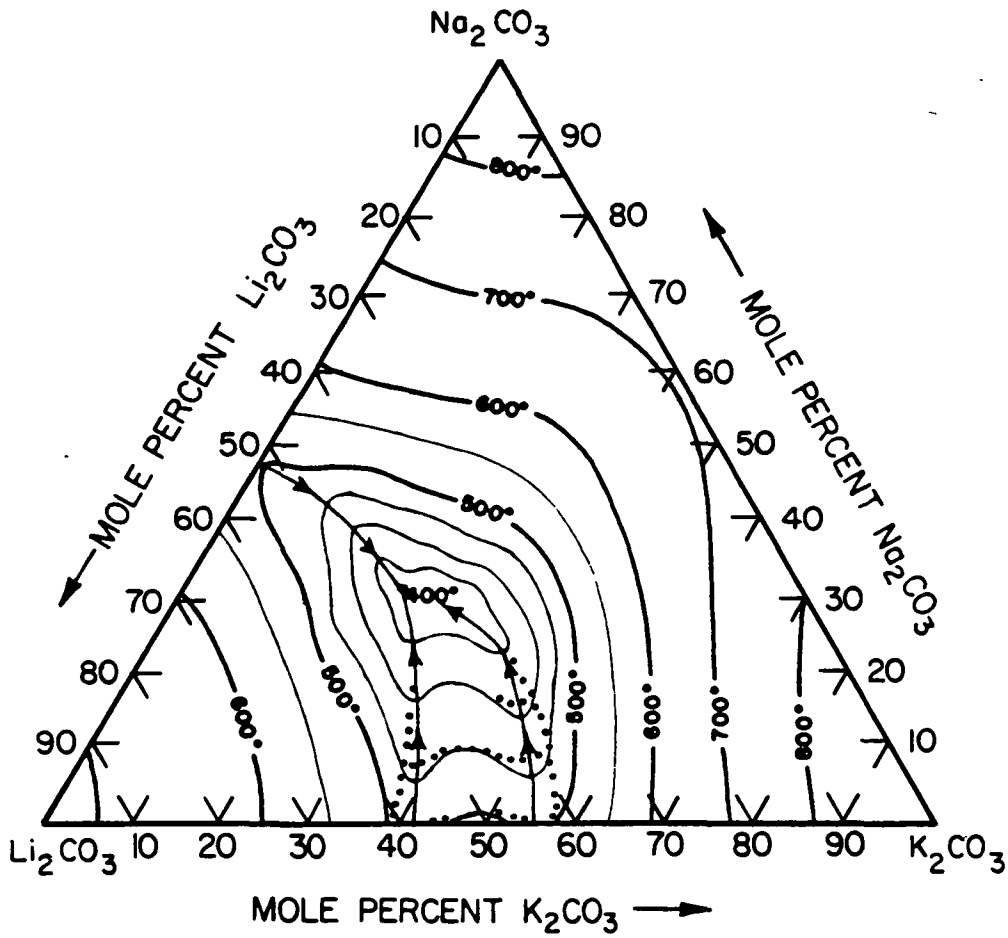

A76122832

Figure E-2. PHASE DIAGRAM FOR THE $(Li\text{-}Na\text{-}K)_2CO_3$ SYSTEM[30]

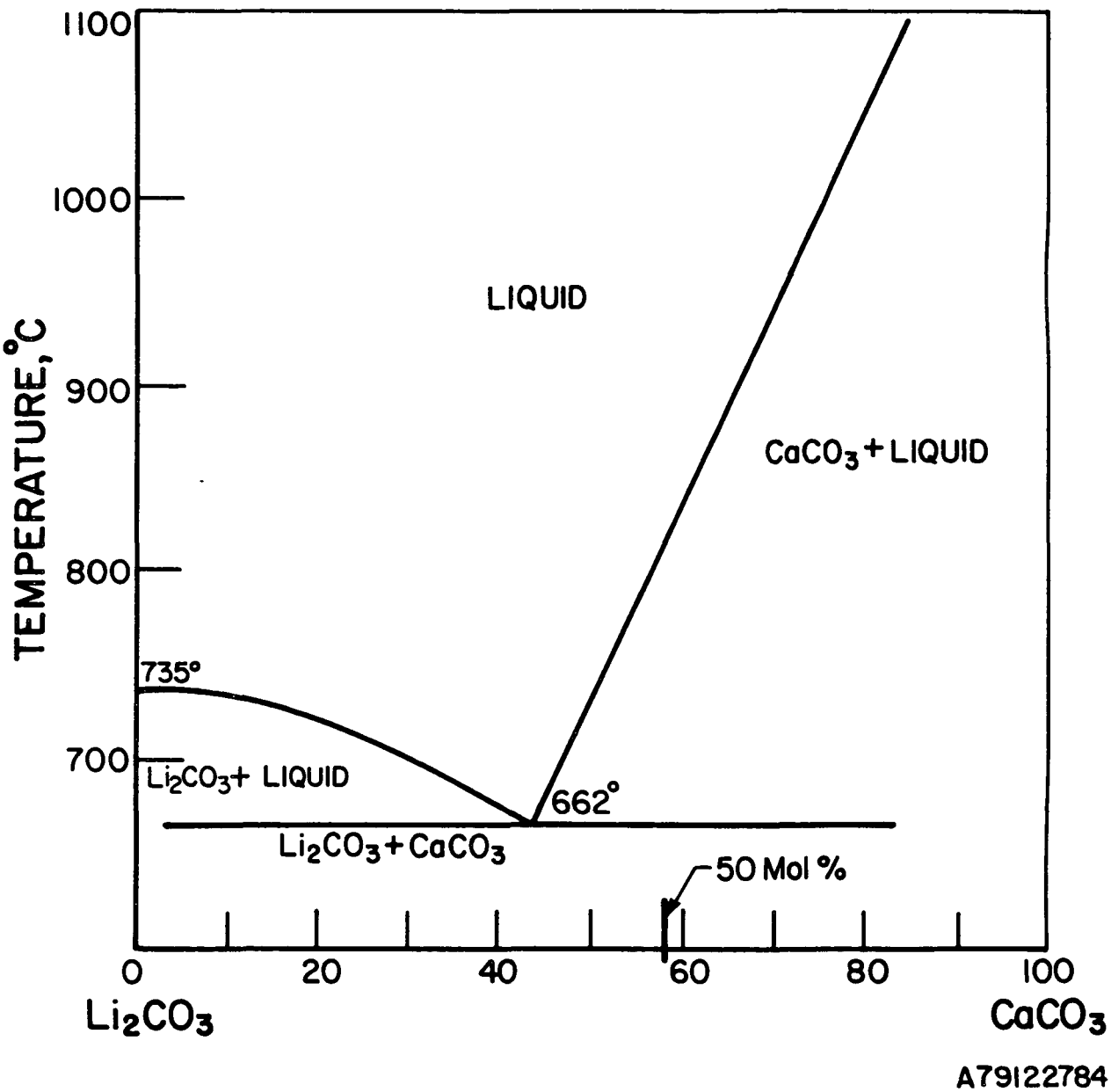

Figure E-3. PHASE DIAGRAM FOR THE Li_2CO_3-$CaCO_3$ SYSTEM[30]

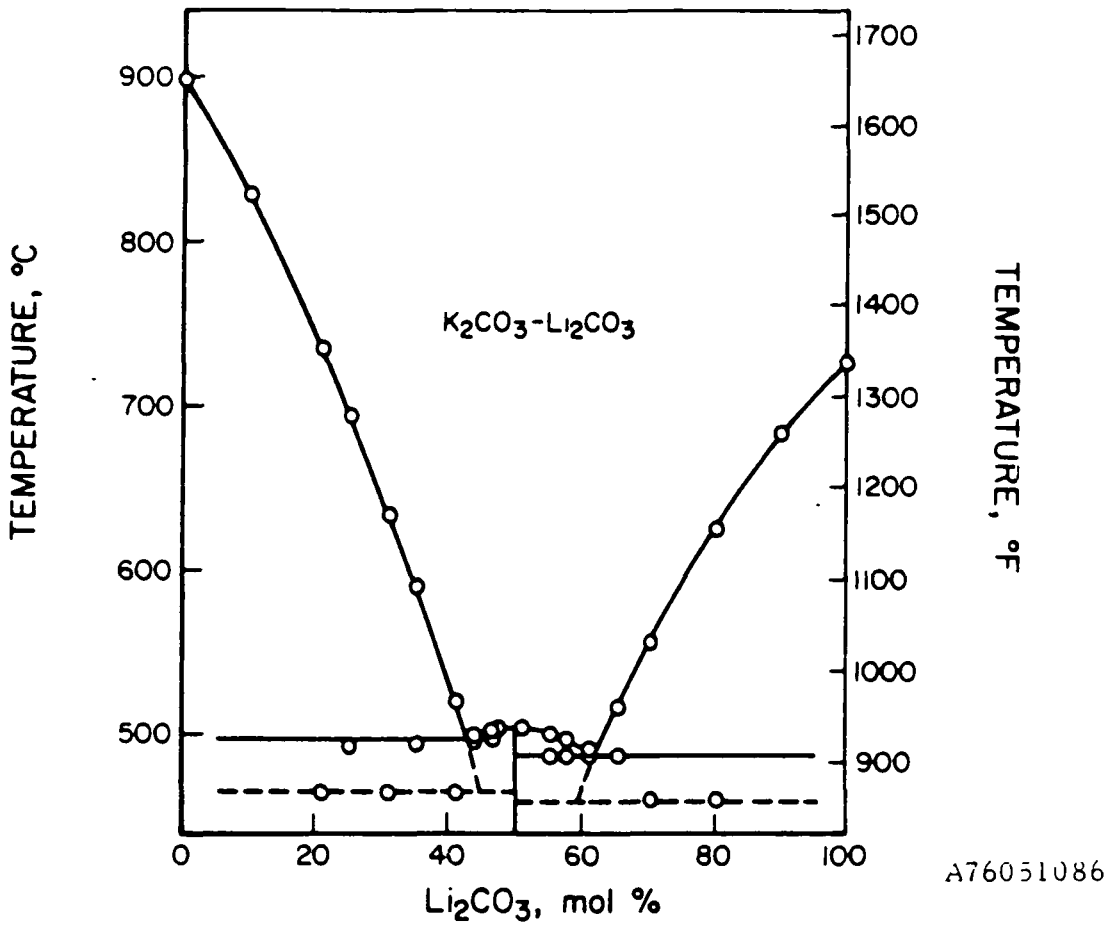

Figure E-4. PHASE DIAGRAM FOR THE K_2CO_3-Li_2CO_3 BINARY SYSTEM

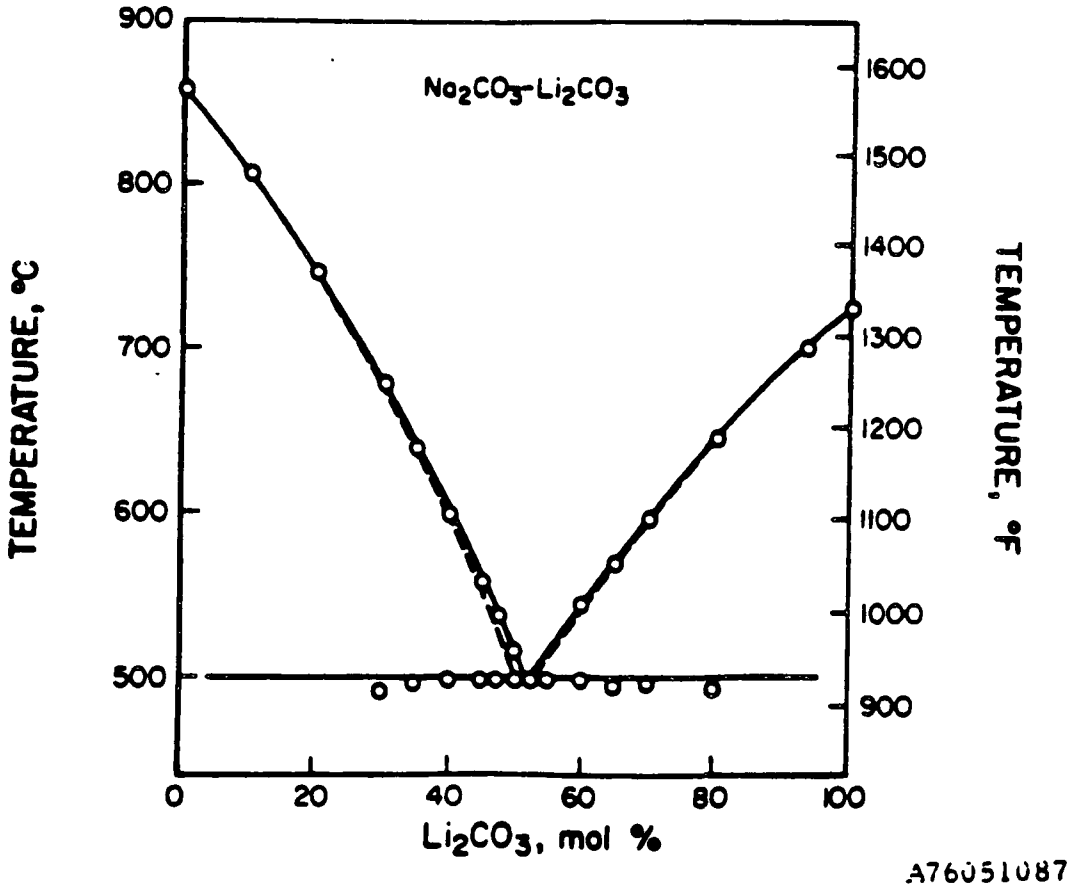

Figure E-5. PHASE DIAGRAM FOR THE Na_2CO_3-Li_2CO_3 BINARY SYSTEM

APPENDIX F. Information for NASA

1 Report No DOE/NASA/0156-83/1 NASA CR 167916	2 Government Accession No	3. Recipient's Catalog No
4 Title and Subtitle High-Temperature Molten Salt Thermal Energy Storage Systems for Solar Applications		5 Report Date July 1983 6. Performing Organization Code
7. Author(s) Randy J. Petri, Terry D. Claar		8 Performing Organization Report No
9. Performing Organization Name and Address Institute of Gas Technology IIT Center, 3424 S. State St. Chicago, Illinois 60616		10 Work Unit No 11 Contract or Grant No DEN 3-156
12. Sponsoring Agency Name and Address National Aeronautics and Space Administration Washington, DC 20546		13. Type of Report and Period Covered 8/6/79-12/31/80 14. Sponsoring Agency Code

15. Supplementary Notes

Project Manager, Richard W. Vernon, NASA Lewis Research Center, Cleveland, Ohio

16. Abstract

Experimental results of compatibility screening studies of 100 salt/containment/thermal conductivity enhancement (TCE) combinations for the high-temperature solar thermal application range of 704° to 871°C (1300° to 1600°F) are presented. Nine candidate containment/HX alloy materials and two TCE materials were tested with six candidate solar thermal alkali and alkaline earth carbonate storage salts (both reagent- and technical-grade of each). Compatibility tests were conducted with salt encapsulated in ~6.0-inch x 1-inch welded containers of test material from 300 to 3000 hours. Compatibility evaluations were end-application oriented, considering the potential 30-year lifetime requirement of solar thermal power plant components. Analyses were based on depth and nature of salt-side corrosion of materials, containment alloy thermal aging effects, weld integrity in salt environment, air-side containment oxidation, and chemical and physical analyses of the salt.

A need for more reliable, and in some cases first-time-determined, thermophysical and transport property data was also identified for molten carbonates in the 704° to 871°C temperature range. In particular, accurate melting point (mp) measurements were performed for Li_2CO_3 and Na_2CO_3 while melting point, heat of fusion, and specific heat determinations were conducted on 81.3 weight percent Na_2CO_3-18.7 weight percent K_2CO_3 and 52.2 weight percent $BaCO_3$-47.8 weight percent Na_2CO_3 to support future TES system design and ultimate scale-up of solar thermal energy storage (TES) subsystems.

17. Key Words (Suggested by Author(s)) Thermal storage Phase-change media Solar thermal storage Carbonates	18. Distribution Statement Unclassified - unlimited Star Category 44 DOE Category UC-94a		
19. Security Classif (of this report) Unclassified	20 Security Classif (of this page) Unclassified	21. No of Pages 177	22. Price*

* For sale by the National Technical Information Service, Springfield, Virginia 22161

NASA-C-168 (Rev 10-75)

PRECEDING PAGE BLANK NOT FILMED

PAGE ____ INTENTIONALLY BLANK

Distribution List for Final Report
DEN 3-156

	No. of Copies
Albuquerque Operations Office P.O. Box 5400 Albuquerque, NM 87115 Attn: D. K. Nowlin	1
Argonne National Lab. 9700 South Cass Avenue Argonne, IL 60439 Attn: Dr. Magdy Farahat	1
Arizona Public Service 411 North Central Phoenix, AZ 85036 Attn: E. R. Weber	1
Badger Energy, Inc. 1 Broadway Cambridge, MA 02142 Attn: Fred Gardner	1
Bechtel Corporation 50 Beale Street San Francisco, CA 94119 Attn: T. E. Walsh	1
Biphase Energy Systems 2800 Airport Boulevard Santa Monica, CA 90405 Attn: Walter Studhalter	1
Black & Veatch P.O. Box 8405 Kansas City, MO 64114 Attn: Sheldon L. Levy	1
Boeing Engineering & Construction Division of The Boeing Company P.O. Box 3707 Seattle, WA 98124 Attn: J. Shroeder W. Beverly W. Engle	 1 1 1
Calmac Manuf. Corp. P.O. Box 710 Englewood, N. J. 07631 Attn: Calvin D. MacCracken	1

Distribution List — Cont.

	No. of Copies
Central Electricity Generating Board Research Division Marchwood Engineering Laboratories Marchwood Southampton Hampshire SO4 4ZB, England Attn: Dr. Ian Glendenning	1
Combustion Engineering, Inc. 1000 Prospect Hill Rd. Windsor, CT 06095 Attn: C. di Lauro	1
Comstock & Wescott, Inc. 765 Concord Avenue Cambridge, MA 02138 Attn: Richard E. Rice	1
DOE/ETS Division of Planning & Technical Transfer 600 E. Street Washington, D.C. 20545 Attn: Leslie S. Levine	1
U.S. Department of Energy 1000 Independence Ave., Forrestal Bldg. Washington, D.C. 20585 Attn: Karl Bastress	1
U.S. Department of Energy 1000 Independence Ave., CE141 Washington, D.C. 20585 Attn: Rufus W. Shivers	1
U.S. Department of Energy Division of Energy Storage Systems Washington, D.C. 20545 Attn: G. F. Pezdirtz	1
J. Swisher	1
J. Gahimer	1
M. Gurevich	1
S. Ruby	1
U.S. Department of Energy San Francisco Operations Office 1333 Broadway Oakland, CA 94612 Attn: D. Elliot	1
R. Hughey	1

	No. of Copies
U.S. Department of Energy Division of Central Solar Technology Washington, D.C. 20545 Attn: M. U. Gutstein	1
Dynatech R/D Company 99 Erie Street Cambridge, MA 02139 Attn: Dr. R. P. Tye	1
Howard Edde, Inc. 1402-140th Place NE Bellevue, WA 98007 Attn: Howard Edde	1
Edison Electric Institute 90 Park Avenue New York, NY 10016 Attn: J. Karp	1
Electric Power Research Institute 3412 Hillview Avenue P.O. Box 10412 Palo Alto, CA 94303 Attn: Dr. T. Schneider Dr. F. Kalhammer W. A. Stevens	1 1 1
Exxon Research and Engineering Company P.O. Box 45 Linden, N.J. 07036 Attn: R. P. Cahn	1
General Atomic Company P.O. Box 81608 San Diego, CA 92138 Attn: D. Vrable	1
General Electric Company — TEMPO P.O. Drawer QQ Santa Barbara, CA 93102 Attn: W. Hausz	1
General Electric Company 1 River Road Schenectady, NY 12345 Attn: Eldon Hall	1

Distribution List — Cont.

	No. of Copies
General Electric Company Advanced Energy Programs P.O. Box 15132 Cincinnati, OH 45215 Attn: W. F. Zimmerman	1
Geoscience Ltd. 410 South Cedros Avenue Solana Beach, CA 92075 Attn: Dr. H. Poppendiek	1
Graz University of Technology Obere Teichstrasse 21/i A-8010 Graz, Austria Attn: Prof. P. V. Gilli	1
Grumman Aerospace Corporation MS B09-25 Bethpage, NY 11714 Attn: Robert Haslett Joseph Alario	1 1
Honeywell, Inc. Energy Resources Center 2600 Ridgeway Parkway Minneapolis, MN 55413 Attn: R. LeFrois	1
Indian Institute of Technology Department of Mechanical Engineering Madras 600036, India Attn: Dr. M. V. Krishna Murthy	1
Jet Propulsion Laboratory California Institute of Technology 4800 Oak Grove Drive Pasadena, CA 91103 Attn: J. Stearns R. Manvi	1 1
Midwest Research Institute 425 Volker Boulevard Kansas City, MO 64110 Attn: K. P. Ananth	1

Distribution List — Cont.

	No. of Copies
National Aeronautics and Space Administration Lewis Research Center 21000 Brookpark Road Cleveland, OH 44135	
Attn: Arno W. Nice, MS: 500-202	1
Norman T. Musial, MS: 500-311	1
Leonard W. Schopen, MS: 500-305	1
Linda M. Finke, MS: 500-202	1
Report Control Office, MS: 5-5	1
Library, MS: 60-3	2
Richard W. Vernon, MS: 500-202	48
National Aeronautics and Space Administration Headquarters Washington, D.C. 20546	
Attn: RG-14/W. Johnson	1
NASA Scientific & Technical Information Facility P.O. Box 8757 Baltimore/Washington International Airport, MD 21240	
Attn: Accessioning Department	30
Northern States Power Company 414 Nicollet Avenue Minneapolis, MN 55401	
Attn: Les Weber, Vice Pres. of Research	1
Oak Ridge National Laboratory Building 9204-1, Mail Stop 3 P.O. Box Y Oak Ridge, TN 37830	
Attn: D. M. Eissenberg	1
J. F. Martin	1
M. Olszewski	1
Ontario Hydro 700 University Avenue Toronto, Ontario M5G1X6, Canada	
Attn: A. G. Barnstaple	1
Pennwalt Corp. P.O. Box C, 900 First Ave. King of Prussia, PA 19406	
Attn: Johnson C. H. Chen	1

	No. of Copies
R&D Associates P.O. Box 9695 Marina del Rey, CA 90291 Attn: R. P. Hammond	1
Rocket Research Company York Center Redmond, VA 98052 Attn: D. D. Huxtable	1
Rockwell International Rocketdyne Division 6633 Canoga Avenue Canoga Park, CA 91304 Attn: Richard Morgan	1
Rockwell International Energy Systems Group 11716 Monogram Avenue Granada Hills, CA 91344 Attn: Jack Rosemary	1
Sandia Laboratories Albuquerque Albuquerque, NM 87115 Attn: J. F. Banas	1
Sandia Laboratories Livermore P.O. Box 969 Livermore, CA 94550 Attn: A. C. Skinrood L. Radosevish T. D. Brumleve W. S. Winter, Jr. J. D. Gilson	 1 1 1 1 1
Sigma Research, Inc. 2950 George Washington Way Richland, WA 99352	1
Solar Resources, Inc. 5401 McConnell Avenue Los Angeles, CA 90066 Attn: Ralph E. Bartera	1
Stone & Webster 245 Summer Street P.O. Box 2325 Boston, MA 02107 Attn: K. E. Hogeland	1

	No. of Copies
Swiss Federal Institute of Reactor Research 5303 Wurenlinged Switzerland Attn: Professor M. Taube	1
Tennessee Valley Authority 1360 Commerce Union Bank Building Chattanooga, TN 37401 Attn: Dr. A. Manaker	1
University of Delaware Department of Chemical Engineering Newark, DE 19711 Attn: C. E. Birchenall	1
University of Stuttgart Institute for Nuclear Energy & Energy Systems (IKE) Pfaffenwaldring 31, Postfach 80 11 40 7000 Stuttgart 80, Federal Republic of Germany Attn: Manfred Groll	1
Westinghouse Electric Corporation P.O. Box 10864 Pittsburgh, PA 15236 Attn: M. K. Wright W. Lundberg	1 1
Xerox Electro-Optical Systems 300 North Halstead Street Pasadena, CA 91107 Attn: William Mortenson	1

179/PRE/distlist